

MODEL PREDICTIVE CONTROL (MPC) PERFORMANCE FOR CONTROLLING
REACTION SYSTEMS

A THESIS SUBMITTED TO
THE GRADUATE SCHOOL OF NATURAL AND APPLIED SCIENCES
OF
MIDDLE EAST TECHNICAL UNIVERSITY

BY

İŞİK AŞAR

IN PARTIAL FULFILLMENT OF THE REQUIREMENTS FOR THE DEGREE OF
MASTER OF SCIENCE
IN
CHEMICAL ENGINEERING

JUNE 2004

Approval of the Graduate School of Natural and Applied Sciences

Prof. Dr. Canan Özgen
Director

I certify that this thesis satisfies all the requirements as a thesis for the degree of Master of Science.

Prof. Dr. Timur Doğu
Head of Department

This is to certify that we have read this thesis and that in our opinion it is fully adequate, in scope and quality, as a thesis and for the degree of Master of Science.

Prof. Dr. Kemal Leblebicioğlu
Co-supervisor

Prof. Dr. Canan Özgen
Supervisor

Examining Committee Members

Prof. Dr. Güniz GÜRÜZ

Prof. Dr. Canan ÖZGEN

Prof. Dr. Kemal LEBLEBİCİOĞLU

Prof. Dr. İnci EROĞLU

Prof. Dr. Isık ÖNAL

I hereby declare that all information in this document has been obtained and presented in accordance with academic rules and ethical conduct. I also declare that, as required by these rules and conduct, I have fully cited and referenced all material and results that are not original to this work.

Name, Last name : Işık Aşar

Signature :

ABSTRACT

MODEL PREDICTIVE CONTROL (MPC) PERFORMANCE FOR CONTROLLING REACTION SYSTEMS

Aşar, Işık

M.S., Department of Chemical Engineering

Supervisor: Prof. Dr. Canan ÖZGEN

Co-Supervisor: Prof. Dr. Kemal LEBLEBİCİOĞLU

June 2004, 145 pages

In this study, the performance of the Model Predictive Controller (MPC) algorithm is investigated in two different reaction systems. The first case is a saponification reaction system where ethyl acetate reacts with sodium hydroxide to produce sodium acetate and ethanol in a CSTR. In the reactor, temperature and sodium acetate concentration are controlled by manipulating the flow rates of ethyl acetate and cooling water. The model of the reactor is developed considering first principal models. The experiments are done to obtain steady state data from the reaction system and these are compared with the model outputs to find the unknown parameters of the model. Then, the developed model is used for

designing SISO and MIMO-MPC considering Singular Value Decomposition (SVD) technique for coupling.

The second case is the reaction system used for the production of boric acid by the reaction of colemanite and sulfuric acid in four CSTR's connected in series. In the reactor, the boric acid concentration in the fourth reactor is controlled by manipulating the sulfuric acid flow rate fed to the reactor. The transfer functions of the process and disturbance (colemanite flow rate) are obtained experimentally by giving step changes to the manipulated variable and to the disturbance. A model-based and constrained SISO-MPC is designed utilizing linear step response coefficients.

The designed controllers are tested for performance in set point tracking, disturbance rejection and robustness issues for the two case studies. It is found that, they are satisfactory except in robustness issues for disturbance rejection in boric acid system.

Keywords: Model Predictive Control, CSTR, Saponification, Boric Acid

ÖZ

REAKSİYON SİSTEMLERİNDE MODEL ÖNGÖRÜMLÜ DENETLEYİCİ PERFORMANSI

Aşar, Işık

Yüksek Lisans, Kimya Mühendisliği

Tez Yöneticisi: Prof. Dr. Canan ÖZGEN

Ortak Tez Yöneticisi: Prof. Dr. Kemal LEBLEBİCİOĞLU

Haziran 2004, 145 sayfa

Bu çalışmada, Model Öngörümlü Deneyleyicilerin (MÖD) performansı iki farklı reaksiyon sistemi için incelenmiştir. Önce, sabunlaştırma reaksiyonu olan etil asetatın sodyum hidroksit reaksiyonu ile sodyum asetat ve etanole dönüşen tepkime kabı ele alınmıştır. Bu tepkime kabında, reaktör sıcaklığı ve sodyum asetat konsantrasyonu, etil asetat ve soğutma suyu akış hızı ile denetlenmiştir. Madde ve enerji denklemleri kullanılarak reaktörün dinamik modeli geliştirilmiştir. Modeldeki bilinmeyen parametreleri elde etmek için yatışkın durum deneyleri yapılmıştır. Geliştirilen model, tek girdili tek çıktılı (TGTÇ) ve çok girdili çok çıktılı (ÇGÇK)-MÖD tasarlamak için kullanılmıştır.

Daha sonra, kolemanit ile sülfürik asidin dört adet sürekli karıştırıcı tank reaktöründeki reaksiyonu sonucunda elde edilen borik asit sistemi incelenmiştir. Bu sistemde, dördüncü reaktördeki borik asit konsantrasyonu, sülfürik asidin akış hızı ile denetlenmesi incelenmiştir. Sistemin ve bozan etkenin (kolemanit akış hızı) aktarım fonksiyonlarını elde etmek için ayarlanan değişkene ve bozan etkene adım değişikliği verilerek borik asit konsantrasyonunun cevap eğrisi elde edilmiştir. Aktarım fonksiyonları TGTÇ-MÖD tasarlamak için kullanılmıştır.

Her iki reaktör sistemi için tasarlanan denetleyicilerin performansları, istek değeri takibi, bozan etkenin ortadan kaldırılması ve gürbüzlük açılarından incelenmiştir. Tasarlanan denetleyicilerin, istek değeri takibi ve bozan etkenin ortadan kaldırılmasına göre başarılı oldukları bulunmuştur. Ancak, borik asit üretiminde kullanılan reaktörün, bozan etkenin performansının gürbüz olmadığı diğerlerinin ise gürbüz olduğu belirlenmiştir.

Anahtar Kelimeler: Model Öngörümlü Denetim, Sürekli Karıştırılan Tank Reaktörü, Sabunlaştırma, Borik Asit

To My Family,

ACKNOWLEDGEMENTS

First, I would like to thank my supervisor Prof. Dr. Canan Özgen for her valuable support, encouragement and guidance, for her kindly and lovely attitude throughout this study.

I would like to thank to Prof. Dr. Kemal Leblebiciođlu, my co-supervisor, for his support.

I would also like to thank Prof. Dr. Işık Önal for his help and Prof. Dr. İnci Erođlu and Gaye Çakal to let me use their experimental system and thank to Gaye Çakal, Anıl Erdođdu, Deniz Gürhan for their help and support during the boric acid experimental studies.

I am very grateful to my parents for their endless love, trust and sacrifices for me. I would like to thank to my control team members; Ugur Yıldız, who always listening my problems without grumbling and trying to solve them, Almıla Bahar, Necati Günaydın, Evren Guner, Salih Obut, Oluş Özbek for their help and friendship. I would like to thank my best friend Yalçın Yıldız who was with me all the way and always support me. I would like to thank also to İsmail Dođan, Alper Uzun, Ural Yađşı, Deđer Şen and my friends that I could not mention here.

TABLE OF CONTENTS

PLAGIARISM	iii
ABSTRACT	iiiv
ÖZ.....	vii
DEDICATION.....	viii
ACKNOWLEDGEMENTS	ixx
TABLE OF CONTENTS	x
LIST OF TABLES	xiii
LIST OF FIGURES	xv
NOMENCLATURE.....	xx
CHAPTER	
1. INTRODUCTION.....	1
2. LITERATURE SURVEY.....	4
2.1 Model Predictive Control (MPC).....	4
2.2 Boric Acid Studies.....	14
3. BORON.....	16
3.1 Boric Acid.....	18
3.1.1 Properties of Boric Acid	18
3.1.2 Boric Acid Production.....	18
4. MODEL PREDICTIVE CONTROL (MPC)	20
4.1 MPC Strategy	20
4.2 MPC Models	22
4.3 Multi-Input Multi-Output (MIMO) Predictive Control	25
4.4 Objective Function.....	25
4.5 Controller Design.....	26

4.6 Tuning the MPC.....	29
5. CASE STUDY I: SAPONIFICATION REACTION in CSTR	30
5.1 Experimental	31
5.1.1 Experimental Set-up	31
5.1.2 Experimental Procedure.....	32
5.2 Model of the Chemical Reactor	32
5.3 Control Studies	37
6. CASE STUDY II: BORIC ACID PRODUCTION from COLEMANITE and SULFURIC ACID in CSTR.....	38
6.1 Description of the Experimental Set-up.....	38
6.2 The Variables of the System.....	39
6.3 Experimental Studies	40
6.3.1 Dynamic Experiments-Step Change in Acid Feed Flow Rate	41
6.3.2 Dynamic Experiments-Step Change in Colemanite Flow Rate ..	41
7. RESULTS AND DISCUSSION	42
7.1 Case Study I: Saponification Reaction in a CSTR	42
7.1.1 Model Verification	42
7.1.2 Calculation of Step Response Coefficients for MPC.....	44
7.1.3 Pairing Between Controlled and Manipulated Variables.....	46
7.1.4 Design of SISO-MPC	47
7.1.4.1 SISO-MPC Performance in Setpoint Tracking	48
7.1.4.2 SISO-MPC Performance in Disturbance Rejection	51
7.1.5 Design of MIMO-MPC.....	53
7.1.5.1 MIMO-MPC Performance in Setpoint Tracking	53
7.1.5.2 MIMO-MPC Performance in Disturbance Rejection	55
7.1.5.3 MPC Performance for Robustness.....	58
7.2 Case Study II: Boric Acid Production from Colemanite and Sulfuric Acid in Four CSTR's	61
7.2.1 System Identification	61
7.2.1.1 Process Transfer Function Determination	61
7.2.1.2 Disturbance Transfer Function Determination	69
7.2.2 Design of SISO-MPC	75
7.2.2.1 Unconstrained SISO-MPC Performance in Setpoint Tracking.....	75
7.2.2.2 Unconstrained SISO-MPC Performance in Disturbance Rejection.....	76
7.2.2.3 Constrained SISO-MPC Performance in Setpoint Tracking	77

7.2.2.4 Constrained SISO-MPC Performance in Disturbance Rejection.....	80
7.2.2.5 SISO-MPC Performance for Robustness	80
7.2.2.6 Performance of SISO-MPC by Using Approximated Transfer Function Model in Setpoint Tracking	83
7.2.2.7 Performance of SISO-MPC by Using Approximated Transfer Function Model in Disturbance Rejection	85
7.2.2.8 Performance of SISO-MPC by Using Approximated Transfer Function Model for Robustness	86
7.2.3 Design of Cohen-Coon (PID) and ITAE (PID) Controllers.....	88
8. CONCLUSIONS	90
REFERENCES	93
APPENDICES.....	99
A. FORMULATION OF CONTROLLER DESIGN	99
B. EXPERIMENTAL DATA FOR SAPONIFICATION SYSTEM	102
C. SINGULAR VALUE DECOMPOSITION (SVD) ANALYSIS	104
D. SIMULATION PROGRAM FOR SAPONIFICATION SYSTEM	106
D.1 cstr.m	106
D.2 controller.m	116
D.3 glob_decs.m.....	121
D.4 glob_initial.m	123
D.5 stepcoefficients.dat	124
E. EXPERIMENTAL DATA FOR BORIC ACID PRODUCTION SYSTEM	127
F. MPC TOOLBOX IN MATLAB AND SIMULATION PROGRAM FOR BORIC ACID PRODUCTION SYSTEM	133
F.1 MPC Toolbox in Matlab	133
F.2 MPC Simulation Program for Boric Acid Production System	137
F.3 Cohen and Coon (PID) Model by Simulink	141
F.4 ITAE (PID) Model by Simulink.....	141
G. SAMPLE CALCULATIONS	142
G.1 Calculation of Sodium Hydroxide Concentration for Saponification System.....	142
G.2 Calculation of Cohen and Coon (PID) and ITAE (PID) Design Parameters	143
G.3 Determination of Boric Acid Concentration	144

LIST OF TABLES

3.1 Important Boron Minerals	17
3.2 Distribution of Boron Minerals.	17
5.1 Operating Conditions and Found Parameters	36
7.1 Different τ_1 values with SSE score for process transfer function	62
7.2 Different τ_2 values with SSE score for process transfer function	63
7.3 Different τ_3 values with SSE score for process transfer function	64
7.4 Different τ_4 values with SSE score for process transfer function	64
7.5 Different τ_1 values with SSE score for process transfer function	70
7.6 Different τ_2 values with SSE score for process transfer function	71
7.7 Different τ_3 values with SSE score for process transfer function	71
7.8 Different τ_4 values with SSE score for process transfer function	71
B.1 Experimental Data for $F_{EA}= 40$ ml/min, $F_N=40$ ml/min at 30°C	102
B.2 Experimental Data after +10% step input to $F_{EA}= 40$ ml/min, $F_N=40$ ml/min at 30°C	102
B.3 Thermodynamic and Kinetic Data	103
E.1 Experimental Data in Reactor I for Run I	127
E.2 Experimental Data in Reactor II for Run I	127
E.3 Experimental Data in Reactor III for Run I	128
E.4 Experimental Data in Reactor IV for Run I.....	128
E.5 Experimental Data in Reactor I for Run II	128
E.6 Experimental Data in Reactor II for Run II	129

E.7 Experimental Data in Reactor III for Run II.....	129
E.8 Experimental Data in Reactor IV for Run II	129
E.9 Experimental Data in Reactor I for Run III	130
E.10 Experimental Data in Reactor II for Run III	130
E.11 Experimental Data in Reactor III for Run III	130
E.12 Experimental Data in Reactor IV for Run III.....	131
E.13 Experimental Data in Reactor I for Run IV.....	131
E.14 Experimental Data in Reactor II for Run IV.....	131
E.15 Experimental Data in Reactor III for Run IV.....	132
E.16 Experimental Data in Reactor IV for Run IV.....	132

LIST OF FIGURES

4.1 MPC Strategy.....	21
4.2 Basic Structure of MPC.....	22
4.3 An Open Loop Step Response of a Linear Process	23
5.1 Experimental Set-up of Saponification System.....	31
5.2 Saponification Reactor System	37
6.1 Experimental Set-up of Boric Acid Production System.....	39
6.2 Block Diagram of the Boric Acid Production System.....	40
7.1 Experimental and Simulated Data for $F_N=F_{EA}=40$ ml/min at 30°C	43
7.2 Experimental and Simulated Data for +10% step input to $F_{EA}=44$ ml/min and $F_N=40$ ml/min at 30°C	43
7.3 Open loop responses of sodium acetate concentration and reactor tempera- ture to unit step change in ethyl acetate flow rate.....	44
7.4 Open loop responses of sodium acetate concentration and reactor temperature to unit step change in cooling water flow rate.....	45
7.5 Response of C_{NA} to -2% decrease in the set point of C_{NA} and followed by +2% increase in set point of C_{NA} for $f= 1\times 10^{-5}$, 1×10^{-6} and 1×10^{-7} with $C=70$	48
7.6 Response of C_{NA} to -2% decrease in the set point of C_{NA} and followed by +2% increase in C_{NA} for $C= 70, 30$ and 5 with $f= 1\times 10^{-7}$	49
7.7 Response of T to $+3^{\circ}\text{C}$ increase in the set point of T and followed by -3°C decrease in set point of T for $f= 1\times 10^{-1}$, 1×10^{-2} and 2×10^{-3} with $C=14$	50

7.8 Response of T to +3 ⁰ C step change in the set point of T and -3 ⁰ C step change in the set point of T for C= 14, 6 and 2 with f= 2×10 ⁻³	51
7.9 Response of C _{NA} for -10% disturbance changes in flow rate of sodium hydroxide for f= 1×10 ⁻⁵ , 1×10 ⁻⁶ , 1×10 ⁻⁷ with C=70.....	52
7.10 Response of T for -10% disturbance change in cooling water temperature, -1.8 ⁰ C, for f= 1×10 ⁻¹ , 1×10 ⁻² and 2×10 ⁻³ with C=14	52
7.11 Responses of C _{NA} and T to -2 % and +2% step changes in the set point of C _{NA} consecutively for f=1×10 ⁻⁵ , 1×10 ⁻⁶ , 1×10 ⁻⁷ with C=70.....	54
7.12 Responses of C _{NA} and T to -2% step change in the set point of C _{NA} and +2% step change in the set point of C _{NA} consecutively for C=70, 35 and 5 with f= 1×10 ⁻⁷	55
7.13 Responses of C _{NA} and T to -10% disturbance changes in flow rate of sodium hydroxide for f= 1×10 ⁻⁵ , 1×10 ⁻⁶ , 1×10 ⁻⁷ and C=70.	56
7.14 Responses of C _{NA} and T for -10% disturbance change in flow rate of sodium hydroxide for C=70, 30, 5 with f=1×10 ⁻⁷	57
7.15 Responses of C _{NA} and T for 1 ⁰ C decrease in cooling water temperature for f=1×10 ⁻⁷ and C=70	58
7.16 Responses of C _{NA} and T to -2 % and +2% step changes in the set point of C _{NA} consecutively for a 15% change in the model parameter, k, for f=1× 10 ⁻⁷ and C=70.....	59
7.17 Responses of C _{NA} and T to -10% disturbance change in sodium hydroxide flow rate for a 15% change in the model parameter, k, for f=1× 10 ⁻⁷ and C=70.....	59
7.18 Responses of C _{NA} and T to 1 ⁰ C decrease in cooling water temperature for a 15% change in the model parameter, k, for f=1× 10 ⁻⁷ and C=70.....	60

7.19 Response of boric acid concentration in Reactor I to 2.7 g/min step change in acid flow rate	65
7.20 Response of boric acid concentration in Reactor I to 2.7 g/min step change in acid flow rate.....	66
7.21 Response of boric acid concentration in Reactor II to 2.7 g/min step change in acid flow rate.....	66
7.22 Response of boric acid concentration in Reactor III to 2.7 g/min step change in acid flow rate.....	67
7.23 (a) Four CSTR's with inputs and outputs (b) The overall transfer function for four CSTR's	67
7.24 Response of boric acid concentration in Reactor IV to 2.7 g/min step change in acid flow rate obtained from approximated transfer function model for the whole system.....	69
7.25 Response of boric acid concentration in Reactor I to 1 g/min step change in colemanite flow rate	72
7.26 Response of boric acid concentration in Reactor II to 1 g/min step change in colemanite flow rate	72
7.27 Response of boric acid concentration in Reactor III to 1 g/min step change in colemanite flow rate	73
7.28 Response of boric acid concentration in Reactor IV to 1 g/min step change in colemanite flow rate	73
7.29 Response of boric acid concentration in reactor IV to 1 g/min step change in colemanite flow rate obtained from approximated transfer function model for the whole system.....	74
7.30 Change of controlled and manipulated variables wrt time for a 0.3 mol/l step change in the set point of boric acid concentration for $f= 1.00, 0.50, 0.10, 0.05$ and 0.02	76

7.31	Change of controlled and manipulated variables wrt time for a -10% disturbance change in the colemanite flow rate for $f= 1.00, 0.50, 0.10, 0.05$ and 0.02	76
7.32	Change of controlled and manipulated variables in the presence of upper controlled variable constraint wrt time for a 0.3 mol/l step change in the set point of boric acid concentration for $f=0.02$	77
7.33	Change of controlled and manipulated variables in the presence of lower manipulated variable constraint wrt time for a 0.3 mol/l step change in the set point of boric acid concentration for $f=0.02$	78
7.34	Change of controlled and manipulated variables in the presence of upper manipulated variable constraint wrt time for a 0.3 mol/l set point change in boric acid concentration for $f=0.02$	79
7.35	Change of controlled and manipulated variables in the presence of controlled, upper and lower manipulated variable constraint wrt time for a 0.3 mol/l set point change in boric acid concentration for $f=0.02$	80
7.36	Change of controlled and manipulated variables in the presence of lower controlled variable constraint wrt time for a 10% decrease in colemanite flow rate for $f=0.02$	80
7.37	Change of controlled and manipulated variables in the presence of lower manipulated variable constraint wrt time for a 10% decrease in colemanite flow rate for $f=0.02$	81
7.38	Change of controlled and manipulated variables wrt time for a 0.3 mol/l set point change in boric acid concentration when the plant is changed by -10%.....	82
7.39	Change of controlled and manipulated variables wrt time for a 10% decrease in colemanite flow rate when the plant is changed by -10%.....	82

7.40	Change of controlled and manipulated variables wrt time for a 0.3 mol/l step change in the set point of boric acid concentration for $f=1.00, 0.50, 0.10, 0.05$ and 0.02	84
7.41	Change of controlled and manipulated variables wrt time for a 10% decrease in the set point of boric acid concentration for actual and approximated transfer function model with $f=0.02$	84
7.42	Change of controlled and manipulated variables wrt time for a 10% decrease in colemanite flow rate for $f=1.00, 0.50, 0.10, 0.05$ and 0.02	85
7.43	Change of controlled and manipulated variables wrt time for 10% decrease in colemanite flow rate for actual and approximated transfer function model with $f=0.02$	86
7.44	Change of controlled and manipulated variables wrt time for a 0.3 mol/l set point change in boric acid concentration when the approximated plant is changed by -10%.....	87
7.45	Change of controlled and manipulated variables wrt time for a 10% decrease in colemanite flow rate when the approximated plant is changed by -10%.....	87
7.46	Change of controlled and manipulated variables wrt time for a 0.3 mol/l setpoint change of boric acid concentrations for different controllers.....	88
7.47	Change of controlled and manipulated variables wrt time for a 10% decrease in colemanite flow rate for different controllers.....	89
F.1	Cohen and Coon Model by Simulink.....	141
F.2	ITAE (PID) Model by Simulink.....	141

NOMENCLATURE

a	Step response coefficient
A	Dynamic matrix
C	Control horizon
C _p	Heat capacity (J/mol.K)
C _i	Concentration of species i (mol/l)
E	Closed loop prediction error
E'	Open loop prediction error
f	Ratio of diagonal elements of input and output weighting matrices
F	Flowrate (ml/min)
F _{cw}	Flowrate of cooling water (ml/min)
F _{EA}	Flowrate of ethyl acetate (ml/min)
F _N	Flowrate of sodium hydroxide (ml/min)
g	Gradient vector
G	Steady state gain matrix
h	Impulse response coefficient
H	Hessian matrix
H	Heat of reaction (J/mol)
I	Identity matrix
J	Objective function
k	Reaction rate constant (l/mol.min)
K _{MPC}	MPC gain
m	Vector of manipulated variables
M	Model horizon
N	Number of process inputs
P	Prediction horizon
Q	Heat flow to the reactor (J/min)

r	Setpoint
t	Time (min)
T	Temperature of the reactor (K)
T_{a1}	Inlet cooling water temperature (K)
T_{a2}	Outlet cooling water temperature (K)
T_{EA}	Inlet temperature of ethyl acetate (K)
T_N	Inlet temperature of sodium hydroxide (K)
u	Process input
U	Left singular vector of G
UA	Overall heat transfer coefficient times area (J/min.K)
V	Right singular vector of G
V	Volume of the reactor (l)
W_1	Weight of predicted error
W_2	Weight of the input changes

Greek Letters

ρ	Density (g/cm ³)
τ	Process time constant
Θ	Time delay
Σ	Singular values of G
λ	Diagonal element of weighing matrix
Δ	Increment

Subscripts

a1	Inlet cooling water
a2	Outlet cooling water
cw	Cooling Water
E	Ethanol
EA	Ethyl Acetate
N	Sodium Hydroxide
NA	Sodium Acetate
i	i^{th} sampling time
n	normalized value

Superscripts:

*	Corrected value in MPC
---	------------------------

$\hat{}$	Predicted value
T	Transpose
-1	Inverse

Abbreviations:

AMPC	Adaptive Model Predictive Control
AGPC	Adaptive Generalized Predictive Control
CARIMA	Controlled Auto Regressive Integrated Moving Average
CN	Condition Number
CSTR	Continuous Stirred Tank Reactor
DMC	Dynamic Matrix Control
EKF	Extended Kalman Filter
FIR	Finite Impulse Responses
GLC	Globally Linearized Control
GOFMPC	MPC Based on a Generalized Objective Function
GMC	Generic Model Control
GPC	Generalized Predictive Control
IAE	Integral of the Absolute Error
IMC	Internal Model Control
LMI	Linear Matrix Inequality
LMPC	Linear Model Predictive Control
LQI	Linear Quadratic Control with Integrator
MAC	Model Algorithmic Control
MPC	Model Predictive Controller
MPHC	Model Predictive Heuristic Control
NARX	Nonlinear Autoregressive Model with Exogenous Inputs
NC	Number of Components
NMPC	Nonlinear Model Predictive Control
PI	Proportional Integral
SMPC	Simplified Model Predictive Control
SVD	Singular Value Decomposition
QDMC	Quadratic Dynamic Matrix Control
QOFMPC	MPC Based on a Quadratic Objective Function
QP	Quadratic Programing

CHAPTER 1

INTRODUCTION

Reactors are one of the most major equipments in the chemical industries. Their controls in different levels are important for achieving high yields, rates and to reduce side products if possible.

The performance of the use of Model Predictive Controller (MPC) in reactors is investigated in this study. "MPC is the family of controllers in which there is a direct use of an explicit and separately identifiable model" (Prett and Garcia, 1988). MPC algorithm can be described shortly by a model that must be obtained off-line, an objective function, a reference trajectory to follow and the constraints (input/output) to apply. MPC is a user friendly and applicable technique for different industrial needs, where, the objective function, the model and optimization method are flexible. The advantages of MPC compared with many other control techniques can be listed as follows (Li et al., 1989):

- It can use step and impulse response data which can easily be obtained,
- It can handle input/output constraints directly,
- It gives satisfactory performance even with time delays and high nonlinearities,

- It can be used in multivariable format,
- It is robust in most cases,
- Implementation of the technique is simple,
- It can optimize over a trajectory,
- It can be used to control various processes, whether simple or complex ones.

In this study, two case studies are considered; a saponification reaction system and boric acid production system. In the saponification system, a CSTR is used. The system is simple to model theoretically. Thus, it is aimed to investigate for the MPC performance for a system which can easily be modeled theoretically. However, unknown parameters of the model are found experimentally at steady state conditions. Thus, a dynamic theoretical model is checked with dynamic experiments. As a result of a good match between experimental and model results, the developed model is used for designing MPC. A multi-input multi-output (MIMO)-MPC is used for the control of temperature of the reactor and sodium acetate concentration which is obtained from the reaction of sodium hydroxide and ethyl acetate in the CSTR. In the simulation studies, previously written software by Dokucu (2002) in Fortran and modified by Bahar (2003) in MATLAB is adopted for the control of the system in a MIMO structure.

The second case study is done in a boric acid production system where boric acid is produced by the reaction between colemanite and sulfuric acid in four CSTR's connected in series. The control of this system necessitates the design of a MIMO-MPC where the controlled variables must be the temperatures in the four reactors and boric acid concentration in the fourth reactor. However, it is planned to keep temperature constant in all the reactors due to the complexity

of the experimental system and the difficulty of performing experiments at different temperatures. Therefore, in the scope of this study only concentration of boric acid is considered as the controlled variable. Experiments are performed by giving step change to the manipulated variable and to the disturbance, and by obtaining the response of the boric acid concentration to obtain the process and disturbance transfer functions. The transfer functions are then used in the design of SISO-MPC.

The performances of the designed controllers are checked for setpoint tracking, disturbance rejection and robustness for the two systems.

CHAPTER 2

LITERATURE SURVEY

2.1 Model Predictive Control (MPC)

Model predictive control (MPC) technique started to be implemented in industrial applications practically since 1970's. The studies related with MPC initialized with Richalet et al. (1978) as Model Predictive Heuristic Control (MPHC) technique and named as Model Algorithmic Control (MAC). This strategy is constructed basing on three issues. The first is to represent the multivariable process to be controlled by its impulse response model. The model's inputs and outputs are updated according to the actual state of the process since it is used for on-line prediction. The second issue is to use reference trajectory for the closed-loop behavior of the plants. This trajectory is initiated on the actual output of the process and tends to approach the desired set point. The third issue is to compute the control variables in a heuristic way that, when applied to the model, they change outputs as close as possible to the desired reference trajectory.

Rouhani and Mehra et al. (1982) suggested mathematical issues for the utilization of model algorithmic control (MAC) analysis and defined the fundamental components of the control structure. They analyzed the stability

and the robustness of both of the deterministic and stochastic systems of SISO system. They verified analytically and experimentally that slowing down the reference trajectory strengthens the robustness of the control.

After the developments of MPHC and MAC, dynamic matrix control (DMC) was used as a new technique by Cutler and Ramaker in 1979. The characteristics of this technique when compared with previous ones are as follows; 1) step response model replacing the impulse response model, 2) quadratic performance objective function over a finite horizon is used, 3) future behavior of the plant is organized in accordance with the setpoint and optimal control inputs are computed to avoid least square problems.

In 1986, Garcia and Morshedi presented quadratic dynamic matrix control (QDMC) in which they concentrated on the associated variable constraints. They established the relationship between the input and output inequality constraints and the manipulated inputs by dynamic matrix. The QDMC algorithm enabled a satisfactory and robust control by maintaining the controlled variables within the constraints.

Clarke et al. (1987) proposed a new control algorithm called Generalized Predictive Control (GPC). This method was claimed to be applicable also to open loop unstable systems, non-minimum phase plants and poorly identified plants with unknown order or dead time. Controlled Auto Regressive Integrated Moving Average (CARIMA) model was used in order to model the disturbances by defining the developed process model in discrete time and by dividing disturbance by the differencing operator.

Lee and Sullivan et al. (1988) developed a generic model control (GMC) algorithm. The advantage of this method was that easy online implementation took place. Finally, various control strategies could be derived in the presence of suitable problem formulation and a reasonable selection of performance index.

Garcia et al. (1989) included in their papers some MPC algorithms such as Dynamic Matrix Control (DMC), Model Algorithmic Control (MAC) and Internal Model Control (IMC) and made their comparisons. They suggested that there is a significant advantage of MPC in terms of the overall operating objectives of the process industries which is the flexible constraint handling capability. They also investigated the applications of MPC to nonlinear systems and identified it is main attractions. It was concluded that in spite of not being inherently more or less robust than classical feedback, MPC can be adjusted more easily.

Riggs and Rhinehart et al. (1990) compared nonlinear internal model control (IMC) and generic model control (GMC) on a SISO exothermic CSTR and SISO heat exchanger. The advantage of choosing these systems was that, they could be easily adjusted so as to change process nonlinearity and process/model mismatch. They concluded that these nonlinear process model based control methods were relatively insensitive to process/model mismatch and have relatively wide tuning bands.

Sistu and Bequette et al. (1992) studied a comparison of globally linearizing control (GLC), a differential geometry based control, and nonlinear predictive control (NLPC), an optimization based technique, for temperature control of an exothermic continuous stirred tank reactor (CSTR). GLC linearize the output/input or the state/input closed loop nonlinear system. This technique was

only used on minimum phase systems, in which the inverse dynamics were stable. All state variables assumed to be measured for GLC. If there were unmeasured state variables, estimation techniques must be used. The results were obtained for considering perfect model, with measured and unmeasured disturbances, an uncertain model, and finally constraints on manipulated variable. For an unconstrained case, GLC gave same performance to NLMPC. However, NLMPC gave better performance than GLC considering constraints on manipulated variable.

Özgülşen et al. (1993) developed a nonlinear model predictive control (NMPC) strategy for controlling periodically forced processes. The system was a non-adiabatic CSTR where ethylene oxide was produced by catalytic oxidation of ethylene with air. Nonlinear autoregressive model with exogenous inputs (NARX) model of the forced CSTR was built by using an orthogonal forward regression estimator for off-line identification of the system and incorporated into NMPC algorithm. The effect of dead time on controller performance was not included in this study. The performance of the predictive controller was investigated considering unmeasured disturbances and parametric uncertainty, and gave good performance.

Lee et al. (1994) proposed a new control scheme, which consisted of an Adaptive Model Predictive Control (AMPC) and state feedback control, for unstable nonlinear processes. Then, the final control inputs were the summation of feedback outputs and the control actions of the AMPC. The control law of AMPC was similar to that of Dynamic Matrix Control (DMC) but the output prediction was obtained by ARMA models, which is very useful for model parameter identification, in AMPC. The advantages of this proposed method were easy

implementation to unstable nonlinear processes with robustness and simplicity of design. The performance of AMPC was tested by a jacketed continuous stirred tank reactor (CSTR) and two jacketed CSTRs in series with a separator and compared with Generalized Predictive Control (GPC) and Adaptive Generalized Predictive Control (AGPC). The results showed that AGPC gave good performance for good set-point tracking, in contrast GPC failed to overcome the effect of process change, and AMPC showed better stable control performance than the AGPC.

Afonso et al. (1996) investigated the performance of a receding horizon model predictive control (MPC) applied to a continuous stirred tank reactor (CSTR), where a pseudo zero order exothermic chemical reaction was simulated in order to control temperature and level of a CSTR. By making MPC algorithm formulation, the manipulated variables were calculated so as to minimize an objective function considered desired trajectories over the horizon. The control law was obtained at each iteration by the solution of quadratic program. The performance of receding horizon model predictive control applied in a CSTR was compared with PI controller. It can be said that MPC gave better performance than PI controller, operating in steady state or dynamically, despite both MPC and PI strategies showed the similar performance for level control.

Al-Ghazzawi et al. (2001) used the closed-loop prediction of the output and its sensitivity to the tuning parameters in order to establish an on-line tuning algorithm. Linear model predictive controllers (LMPC) based on finite impulse response (FIR) models were developed. It was not obligated that dynamic output constraints over the prediction horizon was utilized for the on-line optimization since hard dynamic output constraints were not made use of commercial MPC

software. Al-Ghazzawi developed analytical expressions for the sensitivity of the closed-loop response of MPC with respect to output and input weights of the objective function. Both of the control and prediction horizon were kept constant predetermined values by depending on conventional tuning guidelines. The performance of the proposed strategy was illustrated by using a linear model for a three product distillation column and a non-linear model for a CSTR. In CSTR, a linearized model was developed and converted to FIR to use it for MPC algorithm. The set point tracking, disturbance rejection and effect of modeling errors were considered, the performance of proposed method gave good results. There is also a comparison of the proposed on-line tuning method with an existing off-line tuning method. The off-line method had the control performance better than the proposed method. In addition to that, off-line method expressed a considerably high sluggish response in distillation column example and unstable response in the CSTR example.

Wu et al. (2001) studied linear matrix inequality (LMI) based robust MPC for a class of uncertain linear systems with time varying, linear fractional transformation (LFT) perturbations. This class of uncertain systems was utilized for modeling of nonlinear systems. An adequate state-feedback synthesis condition was developed and formulated as LMI optimization. Then, the control action could be calculated on-line. The stability of robust MPC was decided by the feasibility of the optimization problem. The performance of the robust MPC technique was implemented to an industrial CSTR with explicit input and output constraints for set point tracking without disturbance and disturbance rejection. According to simulation results, it was concluded that robust MPC technique was capable of incorporating model mismatch and constraints as well as stability guarantee.

Park et al. (2001) studied a linear matrix inequality (LMI)-based robust model predictive control (MPC) so as to control the monomer conversion and the weight-average molecular weight of polymer product in a CSTR for the polymerization of methyl methacrylate (MMA) with the polytopic uncertain model. The controller was designed to minimize an upper bound objective function subject to constraints on the control input and plant output. The controller performance was checked for two cases; SISO and MIMO. In the SISO system, the manipulated variable was the jacket inlet temperature and the controlled variable was the monomer conversion. In MIMO system, the manipulated variables were the jacket inlet temperature and the feed flow rate, the controlled variables were the monomer conversion and the weight average molecular weight. According to the simulation results, it can be shown that the LMI-based robust model predictive controller gave good performance for the property of continuous polymerization reactor and the robust stability was guaranteed. It can be concluded that LMI-based robust MPC was so applicable to polymerization processes.

Santos et al. (2001) implemented a Newton-type nonlinear model predictive control (NMPC) algorithm in a continuous stirred tank reactor (CSTR) to control the liquid level and temperature by manipulating the outlet of the reactor and coolant flow rate. NMPC utilized the nonlinear dynamic model in order to predict the effect of sequences of control steps on the controlled variables. It is very useful for processes operating at or near singular points which can't be captured by linear models. NMPC formulation involves integral action to eliminate the steady state offset due to disturbances and model mismatch. The set point changes operating at an unstable point, influence of saturation constraints and effects of unmeasured disturbances and model mismatch to the NMPC controller

were considered with experimental and simulation. Although comparison of simulated and experimental results gave good results, several sources of unmeasured disturbances and model mismatch were observed in this system. In spite of model mismatch and unmeasured disturbances, nonlinear model predictive controller performed well for setpoint tracking and disturbance rejection. In order to accomplish better performance, on-line parameter estimation can be considered.

Seki et al. (2001) developed a nonlinear model predictive control (NMPC) and applied it to an industrial polypropylene semi-batch reactor and a high density polyethylene (HDPE) continuous stirred tank reactor. The developed NMPC algorithm was composed of an optimal trajectory generator and a feedback tracking controller. Linear quadratic control with integrator (LQI) was solved with the successively linearized nonlinear process model. Optimal trajectory generator did not include process constraints, therefore, so as to satisfy the constraints, the feedback tracking controller, which solved a quadratic programming (QP) by using the local linearization of the model around the trajectory, was used. A state estimator was designed in order to provide offset-free responses of the outputs to constant set points. In semi-batch reactor, the NMPC prevented thermal runaway of the reactor temperature control because of the heat removal constraint. In the high density polyethylene reactor, the NMPC improved the performance of the grade changeover operation. In order to improve the performance of the control system, the optimal grade transition trajectories can be employed as the set points to the controlled variables.

Nagrath et al. (2002) developed a MPC-based cascade control approach and applied it to an open loop unstable jacketed exothermic CSTR, where the jacket temperature was used as a secondary measurement so as to see disturbances in jacket feed temperature and reactor feed flow rate. State estimation was accomplished by using a discrete dynamic Kalman filter, while a quadratic programming (QP)-based optimization for the predictive controller explicitly handled the manipulated variable constraints. The MPC-based cascade strategy was compared to classical cascade control, and it can be shown that MPC-based cascade method performed better than it in the presence of constraints on jacket flow rate.

Prasad et al. (2002) studied a multivariable multi-rate NMPC and applied it to styrene polymerization continuous stirred tank reactor in order to control number average molecular weights (NAMW) and polydispersity (PD). The NMPC algorithm included a multi-rate extended Kalman Filter (EKF) in order to handle state variable and parameter estimation. The multi-rate EKF was used for the design of the augmented disturbance model as estimator. Plant-model structural mismatch, parameter uncertainty and disturbances were considered for control simulations in open loop unsteady state CSTR. The results showed that the proposed multi-rate NMPC algorithm gave good performance compared with linear multi-rate and nonlinear single-rate MPC algorithms.

Cervantes et al. (2002) presented a NMPC based on a Wiener piecewise linear model. The L-N approach was used for Wiener model identification since it is straightforward and guarantees an accuracy of the static nonlinearity. In this approach, firstly the linear block is identified using a correlation technique and then, the intermediate signal is generated from the input signal and finally the

static non-linearity is estimated. A good representation of the inverse of the nonlinearity is necessary to implement NMPC algorithm. In order to identify it, direct identification, which is the identification of the nonlinear element of the model but switching inputs and outputs, is used. This proposed technique was illustrated by a SISO CSTR and a MIMO polymerization reactor and the response of NMPC and LMPC are compared. The results showed that the LMPC step response to a lower set point was slower but LMPC was faster for an upper step input.

Wang et al. (2003) proposed an alternative robust MPC design strategy for dealing with model-plant mismatch based on the use of a generalized objective function. The stability of the proposed controller might be verified by using a generalized positive definite objective function due to the conventional quadratic function. Under the circumstances of stability consideration, the infinite prediction horizon was selected. For the sake of feasibility, if the manipulated variable constraints are the only constraints, the optimization problem is always feasible. The optimization was infeasible by the state constraints. The performances of the proposed MPC based on a generalized objective function (GOFMPC), a conventional MPC based on quadratic objective function (QOFMPC) and the min-max algorithm were compared in CSTR. In this study, unconstrained case was also considered. All three controllers gave good performance in the presence of model-plant mismatch. If there is no model-plant mismatch, the response of GOFMPC was faster than that of min-max method, but slightly slower than that of QOFMPC.

Özkan et al. (2003) presented a MPC algorithm depend on multiple piecewise linear models and applied it to copolymerization of methyl methacrylate and

vinyl acetate in CSTR. The control approach based on a receding horizon scheme with the quadratic objective function consisting of a finite horizon cost and an infinite horizon cost. The finite horizon cost is composed of the future control outputs that force the system in order to move the desired operating point. The infinite horizon cost has an upper bound and takes the system to the desired steady-state operating point. The proposed control method gave good performance in the case of disturbance rejection.

2.2 Boric Acid Studies

Gürbüz (1998) looked at the solubility of colemanite in distilled water and boric acid solutions. In this study, boric acid concentrations were chosen as 7.5 %, 10 % and 20 % H_3BO_3 . According to the results obtained, dissolution of colemanite is a very fast reaction in both water and boric acid solutions, and all boric acid concentrations reached saturation during the first five minutes. Dissolution of colemanite in distilled water increased the pH of solution at a considerably high measure. On the other hand, in boric acid solutions the pH variation was observed to be less and seemed to be constant, that is, it is independent of solution concentration.

Tunç and Kocakerim (1998) investigated how reaction temperature, particle size, acid concentration, stirring rate and solid-liquid ratio affect dissolution kinetics of colemanite in H_2SO_4 solutions. It came out to be that rate of conversion increased by decreasing particle size and solid-liquid ratio, and by increasing both temperature and stirring rate. Also, conversion rate increased with increasing acid concentration up to 1 M, after exceeding the acid concentration of 1 M, it decreased.

Kalafatoğlu (2000) studied dissolution characteristics of Hisarcık colemanite in the presence of sulfuric acid. In this study, compositions of reaction solutions with different initial concentrations of sulfuric acid were obtained. Due to stoichiometric ratio, the calcium content showed a minimum at 5 % H₂SO₄ concentration. At the concentrations below this level, dissolved calcium was in equilibrium with colemanite, whereas above this level on account of the reaction conditions, because of supersaturation, high calcium solubilities were observed.

Çetin et al. (2001) studied the formation and growth kinetics of gypsum during dissolution of colemanite in sulfuric acid in a batch reactor by changing temperature (60-90°C), stirring rate (150-400 rpm), and initial concentrations of the reactant. The initial CaO / H₂SO₄ ratio was changed between 0.21-0.85 by keeping initial concentrations of sulfate at 0.623 mol/l and 0.85-3.41 by keeping initial concentrations of colemanite at 0.777 mol/l. Boric acid production reaction is a very fast reaction and almost all of the boric acid was produced in the first minute. It was found that dissolution of colemanite in sulfuric acid was independent of the stirring rate in the range of 150-400 rpm. Also, it was observed that boric acid concentration in the solution decreased by decreasing initial concentration of sulfuric acid.

CHAPTER 3

BORON

Boron is one of the most important elements in the world whose compounds are used in manufacture of glasses, porcelain, soaps, detergents, textile, nuclear reactors and material processing. Its color is black and it is a better semiconductor than a metal. It has a great affinity for oxygen. In nature, boron always occurs in the oxygenated state, mainly as borate. On account of this characteristic, boron is available as approximately 230 boron minerals, the principal of which are listed in Table 3.1.

Turkey has the largest share of known boron minerals. Borate producing countries with their corresponding minerals and reserves are presented in Table 3.2.

Table 3.1 Important boron minerals (Tübitak, 2002)

Mineral	Formula	B₂O₃, wt%
Colemanite	2CaO.3B ₂ O ₃ .5H ₂ O	50.8
Pandermite	4CaO.5B ₂ O ₃ .7H ₂ O	49.8
Hydroboracite	CaO.MgO.3B ₂ O ₃ .6H ₂ O	50.5
Datolite	Ca ₂ B ₄ Si ₂ O ₁₂ 2H ₂ O	26.7
Tinkal	Na ₂ O.2B ₂ O ₃ .10H ₂ O	36.5
Kernite	Na ₂ O.2B ₂ O ₃ .4H ₂ O	50.9
Ulexite	Na ₂ O.2CaO.5B ₂ O ₃ .16H ₂ O	43.0
Szaybelite	MgBO ₂ (OH)	41.4
Sassolite	B(OH) ₃	56.3

Table 3.2 Distribution of Boron Minerals (KIGEM, 1999)

Country	Principal Minerals	Reserves of B₂O₃, tons	%
Turkey	ulexite, colemanite, tinkal	803,000,000	63
United States	tinkal, kernite, colemanite ulexite	209,000,000	16,4
Russia	datolite, hydroboracite	136,000,000	10,7
Chile	ulexite	41,000,000	3,2
China	ascharite	36,000,000	2,8
Peru	ulexite	22,000,000	1,7
Bolivia		19,000,000	1,5
Argentina	tinkal, kernite, ulexite	9,000,000	0,7
Total		1,275,000,000	100

Tincal is mined in Kirka, colemanite in Emet, Bigadiç and Kestelek, and ulexide is mined in Bigadiç (Özbayoğlu et al., 1992).

3.1 Boric Acid

Boric acid can be found as a hydrate of boric oxide and exists both as a trihydrate, orthoboric acid (H_3BO_3) and monohydrate, metaboric acid (HBO_3). Only the more stable orthoboric acid form is commercially important and usually referred as boric acid.

Boric acid is widely used in glass, ceramic, nuclear power, electronic, medical and pharmaceutical industries.

3.1.1 Properties of Boric Acid

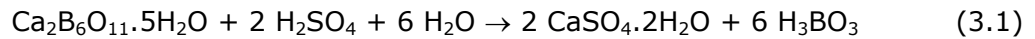
Boric acid is an odorless, white, crystalline, powdered material. It is soluble in hot water, alcohol and glycerin. The solubility of boric acid in water increases rapidly with temperature. The solubility of boric acid in water is increased by the addition of salts, such as KCl, KNO_3 , Na_2SO_4 , whereas the addition of LiCl, NaCl tends to lower the solubility. It behaves as a weak acid in aqueous solutions, pKa of 9.23 at 25°C. Also, it is volatile with steam.

Boric acid reacts with strong bases to form metaborate ion $B(OH)_4^-$ and with alcohols to form borate esters. Boric acid reacts with fluoride ion to form tetrafluoroboric acid $H(F_3BOH)$.

3.1.2 Boric Acid Production

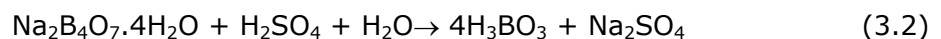
Tincal, kernite, colemanite and ulexide react with strong mineral acids to form boric acid.

In Turkey and Europe, boric acid is produced from crushed colemanite ore by reaction with sulfuric acid. In Bandırma boric acid plant, it is produced in a batch reactor. During calcinations, colemanite decrepitation takes place. Before adding sulfuric acid, ball milling leads to size reduction. The crushed colemanite and sulfuric acid are mixed at 95⁰C. By product gypsum particles and other insolubles are filtered and the hot mother liquor cooled to crystallize boric acid. The boric acid crystals are centrifuged and dried (Özbayoglu et al., 1992). The boric acid production from colemanite with sulfuric acid is as follows:



In order to increase the production rate of boric acid in Turkey, a new plant was constructed and started to operate in Emet, Kütahya in 2003. In this new plant, boric acid production is made by a continuously stirred tank reactor.

In the United States, boric acid is produced by reacting crushed kernite ore with sulfuric acid in recycled weak liquor at 100⁰C. Coarse gangue is separated by rake classifiers and fine particles are settled in a thickener. Boric acid crystallizes from strong liquor, saturated in sodium sulfate in continuous evaporative crystallizers. Crystals are filtered and washed with progressively weaker liquor in a countercurrent circuit. The final product is dried in rotary driers and screened for packaged (Kirk-Othmer, 1992). The reaction is as follows;



CHAPTER 4

MODEL PREDICTIVE CONTROL (MPC)

“Model predictive control refers to the class of control algorithms that compute a manipulated input profile by utilizing a process model to optimize an open loop performance objective subject to constraints over a future time horizon” (Rawling et al., 1993). Recently, the popularity of MPC has been increased for industrial applications and academic world. The reason is the ability of MPC designs to produce high performance control systems having capacity of operating without expert intervention for long durations.

4.1 MPC Strategy (Camacho and Bordons, 1999)

The strategy of MPC can be well understood from Figure 4.1. At the present time n , the future outputs ($y(n+k)$ for $k=1\dots P$) of the system over a prediction horizon (P), are predicted at each instant by using the model of the process, knowing values up to instant n (past inputs and outputs) and future inputs ($u(n), u(n+1), \dots, u(n+C)$) where C is the control horizon. In Figure 4.1, the past inputs ($u(n-k)$ for $k=1\dots M-1$) are expressed by solid lines and the future inputs ($u(n+k)$ for $k=1\dots C$) are shown by dashed lines. The set of future inputs which minimize the objective function are applied to the system. Only the first element

of the future input is applied to the process since a new measurement of the output can be present at the next sampling instant. This procedure is repeated for next sampling time with addition of the new measurements, this is called receding strategy.

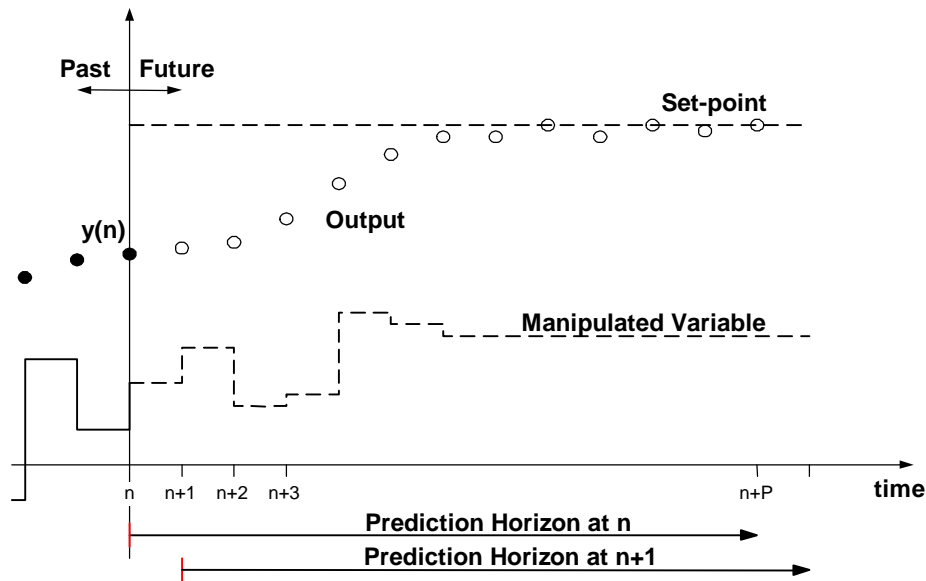


Figure 4.1: MPC Strategy (Garcia et al., 1989).

Figure 4.2 shows the basic structure of MPC. A model is used in order to predict the future outputs based on past inputs and outputs of the system. A comparison is made between the predicted output of the plant and the reference trajectory of it and the future errors of the plant are calculated at each time step. The optimizer calculates the best future inputs considering the objective function and the constraints. Only the first element of this optimal set is applied to the plant and the same procedure repeated at the next sampling time.

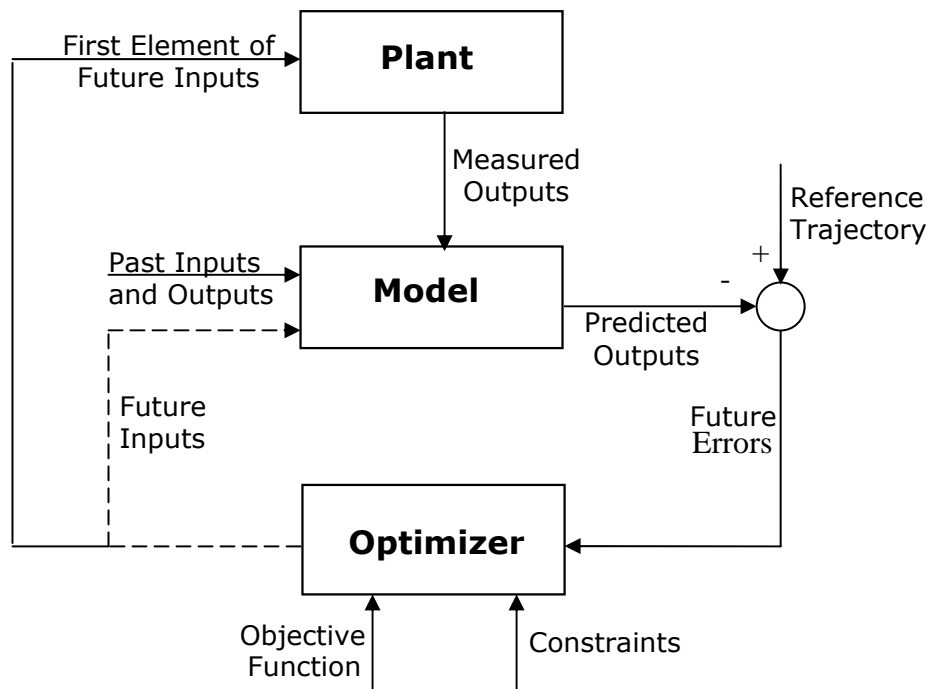


Figure 4.2: Basic Structure of MPC (Camacho and Bordons, 1999).

4.2 MPC Models

The process model is the most important characteristic of MPC. The model is very vital for ability to implement MPC. Many alternative categories of MPC models exist, namely, linear or nonlinear, continuous or discrete-time, distributed parameter or lumped parameter, deterministic or stochastic, input-output or state-space, frequency domain or time domain, first principles or black box.

In the MPC framework mostly used model is discrete step response (convolution) model. The advantage of step response model is that, the model coefficients can be obtained from input output information of the process without assuming a model structure and can be applicable for any linear system. Figure 4.3 shows an

open loop step response of a linear process. A unit step is given to the system so as to obtain a process step response model.

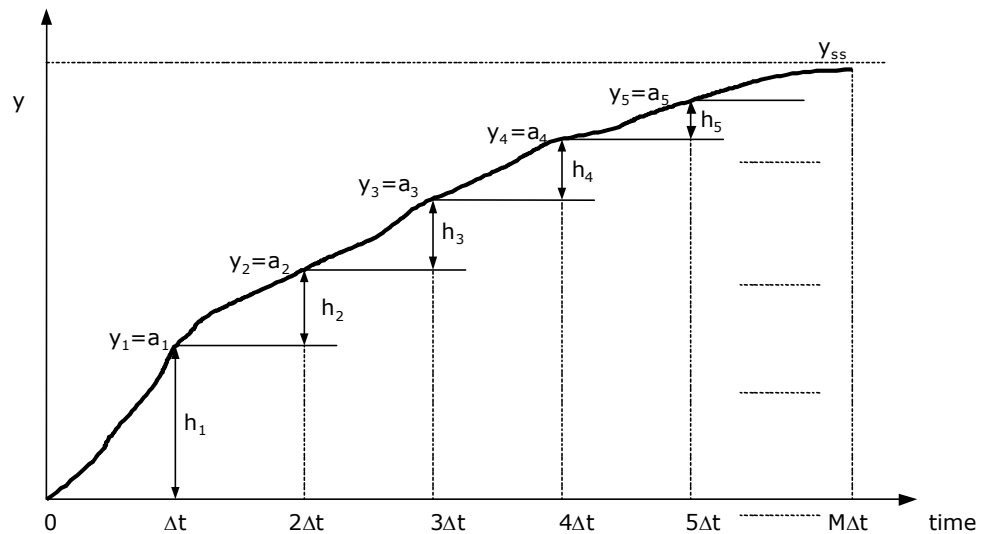


Figure 4.3: An Open Loop Step Response of a Linear Process (Seborg et al., 1989).

In Figure 4.3, the “ a_i ” values are the step response coefficients and “ h_i ” values are the impulse response coefficients. The step response coefficients are the summation of all impulse response coefficients as given in Equation (4.1) (Seborg et al., 1989).

$$a_i = \sum_{j=1}^i h_j \quad (4.1)$$

Using Equation (4.1) for M input changes to predict the system’s output, the discrete convolution model using step response coefficients can be written as in Equation (4.2).

$$\hat{y}_{n+1} = y_0 + \sum_{i=1}^M a_i \Delta u_{n+1-i} \quad (4.2)$$

Rearranging Equation (4.2) for impulse response coefficients, the discrete convolution model in recursive form can be obtained as in Equation (4.3).

$$\hat{y}_{n+1} = \hat{y}_n + \sum_{i=1}^M h_i \Delta u_{n+1-i} \quad (4.3)$$

Equation (4.3) is an open loop prediction, therefore there is no correction for model errors and disturbances that can have occurred at any previous time step.

y_{n+1}^* is used for the corrected prediction of \hat{y}_{n+1} . At any sampling time n , the difference between the actual value (y_n) and the predicted value (\hat{y}_n) is assumed to be constant for next sampling time. This prediction can be formulated as:

$$y_n - \hat{y}_n = y_{n+1}^* - \hat{y}_{n+1} \quad (4.4)$$

In order to obtain recursive form, Equation (4.4) is added to Equation (4.3), resulting in Equation (4.5)

$$y_{n+1}^* = y_n + \sum_{i=1}^M h_i \Delta u_{n+1-i} \quad (4.5)$$

Equation (4.5) is used only for single-step prediction. When the error comes out to be the same for the future times up to prediction horizon (P), the multistep predictions can be expressed as:

$$y_{n+j}^* = y_{n+j-1}^* + \sum_{i=1}^M h_i \Delta u_{n+j-i} \quad \text{for } j = 1, 2, \dots, P \text{ and if } j = 1, y_n^* = y_n \quad (4.6)$$

Equation (4.6) is the final form of multistep convolution model.

4.3 Multi-Input Multi-Output (MIMO) Predictive Control

The step response model is developed for single-input single-output (SISO) systems in Section 4.2. However, most chemical processes are multi-input multi-output systems. Therefore, the step response model for MIMO system with two inputs and two outputs will be developed by using principle of superposition shown in Equation (4.7),

$$y_{1,n+j}^* = y_{1,n+j-1}^* + \sum_{i=1}^M h_{11,i} \Delta u_{1,n+j-i} + \sum_{i=1}^M h_{12,i} \Delta u_{2,n+j-i}$$

$$y_{2,n+j}^* = y_{2,n+j-1}^* + \sum_{i=1}^M h_{21,i} \Delta u_{1,n+j-i} + \sum_{i=1}^M h_{22,i} \Delta u_{2,n+j-i} \quad \text{for } j = 1, 2, \dots, P \quad (4.7)$$

4.4 Objective Function

In order to follow a reference trajectory by the future outputs on the prediction horizon and at the same time to penalize the control effort, an objective function must be developed. A general objective function can be expressed as follows:

$$\min_{\Delta u(n) \dots \Delta u(n+C-1)} \sum_{i=1}^P \|W_1 [\hat{y}(n+i|n) - r(n+i)]\|^2 + \sum_{i=1}^C \|W_2 [\Delta u(n+i-1)]\|^2 \quad (4.8)$$

where the first term is the squared summation of the errors throughout the prediction horizon. The second term is the summation of control effort throughout control horizon. The positive-definite weighing matrices W_1 and W_2 ,

which are usually diagonal matrices, are used to penalize the output and control effort.

4.5 Controller Design

A model based controller can be designed basing on the step response model for MIMO systems. Initially, error must be defined since the controllers behave according to the error. Therefore, subtracting the predicted values from the corresponding setpoints (r), Equation (4.9) can be obtained as

$$\underbrace{\begin{bmatrix} r_1 - y_{1,n+1} \\ r_1 - y_{1,n+2} \\ \vdots \\ r_1 - y_{1,n+P} \\ r_2 - y_{2,n+1} \\ r_2 - y_{2,n+2} \\ \vdots \\ r_2 - y_{2,n+P} \end{bmatrix}}_{\hat{E}} = - \underbrace{\begin{bmatrix} A_{11} & A_{12} \\ A_{21} & A_{22} \end{bmatrix}}_A \underbrace{\begin{bmatrix} \Delta u_{1,n} \\ \Delta u_{1,n+1} \\ \vdots \\ \Delta u_{1,n+C-1} \\ \Delta u_{2,n} \\ \Delta u_{2,n+1} \\ \vdots \\ \Delta u_{2,n+C-1} \end{bmatrix}}_{\Delta u} + \underbrace{\begin{bmatrix} r_1 - y_{1,n} + P_{1,1} \\ r_1 - y_{1,n} + P_{1,2} \\ \vdots \\ r_1 - y_{1,n} + P_{1,P} \\ r_2 - y_{2,n} + P_{2,1} \\ r_2 - y_{2,n} + P_{2,2} \\ \vdots \\ r_2 - y_{2,n} + P_{2,P} \end{bmatrix}}_{\hat{E}'} \quad (4.9)$$

where A_{11} and A_{12} indicate the first manipulated input's effect on the first and second controlled outputs, A_{21} and A_{22} indicate the second manipulated input's effect on the first and second controlled outputs, and $P_{1,p}$ and $P_{2,p}$ are functions of " h_i " as given in Appendix A.

Equation (4.9) can be written in a simpler form as follows:

$$\hat{E} = -A \Delta u + \hat{E}' \quad (4.10)$$

There are two predicted error vectors, namely \hat{E} and \hat{E}' . The vector \hat{E} predicts the current and future errors assuming closed loop prediction whereas the vector is \hat{E}' an open loop prediction since it calculates the past control actions.

Thus, the resulting control law is obtained as follows; (see Appendix A for derivation)

$$\Delta u = (A^T W_1 A + W_2)^{-1} A^T W_1 \hat{E}' = K_{MPC} \hat{E}' \quad (4.11)$$

where K_{MPC} is the matrix of the feedback gains and it is constant for unconstrained control and evaluated only once.

If constraints are imposed on controller and system's output, the minimization becomes more complex due to adding the constraints to objective function. Therefore, the solution cannot be solved explicitly.

Manipulated variable, manipulated rate variable and the output variable constraints are shown in Equations (4.12)-(4.14).

$$u_{\min} \leq u(t) \leq u_{\max} \quad \forall t \quad (4.12)$$

$$\Delta u_{\min} \leq u(t) - u(t-1) \leq \Delta u_{\max} \quad \forall t \quad (4.13)$$

$$y_{\min} \leq y(t) \leq y_{\max} \quad \forall t \quad (4.14)$$

The objective function for quadratic program is as follows:

$$J[\Delta u] = \frac{1}{2} \Delta u^T H \Delta u - g^T \Delta u \quad (4.15)$$

$$\begin{aligned} \text{subject to } C_1 \Delta u &= c_1 \\ C_2 \Delta u &\geq c_2 \end{aligned} \quad (4.16)$$

where H is QP Hessian matrix and g is QP gradient vector. The solution of Equation (4.15) at each sampling time will produce an optimal set satisfying constraints. QP Hessian matrix and QP gradient vector are written as:

$$H = A^T W_1 A + W_2 \quad (4.17)$$

$$g = A^T W_1 E' \quad (4.18)$$

In Equation (4.17), H is fixed at all times. Therefore, a parametric QP algorithm is preferred rather than an algorithm that searches for the minimum in order to reduce the computation time. Hessian matrix is the second derivative and gradient vector is the first derivative. The quadratic dynamic matrix control (QDMC) uses quadratic objective function and minimizes the objective function with quadratic programming algorithm in order to find the optimal set of the future input moves. While formulating the constraints for QP algorithm, the dynamic matrix formulation are preserved.

4.6 Tuning the MPC

The tuning parameters for MPC are the model horizon (M), control horizon (C), prediction horizon (P), weighting matrices for predicted errors (λ_1) and control moves (λ_2) and sampling period (Δt).

The model horizon, M , should be selected to be equal to 99% of the settling time. The control horizon, C , is used in the optimization calculations in order to decrease the predicted errors. It can be selected as the 60% of the open loop settling time. Too large value of C causes an excessive control action whereas a smaller values of C leads to a robust controller which is insensitive to model errors. Prediction horizon, P , which is used as tuning parameter (Maurath *et al.*,1988), is used in the optimization calculations. Increasing P results in more conservative control action but also increases the computational effort. P is chosen as 85% of model horizon (Camacho and Bordons, 1999). The weighting matrix for predicted errors λ_1 is usually selected as identity matrix, I , and the weighting matrix for control moves is chosen as $f \times I$, where f is a scalar design parameter. Larger values of f penalize the control actions more, therefore gives less vigorous control. On the other hand, if the value of f is equal to zero, the controller gains are very sensitive to control horizon C . In order not to lose the important dynamic information, the sampling period (Δt) should be small. However, when the sampling period is too small, model horizon M must be very large, which is not desirable condition (Seborg *et al.*,1989).

CHAPTER 5

CASE STUDY I: SAPONIFICATION REACTION IN CSTR

The MPC methodology explained in Chapter 4 is used in the temperature and product concentration control of saponification reaction in CSTR.

The CSTR is used for an exothermic, irreversible reaction of ethyl acetate (EtOAc) and sodium hydroxide (NaOH) in an aqueous medium to produce sodium acetate (NaOAc) and ethanol (EtOH). The reaction is written as



The experimental set-up and experimental procedure together with the model of the chemical reactor and description of the simulation program will be given below.

5.1 Experimental

5.1.1 Experimental Set-up

The experimental set-up shown in Figure 5.1 is composed of an Armfield CSTR and a bench-mounted main frame carrying a PVC tank divided into two sections fitted with drain taps. Feed liquids are supplied by means of two displacement pumps through two control valves. Liquids within the reactor are mixed by a motor driven stirrer and there is a baffle to obtain homogeneous mixture without vortex formation. Cooling water, the temperature of which is measured by a thermocouple and monitored on the panel, is circulated through a stainless steel coil immersed in the reactor. The system is equipped with a temperature controller.

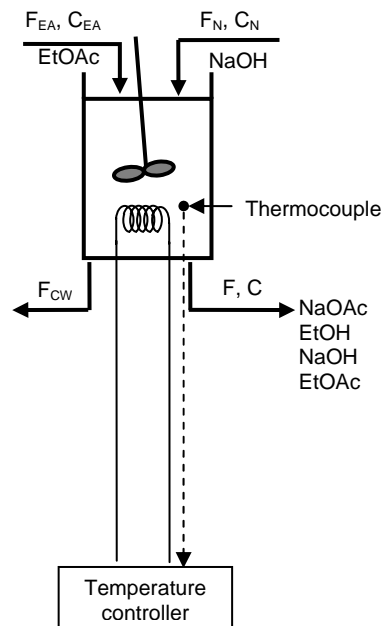


Figure 5.1: Experimental Set-up of Saponification System.

5.1.2 Experimental Procedure

In the experiments, 0.1 M NaOH, 0.1 M EtOAc are used as reactants, where 0.1 M HCl is used to stop the reaction and phenolphthalein is used for titration indicator.

Before starting the experiment, the calibrations of rotameters are done for NaOH and EtOAc separately. The temperature, stirring rate and equal molar flow rates of NaOH and EtOAc are adjusted to 30°C, 90 rpm and 40 ml/min, respectively. The reactants are supplied to the reactor from two feed tanks. The samples can only be taken after reaching the desired level in the CSTR constant volume, 1.24 l. The system is operated to reach the steady state condition while samples are taken every two minutes. Then, the flow rate of ethyl acetate is increased from 40 ml/min to 44 ml/min by giving +10% step change, and the flow rate of other reactant NaOH is kept constant.

The samples of 10 ml are taken from the outlet for analyzing concentrations. The concentration analysis is done by adding 10 ml HCl solution to 10 ml sample immediately. After it is withdrawn, phenol phthalein is used as an indicator. The samples later are titrated with 0.1 M NaOH in order to obtain un-reacted amount of NaOH.

5.2 Model of the Chemical Reactor

The model of the CSTR is developed from material and energy balances. The assumptions are made as follows;

1. Densities and heat capacities of all components are assumed to be constant and equal to that of water due to small fractions of components,

2. The exit coolant temperature is assumed to be 20°C when the coolant inlet temperature is 18°C and the reactor temperature is 30°C assuming a 10°C temperature difference between the reactor and exit coolant temperature,
3. A quasi steady state is assumed for energy balance on heat exchanger and accumulation term is neglected.

Overall mass balance over reactor can be written as

$$\frac{dV}{dt} = F_N + F_{EA} - F_0 \quad (5.2)$$

From Equation (5.2) at constant volume, the outlet flow rate is

$$F_0 = F_N + F_{EA} \quad (5.3)$$

Mass balances of components in the reactor are

NaOH balance:

$$V \frac{dC_N}{dt} = F_N C_{N1} - (F_N + F_{EA}) C_N + r_N V \quad (5.4)$$

EtOAc balance:

$$V \frac{dC_{EA}}{dt} = F_{EA} C_{EA1} - (F_N + F_{EA}) C_{EA} + r_{EA} V \quad (5.5)$$

NaOAc balance:

$$V \frac{dC_{NA}}{dt} = -(F_N + F_{EA}) C_{NA} + r_{NA} V \quad (5.6)$$

EtOH balance:

$$V \frac{dC_E}{dt} = -(F_N + F_{EA}) C_E + r_E V \quad (5.7)$$

where

$$r_N = r_{EA} = -r_{NA} = -r_E = -k C_N C_{EA} \quad (5.8)$$

The energy balance around the reactor is written as

$$\begin{aligned} & \left[V (C_N C_{pN} + C_{EA} C_{pEA} + C_{NA} C_{pNA} + C_E C_{pE}) \right] \frac{dT}{dt} = F_N C_{N1} C_{pN} T_N \\ & + F_{EA} C_{EA1} C_{pEA} T_{EA} - (F_N + F_{EA}) (C_N C_{pN} + C_{EA} C_{pEA} + C_{NA} C_{pNA} + C_E C_{pE}) T \\ & + \Delta H_{rxn} r_N V + \dot{Q} \end{aligned} \quad (5.9)$$

The energy balance on heat exchanger (Fogler, 1999) is

$$\dot{m}_c C_{p_{cw}} T_{a1} - \dot{m}_c C_{p_{cw}} T_{a2} - \frac{UA(T_{a1} - T_{a2})}{\ln[(T - T_{a1})/(T - T_{a2})]} = 0 \quad (5.10)$$

where

$$\dot{m}_c = \frac{F_{cw} \rho_w}{MW} \quad (5.11)$$

Simplifying Equation (5.10),

$$\dot{Q} = \dot{m}_c C_{p_{cw}} (T_{a1} - T_{a2}) = \frac{UA(T_{a1} - T_{a2})}{\ln[(T - T_{a1})/(T - T_{a2})]} \quad (5.12)$$

Solving Equation (5.12) for the exit temperature of the coolant water,

$$T_{a2} = T - (T - T_{a1}) \exp\left(\frac{-UA}{\dot{m}_c C_{p_{cw}}}\right) \quad (5.13)$$

Solving for the heat transfer rate, \dot{Q} , using Equation (5.12) and (5.13), Equation (5.14) is attained as

$$\dot{Q} = \dot{m}_c C_{p_{cw}} \left\{ (T_{a1} - T) \left[1 - \exp\left(\frac{-UA}{\dot{m}_c C_{p_{cw}}}\right) \right] \right\} \quad (5.14)$$

where UA and \dot{m} are unknown and must be evaluated using the experimental data.

Then, the energy balance on reactor is obtained by using Equation (5.14) in Equation (5.9) as follows

$$\begin{aligned} & \left[V (C_N C_{p_N} + C_{EA} C_{p_{EA}} + C_{NA} C_{p_{NA}} + C_E C_{p_E}) \right] \frac{dT}{dt} = F_N C_{N1} C_{p_N} T_N + F_{EA} C_{EA1} C_{p_{EA}} T_{EA} \\ & - (F_N + F_{EA}) (C_N C_{p_N} + C_{EA} C_{p_{EA}} + C_{NA} C_{p_{NA}} + C_E C_{p_E}) T \\ & + \Delta H_{rxn} r_N V + \dot{m}_c C_{p_{cw}} \left\{ (T_{a1} - T) \left[1 - \exp\left(\frac{-UA}{\dot{m}_c C_{p_{cw}}}\right) \right] \right\} \end{aligned} \quad (5.15)$$

The enthalpies and heat capacities of components are obtained from literature (Perry's Chemical Engineering Handbook, 1980). The reaction rate constant, k , is taken from Balland et al. (2000). Cooling water flow rate, F_{cw} , overall heat transfer coefficient times transfer area, UA , are calculated by using the Equations (5.9), (5.12) and (5.13) at steady state condition while concentrations of products and reactants are measured during the experiment. The calculated values of F_{cw} and UA are given in Table 5.1. Model of the reactor is written in MATLAB by using Equations (5.2)-(5.7) and (5.15). Table 5.1 shows the operating, assumed and calculated data. Thermodynamic and kinetic properties are given in Table B.3.

Table 5.1: Operating Conditions and Calculated Parameters

Parameters	Values
F_N	40 ml/min
F_{EA}	40 ml/min
F_{cw} (calculated)	24 ml/min
V_i	0.04 l
C_{N1}	0.1 M
C_{EA1}	0.1 M
C_{Ni}	0.05 M
C_{EAi}	0.05 M
C_{NAi}	0
C_{Ei}	0
T_N	298.15 K
T_{EA}	298.15 K
T_{a1}	291.15 K
T_{a2} (assumed)	293.15 K
UA (calculated)	18.3 J/min.K

5.3 Control Studies

The controlled variables of the system are considered as sodium acetate concentration (C_{NA}) and temperature of the reactor (T) whereas the manipulated variables are selected as ethyl acetate flow rate (F_{EA}) and cooling water flow rate (F_{CW}). A change in a manipulated variable affects both of the controlled variables showing MIMO structure is used. Moreover, inputs such as sodium hydroxide flow rate (F_N) and cooling water temperature (T_{CW}) also affect the controlled variables. They are considered as disturbances. The block diagram of the system to be used in control studies is shown in Figure 5.2.

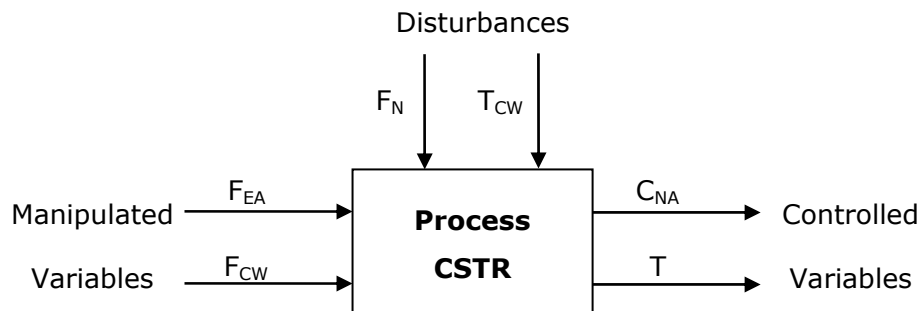


Figure 5.2: Saponification Reactor System.

CHAPTER 6

CASE STUDY II: BORIC ACID PRODUCTION FROM COLEMANITE AND SULFURIC ACID IN CSTR

In this case study, four continuously stirred tank reactors connected in series are used to obtain boric acid by the reaction between colemanite and sulfuric acid as follows:



This chapter is focused on the description of the experimental set-up, the variables of the system and the experimental studies.

6.1 Description of the Experimental Set-up

The boric acid production system which is constructed by Çakal (2004) is shown in Figure 6.1. There are four CSTR's in the reactor system, a liquid feed tank, a colemanite feeder and a filtration unit. Temperatures of all reactors are kept constant. Detailed information about experimental set-up can be found in Çakal (2004).

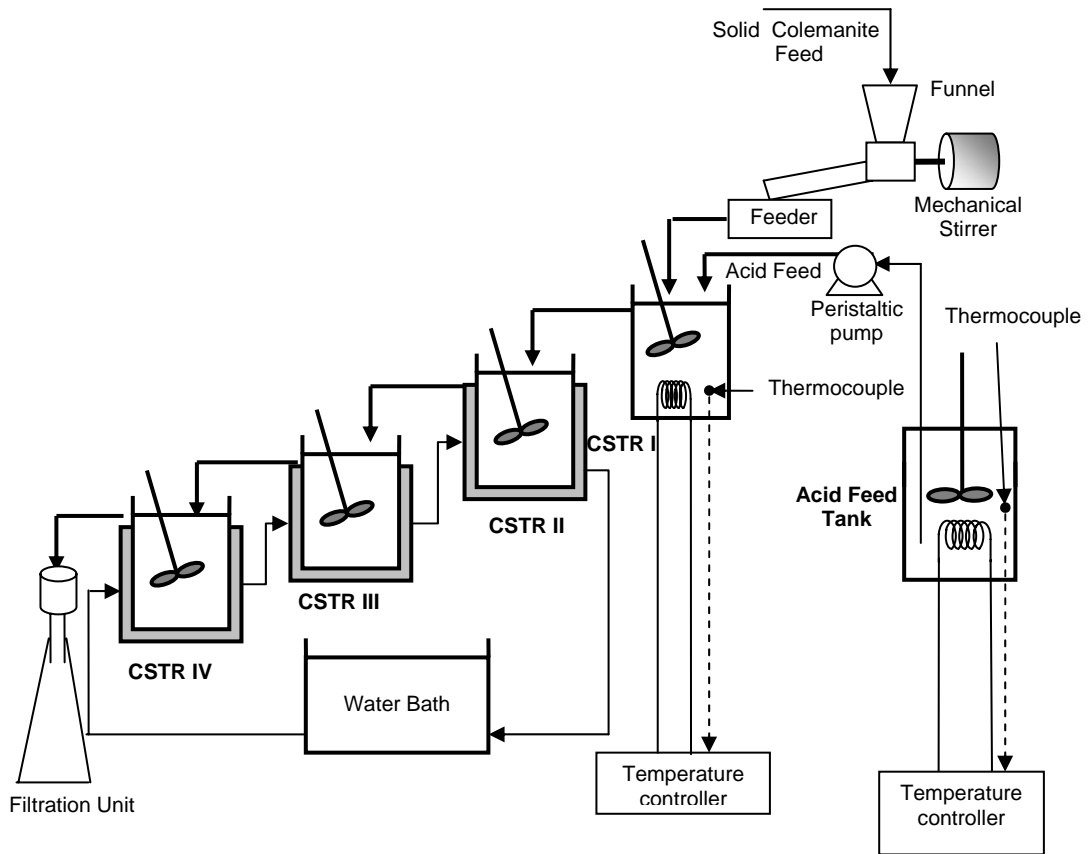


Figure 6.1: Experimental Set-up of Boric Acid Production System.

6.2 The Variables of the System

The aim of this case study is to control the boric acid concentration in the fourth reactor obtained from the reaction between colemanite with sulfuric acid. The controlled variables of the system can be considered as boric acid concentration (C_B) and temperature of the reactors (T). The block diagram of the system is shown in Figure 6.2. As it is well known, there is a strong interaction between concentration and temperature. Therefore, while controlling the boric acid concentration, temperature of the reactors must also be controlled. Heat input, Q , can be considered as a manipulated variable for controlling temperature of the reactors. However, in this study due to the complexity of the experimental system and the difficulty of performing experiments with changing temperature,

it is planned to keep temperature constant in the process and to model and design a controller only for the control of boric acid concentration in the fourth reactor. Thus, the temperature of the first reactor is controlled by a temperature controller and in the other three reactors; hot water supplied from a constant temperature water bath is circulated through their jackets to keep temperature constant.

The boric acid concentration is a function of the acid feed flow rate (F_A) and colemanite flow rate (F_C). However, flow rate of colemanite cannot be fixed continuously as a constant value, it considered as a disturbance to the system. Thus, acid feed flow rate is chosen as manipulated variable in order to control the boric acid concentration.

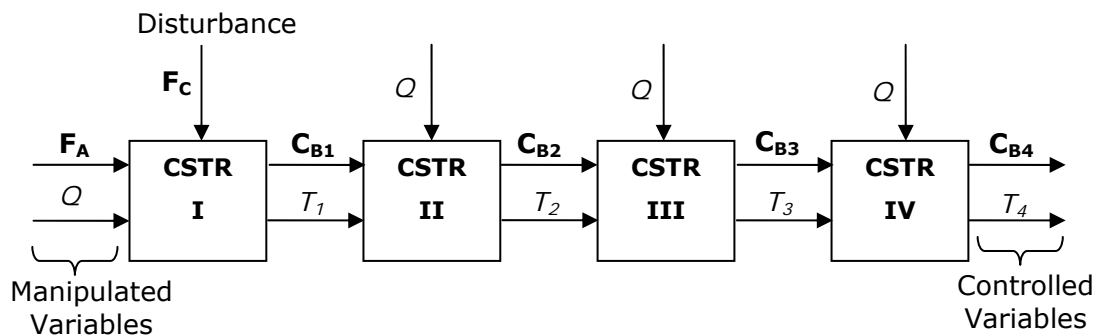


Figure 6.2: Block Diagram of the Boric Acid Production System.

6.3 Experimental Studies

Experiments are performed by giving a step change to the manipulated variable and to the disturbance after reaching the steady state condition, and by obtaining the response of the boric acid concentration to obtain the transfer functions for the process and disturbance.

6.3.1 Dynamic Experiments-Step Change in Acid Feed Flow Rate

The experiments to obtain response data for a change in the acid feed flow rate are performed by two runs. In the first run, the flow rates of colemanite and acid feed are chosen to be 5 g/min and 48.5 g/min respectively, giving $\text{CaO}/\text{SO}_4^{2-}$ molar ratio as 1 for -250 μm size of colemanite. After reaching the steady state condition, the acid feed flow rate is increased from 48.5 g/min to 50.9 g/min reducing the $\text{CaO}/\text{SO}_4^{2-}$ molar ratio to 0.94. In run II, the flow rates of colemanite and acid feed are chosen to be 10 g/min and 70 g/min respectively, giving $\text{CaO}/\text{SO}_4^{2-}$ molar ratio as 1.38 for -250 μm size of colemanite. The flow rate of acid feed is increased from 70 g/min to 72.7 g/min reducing $\text{CaO}/\text{SO}_4^{2-}$ molar ratio was 1.32. The samples from each reactor are collected in 25 min intervals. Boric acid concentrations are calculated by using Equation (G.11).

6.3.2 Dynamic Experiments-Step Change in Colemanite Flow Rate

In addition to acid flow rate, the experiments are done to collect response data for giving a step change in colemanite flow rate from 10 g/min to 11 g/min. In run III, the initial flow rates of colemanite and acid feed are selected to be 10 g/min and 70 g/min respectively giving $\text{CaO}/\text{SO}_4^{2-}$ molar ratio as 1.27 for -150 μm size of colemanite. After giving the step input to the flow rate of colemanite from 10 to 11 g/min as a result $\text{CaO}/\text{SO}_4^{2-}$ ratio is increased to 1.37. In run IV, initially the flow rates of colemanite and acid feed are selected to be 10 g/min and 90 g/min respectively giving $\text{CaO}/\text{SO}_4^{2-}$ molar ratio as 1.00 for -150 μm size of colemanite. After giving the step input to flow rate of colemanite, $\text{CaO}/\text{SO}_4^{2-}$ ratio is increased to 1.09. The samples from each reactor are taken in 25 min intervals.

CHAPTER 7

RESULTS AND DISCUSSIONS

The performance of MPC used to control two different CSTR's is investigated. In the two case studies, the modeling and control studies of saponification reaction in CSTR and of boric acid production by the reaction of colemanite and sulfuric acid in CSTR are studied both experimentally and theoretically. The results of both studies will be given below.

7.1 Case Study I: Saponification Reaction in CSTR

7.1.1 Model Verification

As stated before, the experiments are done to obtain steady state data from the reaction system and these are compared with the model outputs to find the unknown parameters (F_{cw} and UA) of the model. These calculated values are used in the unsteady state modeling studies. The experimental (Table B.1) and modeling results are shown in Figure 7.1 at the same flow rates of sodium hydroxide and ethyl acetate as 40 ml/min and at 30°C until steady state is reached. After reaching the steady state condition, the system is disturbed by +10% step input in EtOAc flow rate, while keeping the NaOH flow rate constant

and the experimental (Table B.2) and theoretical findings are shown in Figure 7.2. It can be seen from Figures 7.1 and 7.2 that there is a good match between experimental and modeling results prevailing the developed model in the design of the MPC.

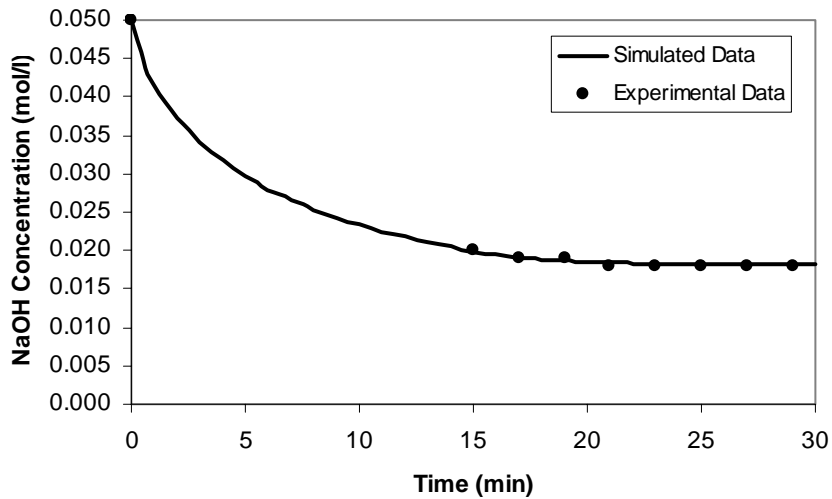


Figure 7.1: Experimental and Simulated Data for $F_N=F_{EA}=40$ ml/min at 30°C .

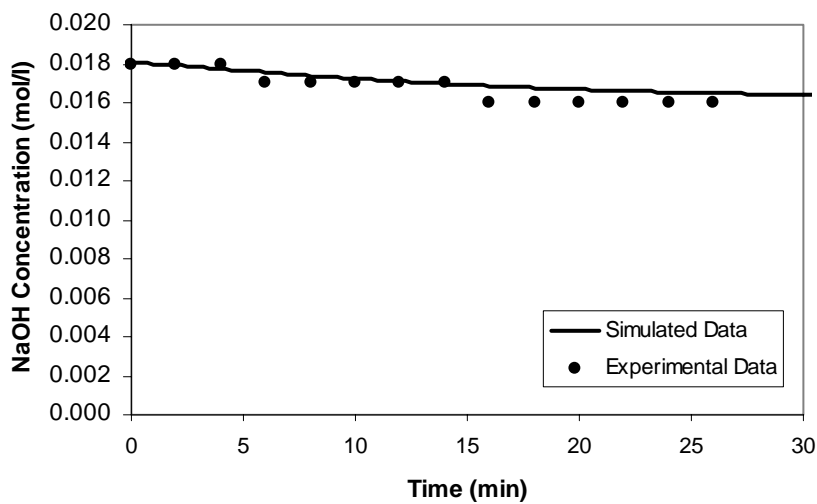


Figure 7.2: Experimental and Simulated Data for +10% step input to $F_{EA}=44$ ml/min and $F_N=40$ ml/min at 30°C .

7.1.2 Calculation of Step Response Coefficients for MPC

In this study, step response model is used for MPC design. In order to get coefficients of step response model, it is necessary to obtain the open loop responses of controlled variables by giving unit step changes to the manipulated variables. The open loop responses of controlled variables, sodium acetate concentration (C_{NA}) and reactor temperature (T), are shown in Figures 7.3 and 7.4 for step input changes in the manipulated variables, ethyl acetate flow rate and cooling water flow rate, respectively.

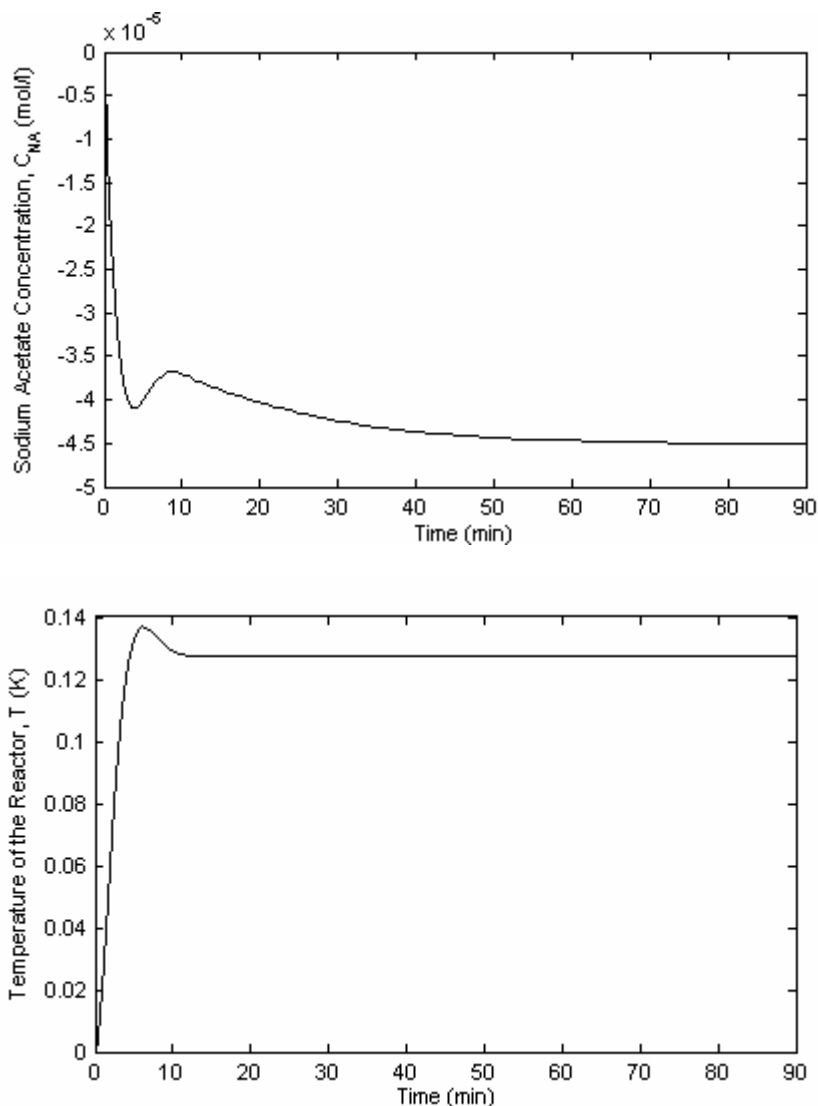


Figure 7.3: Open loop responses of sodium acetate concentration and reactor temperature to unit step change in ethyl acetate flow rate.

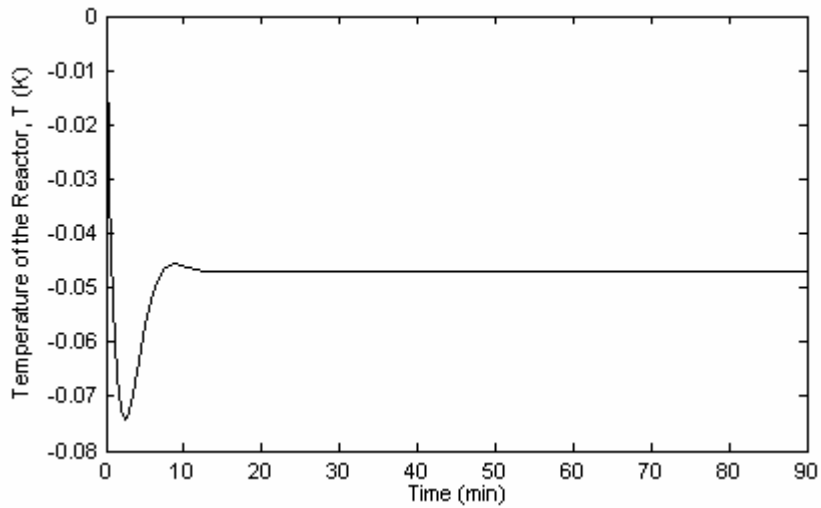
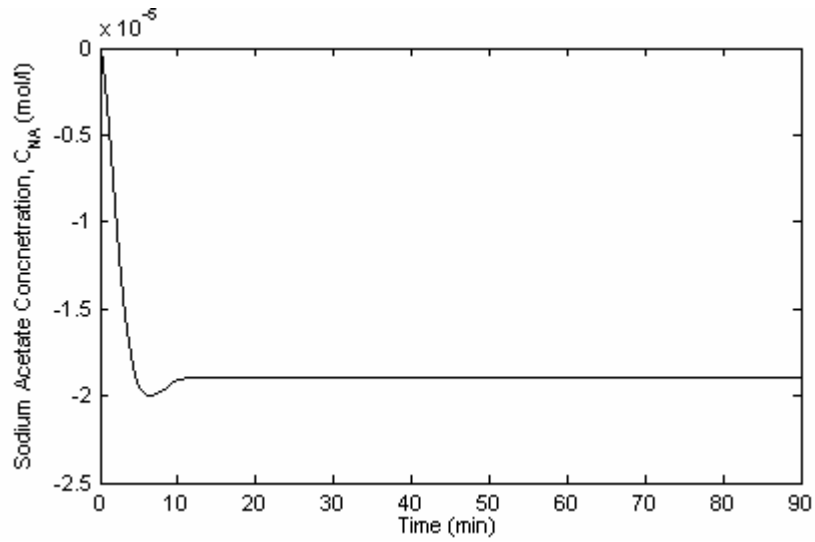


Figure 7.4: Open loop response of sodium acetate concentration and reactor temperature to unit step change in cooling water flow rate.

7.1.3 Pairing Between Controlled and Manipulated Variables

In order to determine the interactions between controlled and manipulated variables of the system and to determine the coupling between variables, Singular Value Decomposition (SVD) method must be used. The short explanation of the SVD method is given in Appendix C.

The steady state gain matrix, G , is obtained from positive unit step changes in both of ethyl acetate and cooling water flow rates. G matrix includes the ratio of the deviations of the output divided by steady state value and the deviations of input divided by steady state value. G is found as

$$\begin{bmatrix} C_{NA} \\ T \end{bmatrix} = \underbrace{\begin{bmatrix} -0.0565 & -0.0143 \\ 0.0169 & -0.0037 \end{bmatrix}}_G \begin{bmatrix} F_{EA} \\ F_{CW} \end{bmatrix} \quad (7.3)$$

Then, U , Σ and V^T are determined by using MATLAB as in (7.4).

$$G = \underbrace{\begin{bmatrix} -0.9654 & 0.2606 \\ 0.2606 & 0.9654 \end{bmatrix}}_U \underbrace{\begin{bmatrix} 0.0603 & 0 \\ 0 & 0.0075 \end{bmatrix}}_\Sigma \underbrace{\begin{bmatrix} 0.9771 & 0.2126 \\ 0.2126 & -0.9771 \end{bmatrix}}_{V^T} \quad (7.4)$$

Largest vector component of column U_1 , C_{NA} , is paired with largest vector component of column V_1 , F_{EA} and largest vector component of column U_2 , T , is paired with largest vector component of column V_2 , F_{cw} .

The condition number is calculated as 8 from Equation (7.2), and the small condition number result indicates good conditioning. Therefore, the SISO control is possible for the pairing between concentration of sodium acetate (C_{NA}) and flow rate of ethyl acetate (F_{EA}), and between temperature of reactor (T) and flow

rate of cooling water (F_{cw}). Since there is a strong interaction between temperature and concentration, MIMO-MPC is also designed and simulated.

7.1.4 Design of SISO-MPC

From the SVD analysis it can be concluded that, concentration of sodium acetate must be controlled by manipulating flow rate of ethyl acetate and temperature of reactor (T) must be controlled by manipulating cooling water flow rate (F_{cw}). The controllers are tested by performing simulations using the MATLAB program (Appendix D) which is composed of a model of the chemical reactor and MPC algorithm which was previously written by Dokucu (2002) in FORTRAN and modified by Bahar (2003) in MATLAB.

In the control loop for sodium acetate concentration, the 99% completion of open loop response of sodium acetate concentration for a unit step change of ethyl acetate flow rate takes place in 58 min time as can be observed from Figure 7.3. Thus, the model horizon (M) is found as 116 by dividing 99% completion time by the controller sampling time of 0.5 min. The prediction horizon (P) is kept constant at 85% of the model horizon as 99. In the second loop for control temperature of the reactor, the model horizon M is found as 24 from Figure 7.4 and prediction horizon P is kept constant at 20. In these two SISO-MPC controllers, the tuning parameters are the control horizon, C, and the $f(\lambda_2/\lambda_1)$ values.

7.1.4.1 SISO-MPC Performance in Set Point Tracking

The two SISO-MPC performances are tested for set-point tracking. The effect of f values and control horizon C are analyzed. The integral absolute error (IAE) scores are evaluated for each controlled output. The set point of sodium acetate concentration (C_{NA}) is changed as magnitude of -2% C_{NA} at 35^{th} min and magnitude of $+2\%$ C_{NA} at 105^{th} min consecutively while keeping reactor temperature constant. The performance of SISO-MPC is shown in Figure 7.5 for different f values, 1×10^{-5} , 1×10^{-6} and 1×10^{-7} and control horizon C is taken as 70.

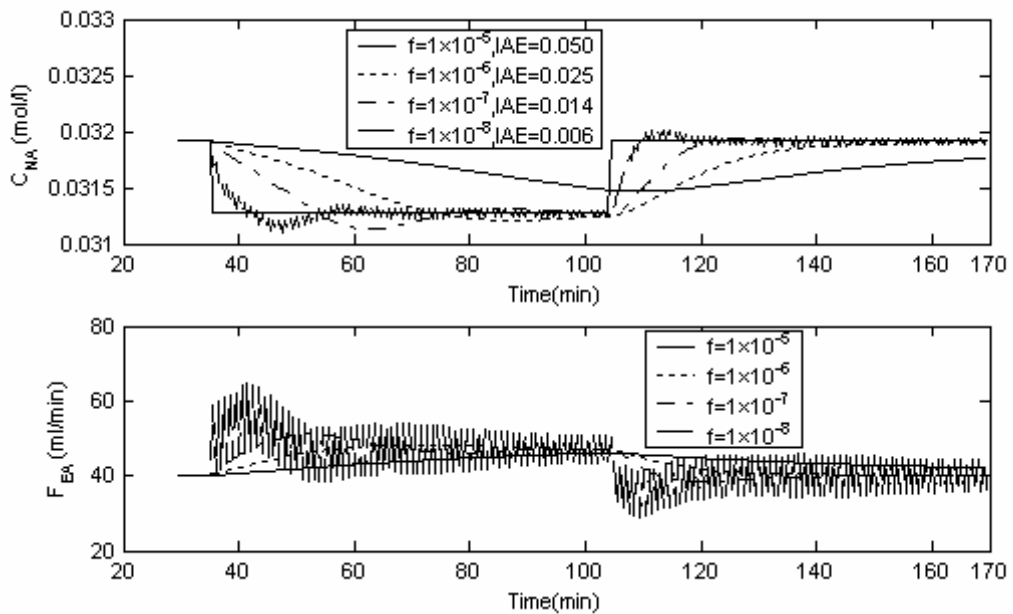


Figure 7.5: Response of C_{NA} to -2% decrease in the set point of C_{NA} followed by $+2\%$ increase in set point of C_{NA} for $f= 1 \times 10^{-5}$, 1×10^{-6} , 1×10^{-7} and 1×10^{-8} with $C=70$.

It can be seen from Figure 7.5 that, there is offset in the response for $f=1 \times 10^{-5}$ whereas for the smallest f value, 1×10^{-8} , sodium acetate concentration reaches the new set point with least response time and IAE score. However, as can be seen from Figure 7.5, the response is highly oscillatory. Therefore, the best f value is chosen as 1×10^{-7} .

In order to observe the effect of control horizon (C), the controller performance is tested with different C values, 70, 30 and 5 with $f=1 \times 10^{-7}$ as shown in Figure 7.6. Small control horizon, $C=5$, give better performance than others due to small response time and less IAE score. The responses of $C=70$ or $C=30$ are almost the same.

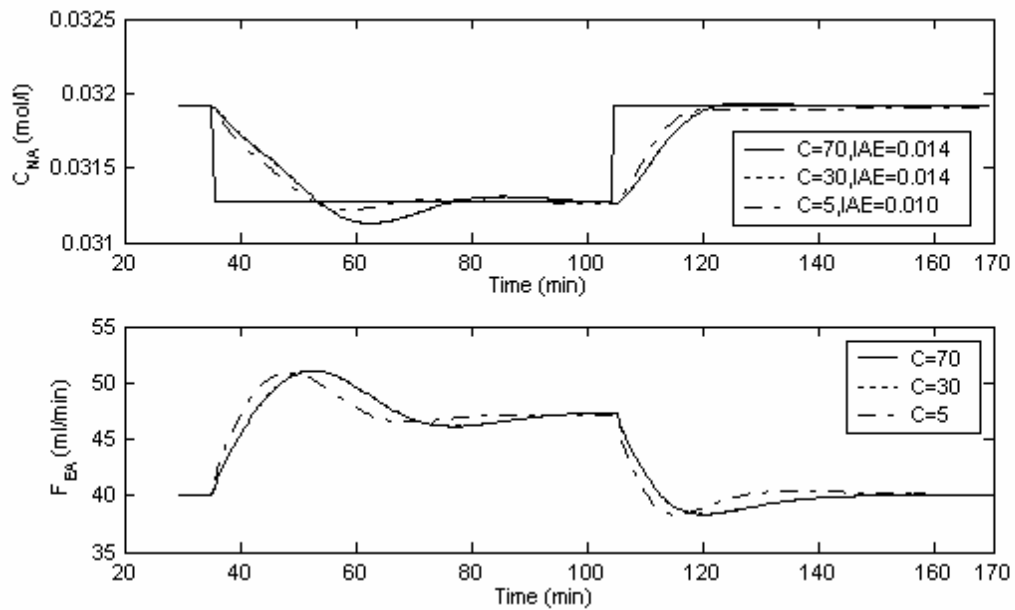


Figure 7.6: Response of C_{NA} to -2% decrease in the set point of C_{NA} and followed by +2% increase in C_{NA} for $C= 70, 30$ and 5 with $f= 1 \times 10^{-7}$.

The performance of SISO-MPC for set point tracking of temperature of reactor is also tested. The consequent set point change is given as +10% of reactor temperature, $+3^{\circ}C$, at 35th min and -10% of reactor temperature $-3^{\circ}C$ at 95th min. The response of temperature of reactor for f values of $1 \times 10^{-1}, 1 \times 10^{-2}$, 2×10^{-3} and 1×10^{-4} control horizon $C=14$ is presented in Figure 7.7.

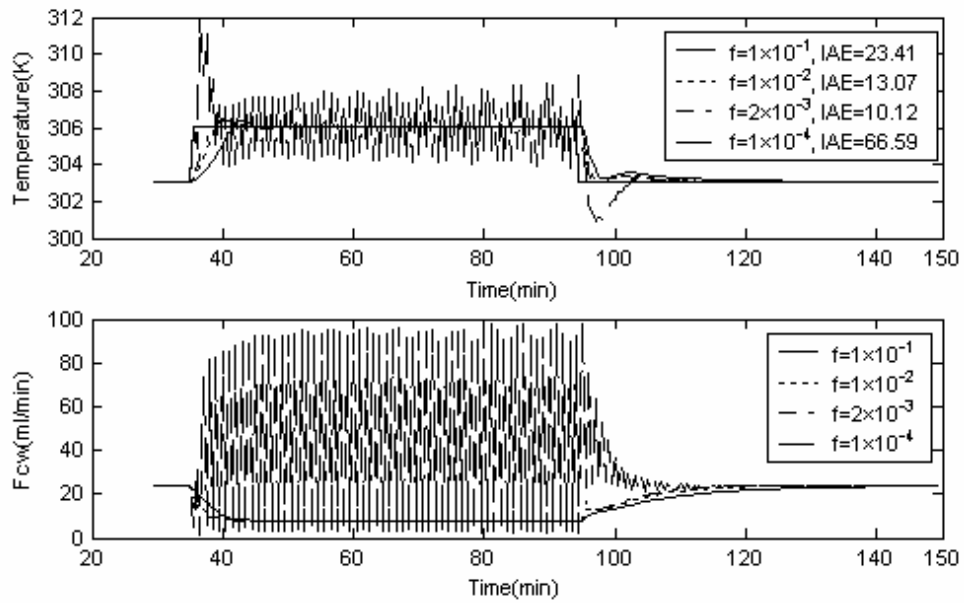


Figure 7.7: Response of T to $+3^{\circ}\text{C}$ increase in the set point of T and followed by -3°C decrease in set point of T for $f=1\times 10^{-1}$, 1×10^{-2} and 2×10^{-3} with $C=14$.

The smallest IAE score is obtained for $f=2\times 10^{-3}$ and the response time is also smaller than others. As can be seen from Figure 7.7 for $f=1\times 10^{-4}$, oscillations are observed for both the controlled and the manipulated variables. Therefore, the best f value is chosen as 2×10^{-3} to control the temperature of the reactor.

In order to see the effect of control horizon (C), the controller performance is tested with three different C values ($C=14$, 8 and 2) with $f=2\times 10^{-3}$ as shown in Figure 7.8. It can be seen for in Figure 7.8, the control horizon doesn't have an important effect on the response of the temperature of the reactor with the almost same IAE scores.

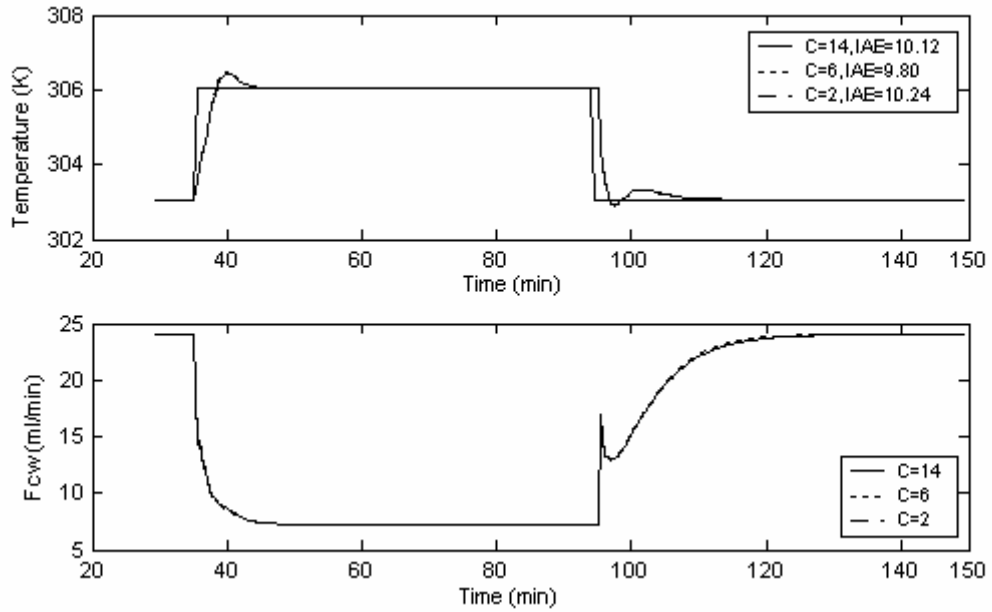


Figure 7.8: Response of T to $+3^{\circ}\text{C}$ step change in the set point of T and -3°C step change in the set point of T for $C= 14, 6$ and 2 with $f= 2 \times 10^{-3}$.

7.1.4.2 SISO-MPC Performance in Disturbance Rejection

The disturbance rejection performance of the SISO-MPC for controlling sodium acetate concentration is tested by disturbing by -10% the sodium hydroxide flow rate (-4 ml/min) at 35^{th} min and the SISO-MPC for controlling the temperature of reactor by disturbing by -10% the cooling water temperature (-1.8°C) at 35^{th} min. In Figure 7.9, the effect of different f values, 1×10^{-5} , 1×10^{-6} and 1×10^{-7} for $C=70$ is shown for disturbance rejection of sodium hydroxide flow rate. It can be seen that C_{NA} is returned to its initial value for $f=1 \times 10^{-6}$ and 1×10^{-7} whereas offset occurred for $f=1 \times 10^{-5}$. It can be concluded that the best performance is obtained for $f=1 \times 10^{-7}$ because of small response time and least IAE score.

In Figure 7.10, the effects of different f values, 1×10^{-1} , 1×10^{-2} and 2×10^{-3} for $C=70$ are shown for disturbance rejection of sodium hydroxide flow rate.

Although all temperature responses attain the initial steady state values for all f values with approximately same response times, the least IAE is obtained for $f=2\times 10^{-3}$. For $f=1\times 10^{-4}$ no logical solution is obtained. Therefore, the best f value is selected as 2×10^{-3} .

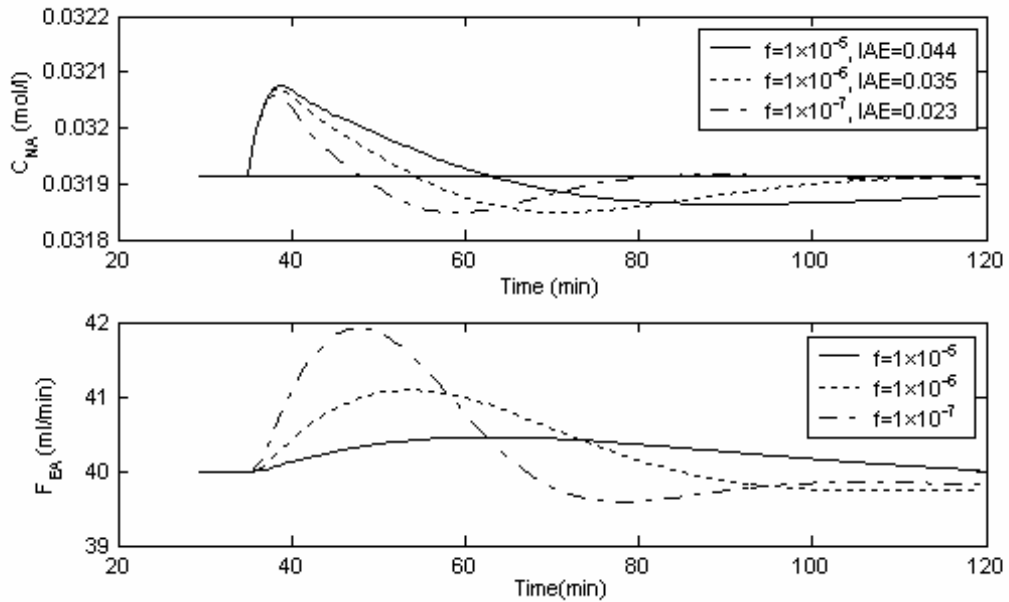


Figure 7.9: Response of C_{NA} for -10% disturbance changes in flow rate of sodium hydroxide for $f=1\times 10^{-5}$, 1×10^{-6} and 1×10^{-7} with $C=70$.

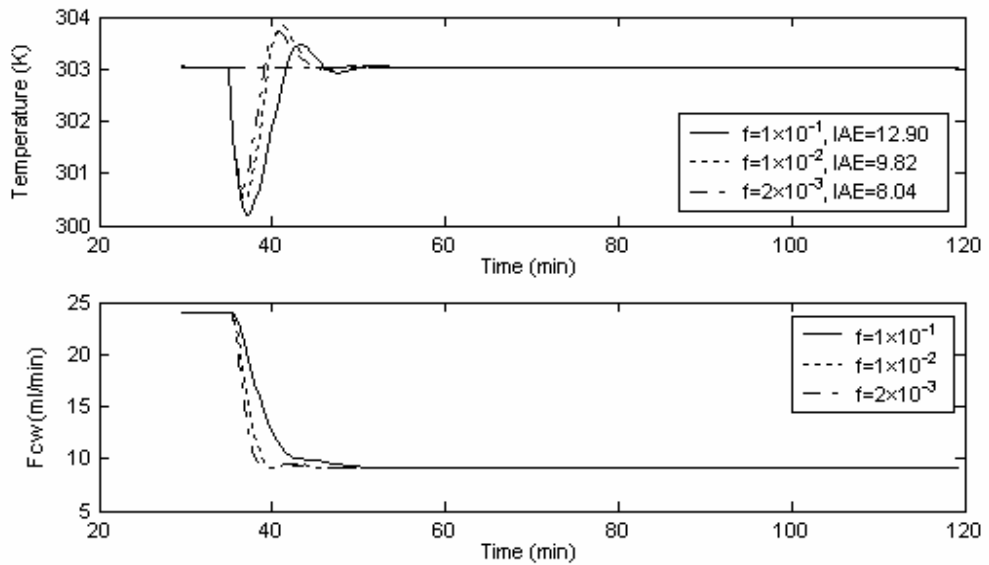


Figure 7.10: Response of T for -10% disturbance change in cooling water temperature, -1.8°C , for $f=1\times 10^{-1}$, 1×10^{-2} and 2×10^{-3} with $C=14$.

7.1.5 Design of MIMO-MPC

The saponification CSTR signal flow diagram is given in Figure 5.2. It is clear that, the reactor temperature and sodium acetate concentration can be controlled by manipulating ethyl acetate and cooling water flow rates. Therefore, the system can be considered also as a MIMO structure. For this 2×2 system, four step response curves given in Figures 7.3 and 7.4 must be utilized to obtain the step response coefficients.

In MIMO system, the model horizon M is determined according to the slowest response output. The slowest step response curve is observed for the sodium acetate concentration to unit step change in F_{ea} (Figure 7.3). Therefore, M is found as 116 by dividing 99% completion time by the controller sampling time of 0.5 min. The prediction horizon (P) is kept constant at 85% of the model horizon as 99. The control horizon (C) is first chosen as 60% of model horizon as 70. Similarly, the control horizon (C) and $f(\lambda_2/\lambda_1)$ are the tuning parameters. Integral Absolute Error (IAE) is the performance index which is calculated for all the outputs of the system utilizing MATLAB program.

7.1.5.1 MIMO-MPC Performance in Set Point Tracking

The set point tracking of the MIMO-MPC is tested by changing the set point of sodium acetate concentration (C_{NA}). The effect of tuning parameters, f and control horizon C , are also analyzed. The range of f values is selected considering the results of SISO-MPC's.

The runs are carried out by changing set-points as follows:

-2% changes in C_{NA} at 35th min, +2% changes in C_{NA} at 95th min while keeping the temperature of reactor constant. The responses of controlled

variables and the controller moves are given in Figure 7.11 for different f values, 1×10^{-5} , 1×10^{-6} and 1×10^{-7} with $C=70$.

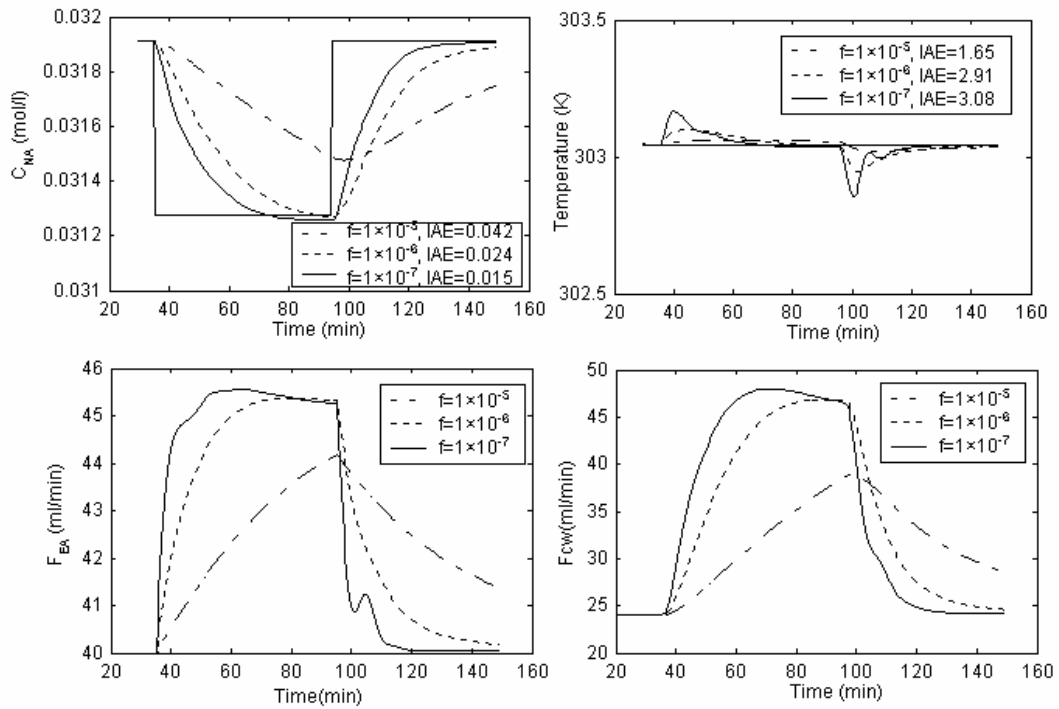


Figure 7.11: Responses of C_{NA} and T to -2% and +2% step changes in the set point of C_{NA} consecutively for $f=1 \times 10^{-5}$, 1×10^{-6} and 1×10^{-7} with $C=70$.

In the response of C_{NA} , offset is observed for $f=1 \times 10^{-5}$. On the other hand, for temperature of reactor least IAE score is obtained for 1×10^{-5} . For the C_{NA} response, IAE scores for the two values of 1×10^{-6} and 1×10^{-7} are approximately same. However, the response time is small for 1×10^{-7} . Therefore, for both control variables the best f value can be considered as 1×10^{-7} for the set point tracking of C_{NA} and to keep temperature of the reactor constant.

The effect of control horizon for set point tracking of C_{NA} is presented in Figure 7.12. Decreasing the control horizon does not have a pronounced performance with the least IAE effect on set point tracking for C_{NA} . However, smallest IAE

score is determined for the temperature of the reactor for $C=70$. Therefore, $C=70$ is selected for this MIMO-MPC.

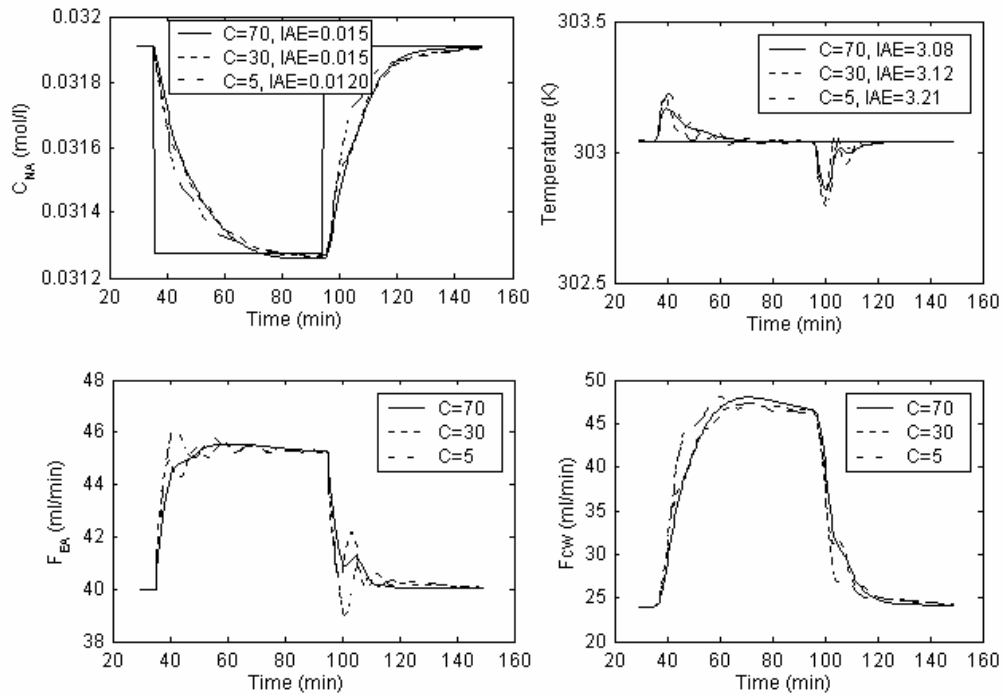


Figure 7.12: Responses of C_{NA} and T to -2% step change in the set point of C_{NA} and +2% step change in the set point of C_{NA} consecutively for $C=70, 35$ and 5 with $f=1 \times 10^{-7}$.

7.1.5.2 MIMO-MPC Performance in Disturbance Rejection

The disturbance rejection performance of MIMO-MPC is tested by disturbing the sodium hydroxide flow rate by step change.

First, the performance of MIMO-MPC is analyzed by giving a -10 % disturbance to sodium hydroxide flow rate at 35th min for $f=1 \times 10^{-5}, 1 \times 10^{-6}$ and 1×10^{-7} with $C=70$, shown in Figure 7.13. The least IAE score and smallest response time is observed for 1×10^{-7} for sodium acetate concentration but higher IAE score for temperature of reactor. The response time for temperature is very small as 5

min. Therefore, the best f value is chosen as 1×10^{-7} . The MIMO-MPC is very satisfactory for disturbance rejection.

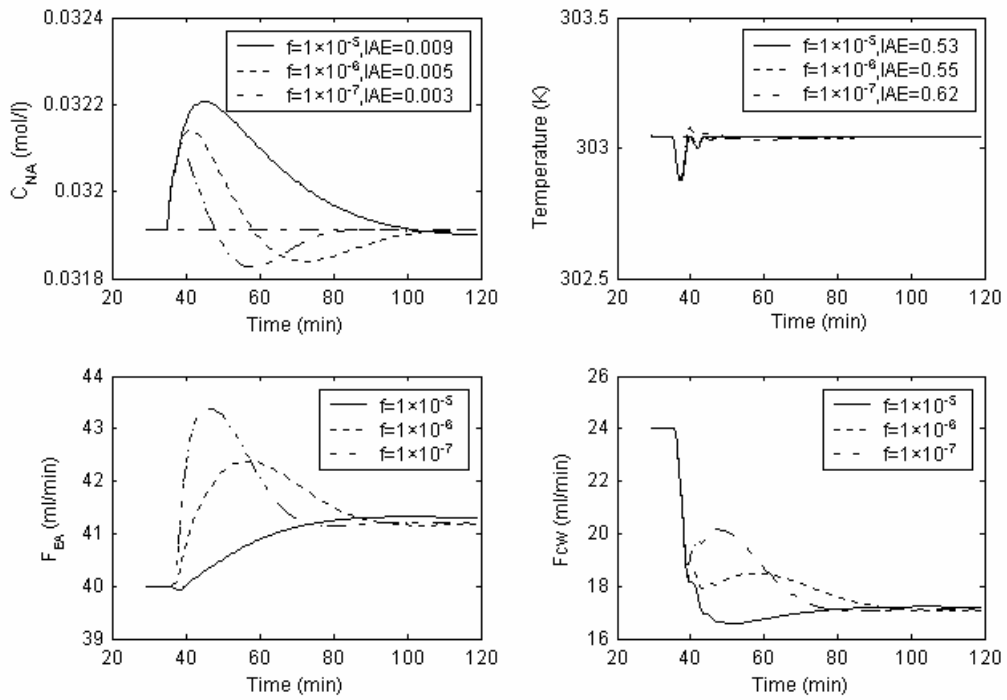


Figure 7.13: Responses of C_{NA} and T to -10% disturbance changes in flow rate of sodium hydroxide for $f=1 \times 10^{-5}$, 1×10^{-6} and 1×10^{-7} with $C=70$.

In Figure 7.14, the effect of control horizon is shown for different C values and $f=1 \times 10^{-7}$. The least IAE score is obtained for $C=30$ for sodium acetate concentration and for $C=70$ for temperature of reactor. The effect of C is not very pronounced in this example. The MIMO-MPC is very satisfactory for disturbance rejection.

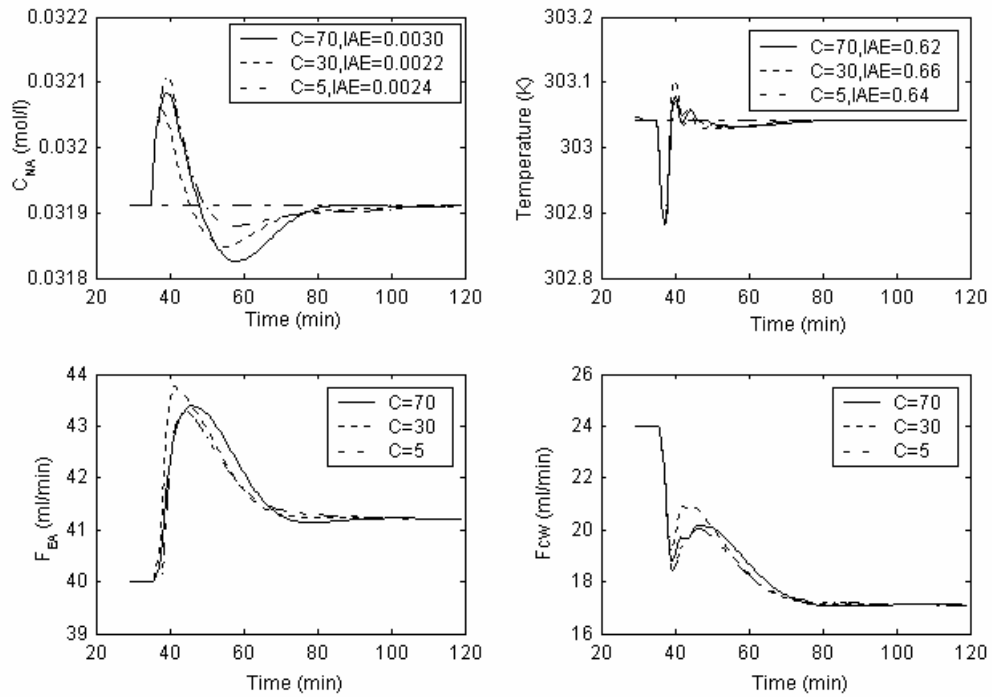


Figure 7.14: Responses of C_{NA} and T for -10% disturbance change in flow rate of sodium hydroxide for $C=70, 30$ and 5 with $f=1 \times 10^{-7}$.

The performance of MIMO-MPC is also analyzed by giving 1°C decrease in cooling water temperature for $f=1 \times 10^{-7}$ and $C=70$. In Figure 7.15, it is seen that both temperature of the reactor and sodium acetate concentration return the initial condition for a small response time and oscillations are observed for temperature of the reactor.

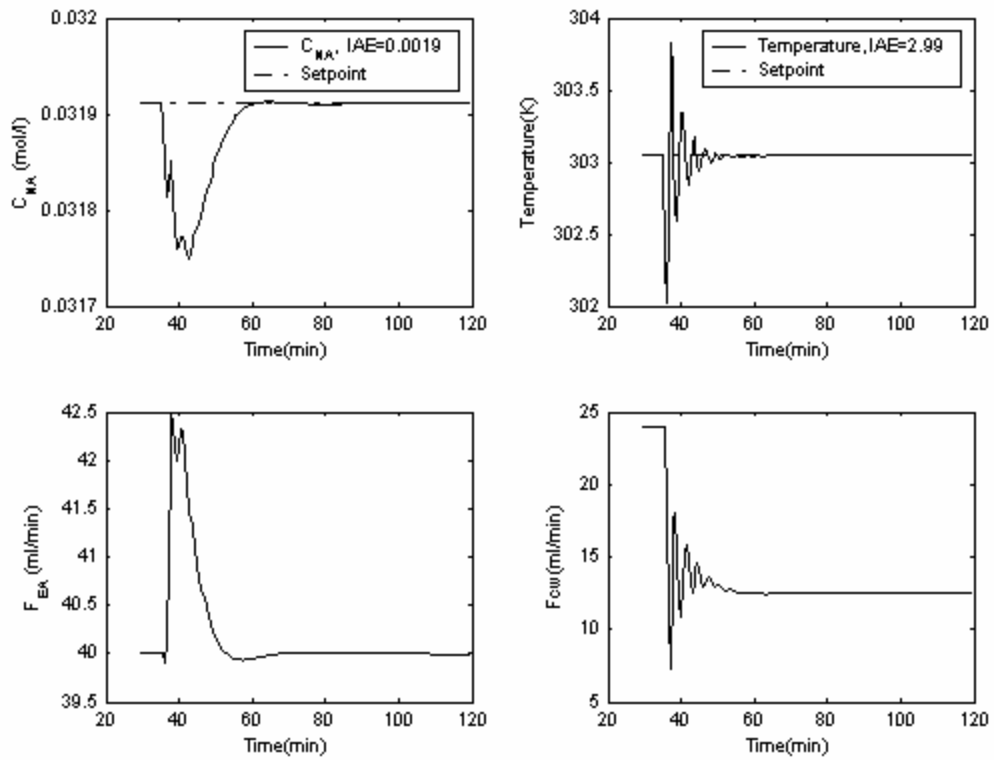


Figure 7.15: Responses of C_{NA} and T for 1°C decrease in cooling water temperature for $f=1 \times 10^{-7}$ and $C=70$.

7.1.5.3 MIMO-MPC Performance for Robustness

The performance of MIMO-MPC is also presented for robustness which is defined to be “insensitive to changes in process conditions and to errors in the assumed process model” (Seborg et al., 1989). In order to analyze the robustness of MIMO-MPC, the reaction rate constant k_0 is decreased from 1.83×10^8 to 1.556×10^8 by 15% to change the model (i.e the plant). When the plant is changed, the initial steady state points of sodium acetate concentration and temperature of the reactor are also changed. Therefore, in using the same step response model, new steady state points are actualized. In Figure 7.16, set point tracking performances of MPC are demonstrated for sodium acetate concentration. In addition to this, MPC is tested for -10% disturbance change in

sodium hydroxide flow rate (-4) and 1°C decrease in cooling water temperature and the responses of controlled and manipulated variables are presented in Figure 7.17 and Figure 7.18. As can be seen from the figures, the controller is robust in spite of variations in the derived model of the process.

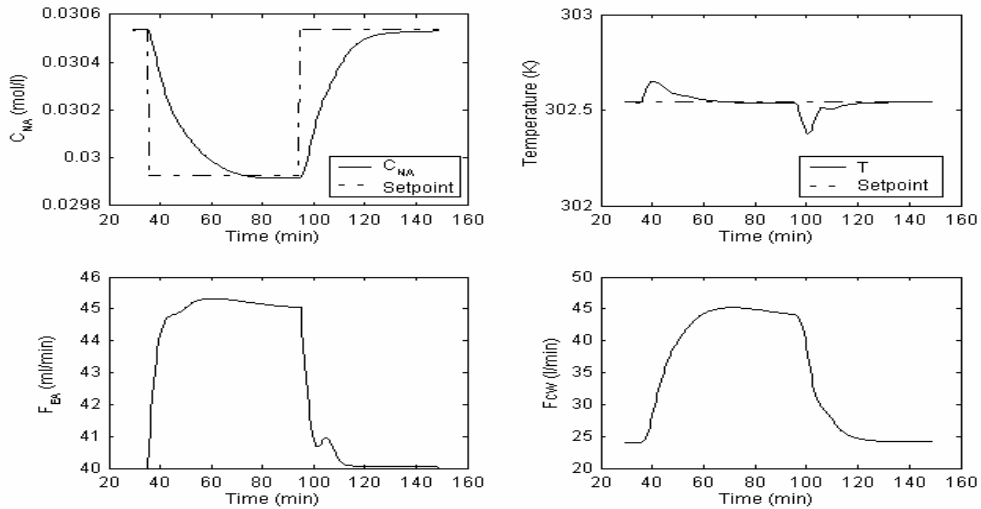


Figure 7.16: Responses of C_{NA} and T to -2 % and +2% step changes in the set point of C_{NA} consecutively for a 15% change in the model parameter, k , for $f=1 \times 10^{-7}$ and $C=70$.

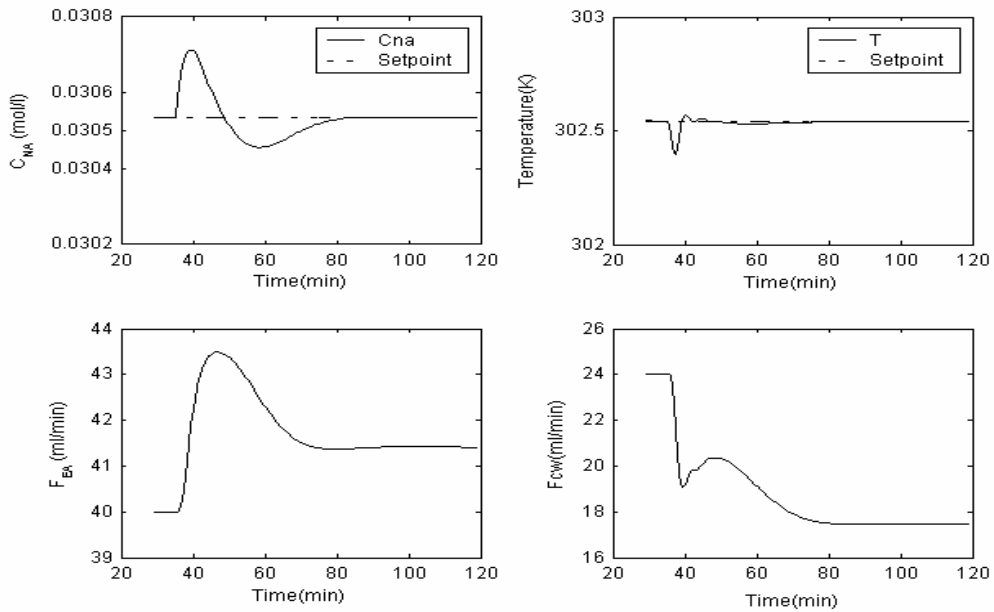


Figure 7.17: Responses of C_{NA} and T to -10%, -4 ml/min, disturbance change in sodium acetate flow rate for a 15% change in the model parameter, k , for $f=1 \times 10^{-7}$ and $C=70$.

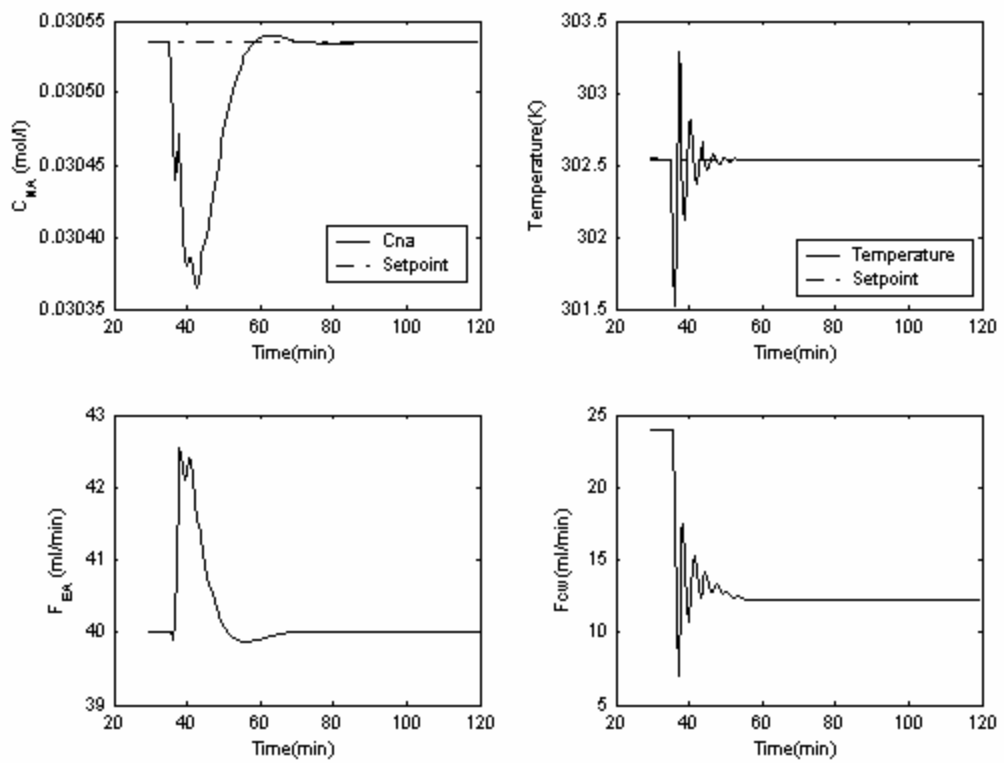


Figure 7.18: Responses of C_{NA} and T to 1°C decrease in cooling water temperature for a 15% change in the model parameter, k , for $f=1 \times 10^{-7}$ and $C=70$

7.2 CASE STUDY II: Boric Acid Production from Colemanite and Sulfuric Acid in Four CSTR's

7.2.1 System Identification

The identification of the boric acid system is done by giving step inputs to acid flow rate (manipulated variable) and to colemanite flow rate (disturbance). The open loop responses of the process are used to find transfer functions as will be explained below.

7.2.1.1 Process Transfer Function Determination

Two experiments are performed in order to observe the effect of acid flow rate on the concentration of boric acid in four reactors. The results of both of the experiments are close to each other. However, in the second experiment, the operation is believed to be more stabilized and therefore, in the evaluation, second experiment results are used.

In the experiment, the acid flow rate is changed by 4% (from 70 g/min to 72.7 g/min), and colemanite flow rate is kept constant at 10 g/min. The experimental data obtained boric acid concentrations in all four reactors are shown in Figures 7.19-7.23 for a 4% increase in acid flow rate. The transfer function that fits the experimental data is found by utilizing the Sundaresan and Krishnaswamy

method (Seborg et al., 1989) as $G = \frac{-0.039e^{-6.4s}}{44s + 1}$. Although a first order transfer

function with time delay is considered, it is observed from the experimental data that delays in the reactor is very small. Thus, 1 min time delay is assumed for the first reactor. This is also considered for the other reactors which are in dimensions same with the first reactor. The time constant of the first reactor is

evaluated as an initial estimate by the above method and then fine tuning in the value is done by considering least Sum of Squared Error (SSE) score. The results of these are given Table 7.1.

Table 7.1: Different τ_1 values with SSE score for process transfer function

τ_1	SSE
44 (Sundaresan)	0.000272
44	0.000140
40	0.000093
36	0.000102

The transfer function of the first reactor is found as in Equation (7.1) by using MATLAB-SIMULINK.

$$\left[y_1' \right] = \left[\frac{-0.039 e^{-s}}{40s + 1} \right] \left[u_1' \right] \quad (7.1)$$

where

y_1' is boric acid concentration of the first reactor in deviation form

u_1' is acid flow rate of the first reactor in deviation form

The response curve of transfer function model of the first reactor is given in Figure 7.19.

The response obtained from the second reactor is actually the response of both the first and the second reactors. Therefore, the transfer function is of second

order representing the first two reactors. The second time constant, τ_2 , is found as 25 with respect to SSE and other trials are given in Table 7.2.

Table 7.2: Different τ_2 values with SSE score for process transfer function

τ_2	SSE
20	0.000239
25	0.000124
30	0.000141

The transfer function of the first two reactors is given in Equation (7.2).

$$\begin{bmatrix} y_2' \end{bmatrix} = \begin{bmatrix} -0.039 e^{-2s} \\ (40s + 1)(25s + 1) \end{bmatrix} \begin{bmatrix} u_1' \end{bmatrix} \quad (7.2)$$

where

y_2' is boric acid concentration in the second reactor in deviation form

The response curve of transfer function model of the first two reactors is given in Figure 7.20.

Consequently, the transfer function of the first three reactors is considered as third order with time delay. Different time constants of third reactor, τ_3 , with SSE scores are tabulated in Table 7.3.

Table 7.3: Different τ_3 values with SSE score for process transfer function

τ_3	SSE
10	0.000375
15	0.000225
20	0.000236

The transfer function of the first three reactors is presented in Equation (7.3).

$$\left[y_3' \right] = \left[\frac{-0.041 e^{-3s}}{(40s + 1)(25s + 1)(15s + 1)} \right] \left[u_1' \right] \quad (7.3)$$

where

y_3' is boric acid concentration in the second reactor in deviation form

The response curve of transfer function model of the first three reactors is given in Figure 7.21.

Finally, the overall process transfer function is considered as fourth order with a delay term. Time constant of the fourth reactor, τ_4 , for different τ_4 values with SSE are given in Table 7.4.

Table 7.4: Different τ_4 values with respect to SSE for process transfer function

τ_4	SSE
10	0.000431
5	0.000427
2	0.000484

The overall process transfer function is expressed as in Equation (7.4).

$$\left[y_4' \right] = \left[\frac{-0.042 e^{-4s}}{(40s + 1)(25s + 1)(15s + 1)(5s + 1)} \right] \left[u_1' \right] \quad (7.4)$$

where

y_4' is boric acid concentration in the second reactor in deviation form

The boric acid concentration response to a step change (4%) in acid flow rate is shown in Figures 7.22. The experimental data are given in Table E.5-E.8.

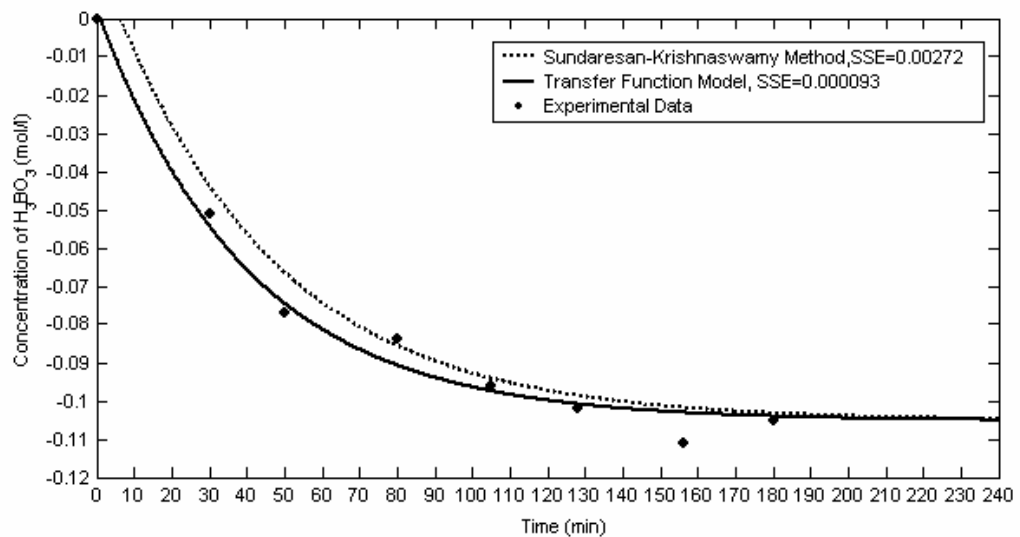


Figure 7.19: Response of boric acid concentration in Reactor I to 2.7 g/min step change in acid flow rate.

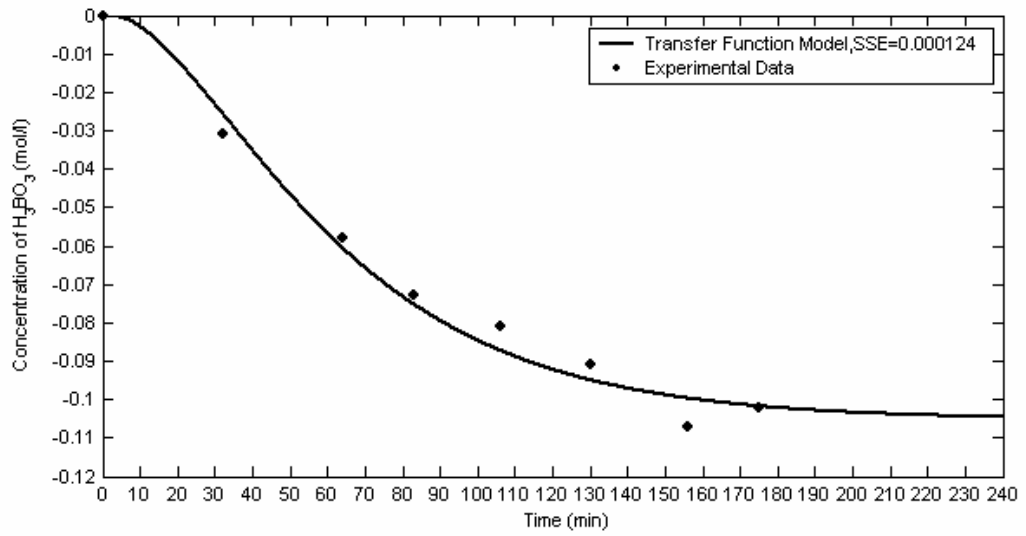


Figure 7.20: Response of boric acid concentration in Reactor II to 2.7 g/min step change in acid flow rate.

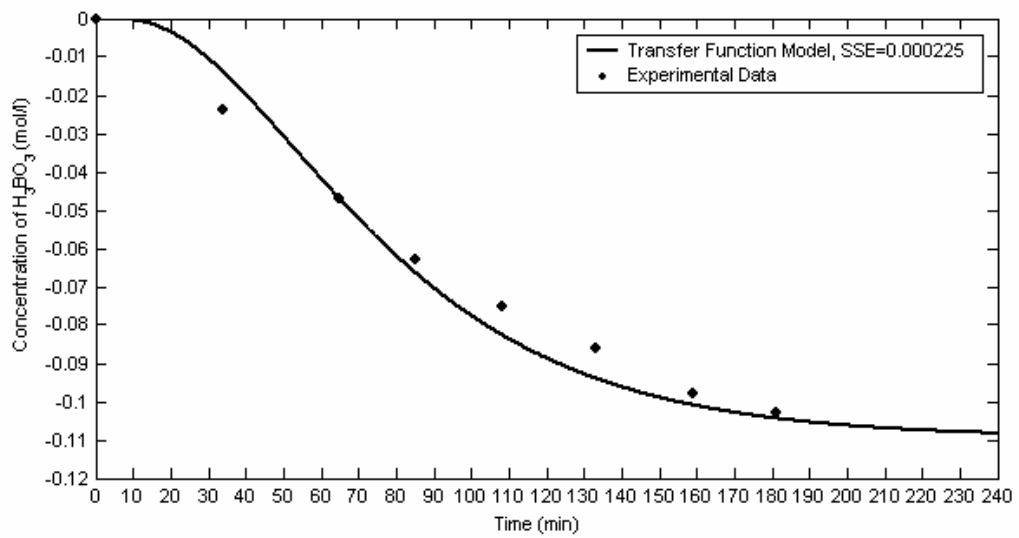


Figure 7.21: Response of boric acid concentration in Reactor III to 2.7 g/min step change in acid flow rate.

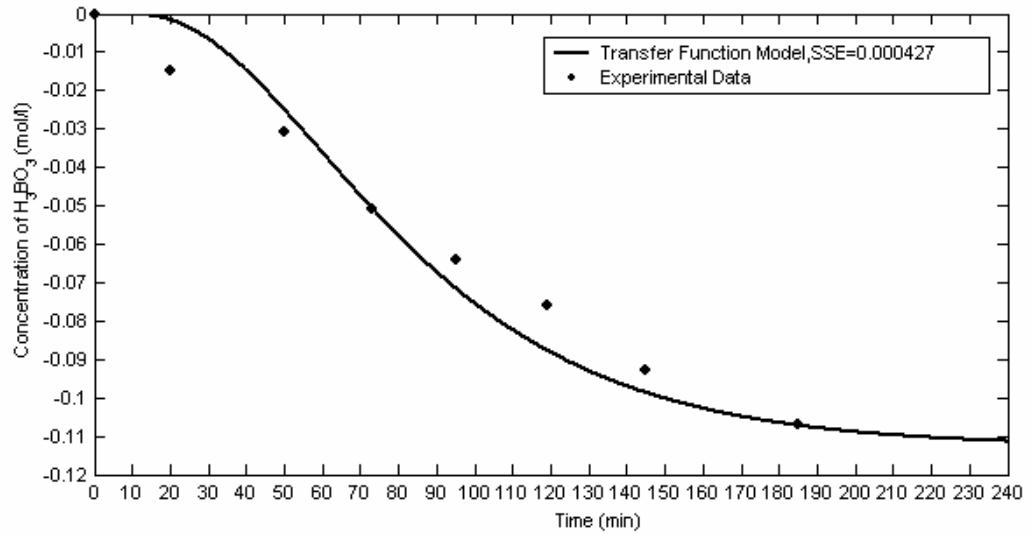
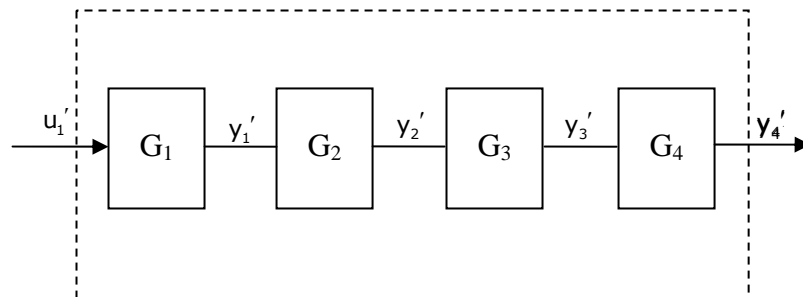
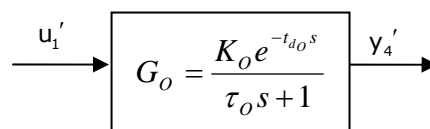


Figure 7.22: Response of boric acid concentration in Reactor IV to 2.7 g/min step change in acid flow rate.

The four reactors in series shown in Figure 7.23(a) can be approximated by a single transfer function as shown in Figure 7.23(b).



(a)



(b)

Figure 7.23: (a) Four CSTR's with inputs and outputs (b) The overall transfer function for the four CSTR's.

The overall transfer function is approximated first order transfer function with time delay as given in Equation (7.5) using the experimental data shown in Figure 7.22.

$$\left[y_4' \right] = \frac{K_o e^{-t_{d_o} s}}{\tau_o s + 1} \left[u_1' \right] \quad (7.5)$$

where

K_o is the overall steady state gain for the four reactors

τ_o is the overall time constant for the four reactors

t_{d_o} is the overall time delay for the four reactors

By using Sundaesan and Krishnaswamy method and approximated transfer function is expressed as in Equation (7.6).

$$\left[y_4' \right] = \left[\frac{-0.042 e^{-31s}}{54s + 1} \right] \left[u_1' \right] \quad (7.6)$$

The comparison of the experimental data obtained from Reactor IV and of the approximated model is shown in Figure 7.24.

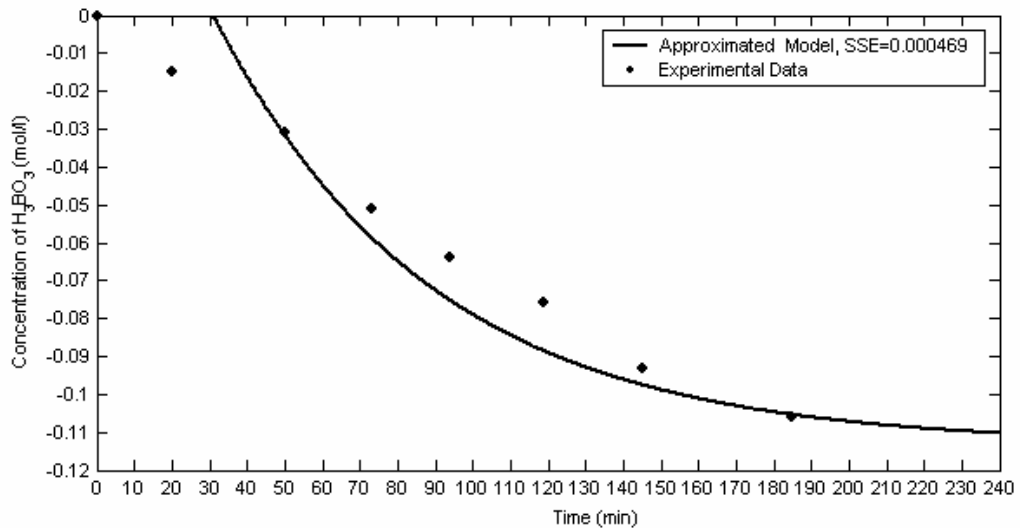


Figure 7.24: Response of boric acid concentration in Reactor IV to 2.7 g/min step change in acid flow rate obtained from approximated transfer function model for the whole system.

7.2.1.2 Disturbance Transfer Function Determination

Run III is done in order to obtain disturbance transfer function for the step change in colemanite flow rate (disturbance). In Run III, colemanite flow rate is increased by 10% (from 10 g/min to 11 g/min) while keeping acid flow rate constant at 70 g/min. The disturbance transfer function for the first reactor is found using the experimental data given in Table E.9-E.12 and shown in Figure 7.25. The parameters of the first order transfer function with delay are found using the Sundaresan and Krishnaswamy as first estimates, $\tau_1 = 43$, $\theta_1 = 6.9$.

However, time delay is not apparently seen in the experimental findings (Figure 7.25). Therefore, as is done in Section 7.2.1.1, time delay terms are taken 1 min for all four reactors. Thus, trials for better τ_1 values are done and response curves are obtained. SSE scores for each τ_1 are given in Table 7.5. Thus, $\tau_1 = 35$ is selected resulting in the least SSE score for which the response is given in Figure 7.25 for a disturbance of 10% in colemanite flow rate.

Table 7.5: Different τ_1 values with SSE score for disturbance transfer function

τ_1	SSE
43 (Sundaresan)	0.001037
43	0.000476
38	0.000254
35	0.000206
32	0.000231

The disturbance transfer function for the first reactor is expressed as in Equation (7.7).

$$\left[y_1' \right] = \left[\frac{0.130 e^{-s}}{35s + 1} \right] \left[d_1' \right] \quad (7.7)$$

where

y_1 is boric acid concentration of the first reactor in deviation form

d_1 is colemanite flow rate of the first reactor in deviation form

The disturbance transfer functions between the disturbance and the boric acid concentration in the effluent leaving each reactor are obtained by a similar procedure and given below. The best τ_2 , τ_3 and τ_4 resulting in SSE score are found as 15, 8 and 7. The different τ_2 , τ_3 and τ_4 values with SSE score are tabulated in Tables 7.6-7.8. The response curves for the disturbance of 10% are shown in Figures 7.26-7.28.

Table 7.6: Different τ_2 values with SSE score for disturbance transfer function

τ_2	SSE
10	0.000757
15	0.000681
20	0.000742

Table 7.7: Different τ_3 values with SSE score for disturbance transfer function

τ_3	SSE
5	0.000470
8	0.000458
10	0.000500

Table 7.8: Different τ_4 values with SSE score for disturbance transfer function

τ_4	SSE
5	0.000265
7	0.000246
9	0.000269

$$\begin{bmatrix} y_2' \end{bmatrix} = \begin{bmatrix} \frac{0.129 e^{-2s}}{(35s + 1)(15s + 1)} \end{bmatrix} \begin{bmatrix} d_1' \end{bmatrix} \quad (7.8)$$

$$\begin{bmatrix} y_3' \end{bmatrix} = \begin{bmatrix} \frac{0.127 e^{-3s}}{(35s + 1)(15s + 1)(8s + 1)} \end{bmatrix} \begin{bmatrix} d_1' \end{bmatrix} \quad (7.9)$$

$$\begin{bmatrix} y_4' \end{bmatrix} = \begin{bmatrix} \frac{0.123 e^{-4s}}{(35s + 1)(15s + 1)(8s + 1)(7s + 1)} \end{bmatrix} \begin{bmatrix} d_1' \end{bmatrix} \quad (7.10)$$

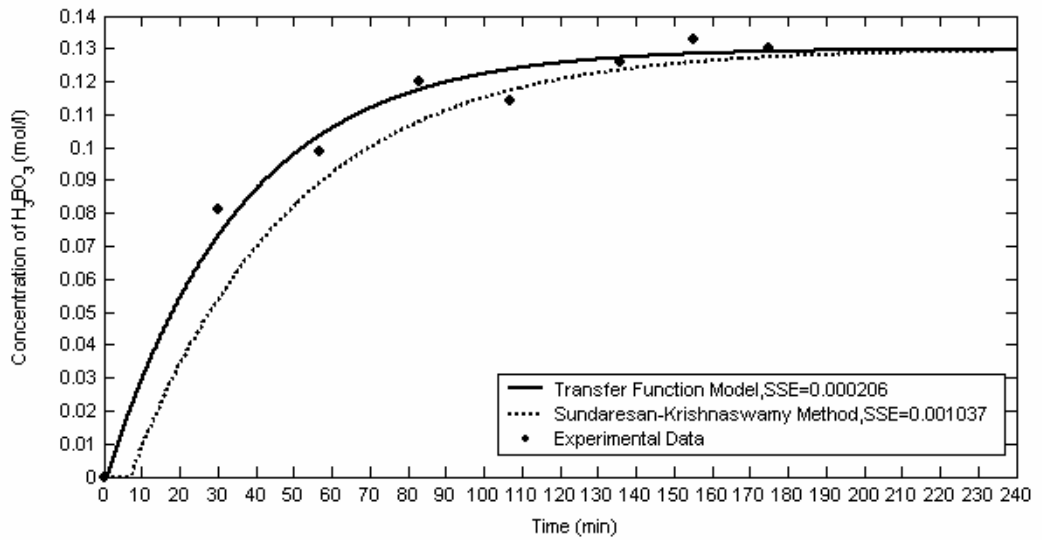


Figure 7.25: Response of boric acid concentration in Reactor I to 1 g/min step change in colemanite flow rate.

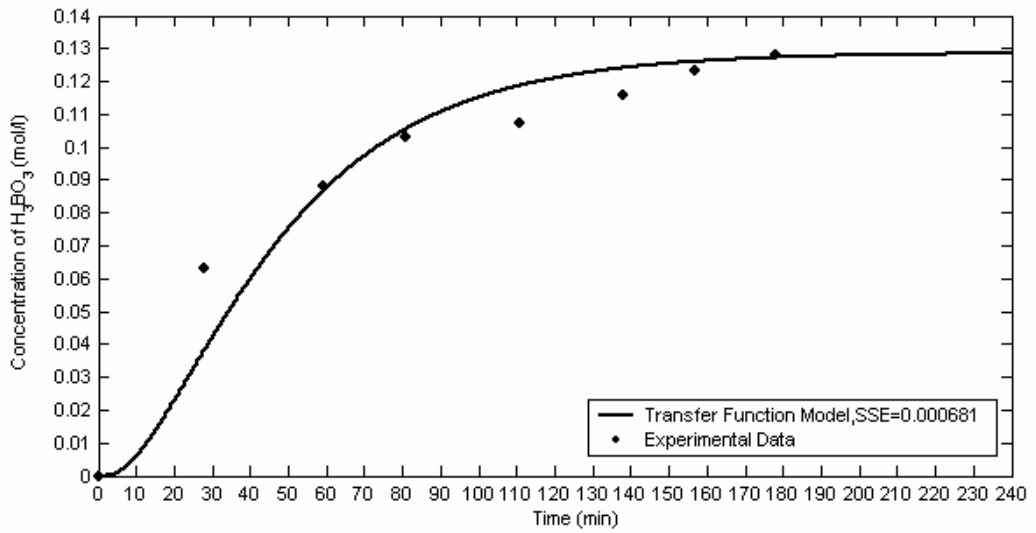


Figure 7.26: Response of boric acid concentration in Reactor II to 1 g/min step change in colemanite flow rate.

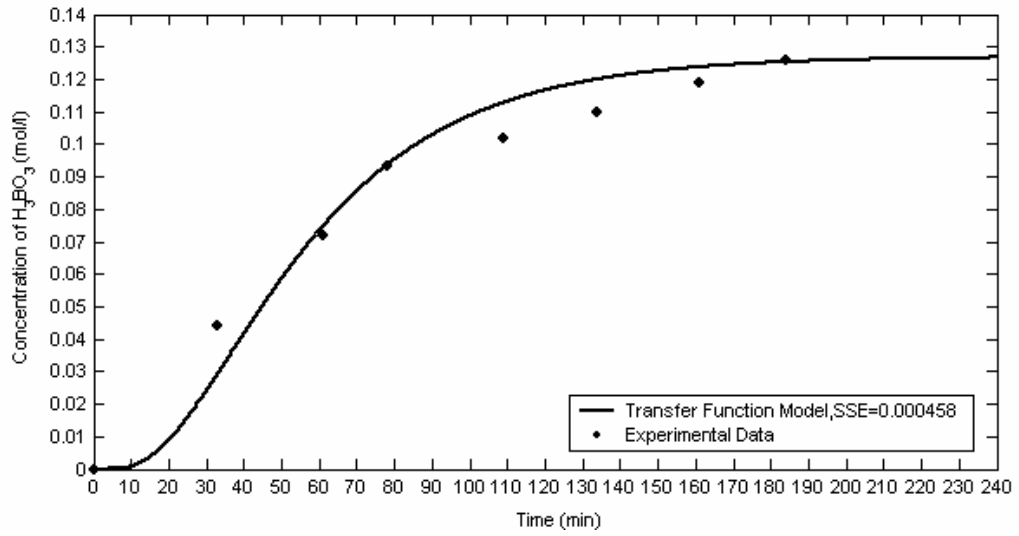


Figure 7.27: Response of boric acid concentration in Reactor III to 1 g/min step change in colemanite flow rate.

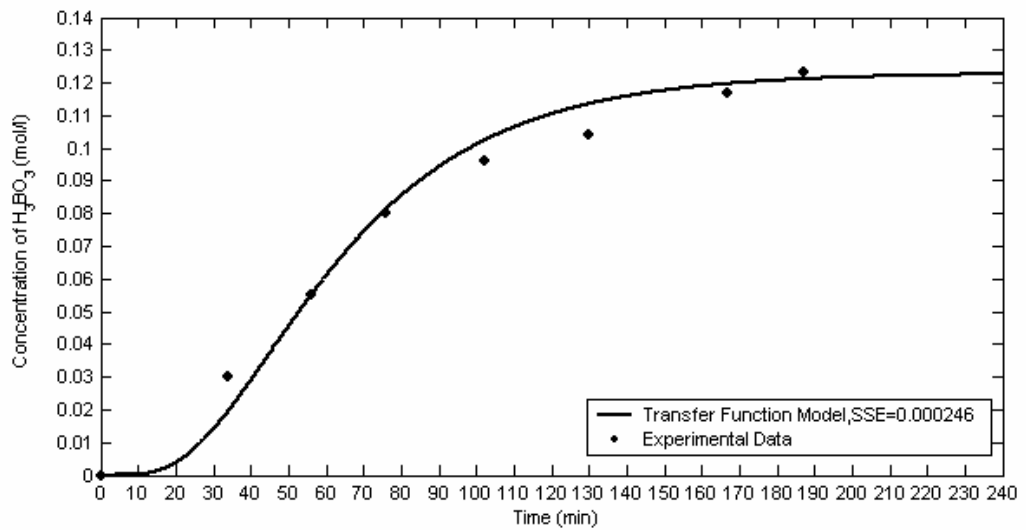


Figure 7.28: Response of boric acid concentration in Reactor IV to 1 g/min step change in colemanite flow rate.

The approximated disturbance transfer function of the four reactors in terms of y_4' and d_1' is obtained using the experimental data given in Table E.9-E.12 by using Sundaresan and Krishnaswamy method. Disturbance transfer function of the four reactors is considered as first order with time delay and given in Equation (7.11).

$$\left[y_4' \right] = \left[\frac{0.123 e^{-29s}}{48s + 1} \right] \left[d_1' \right] \quad (7.11)$$

The comparison of the experimental data points for Reactor IV and the obtained response obtained used the approximated transfer function model given in Equation (7.11) for a 10% step input change in colemanite flow rate is given in Figure 7.29.

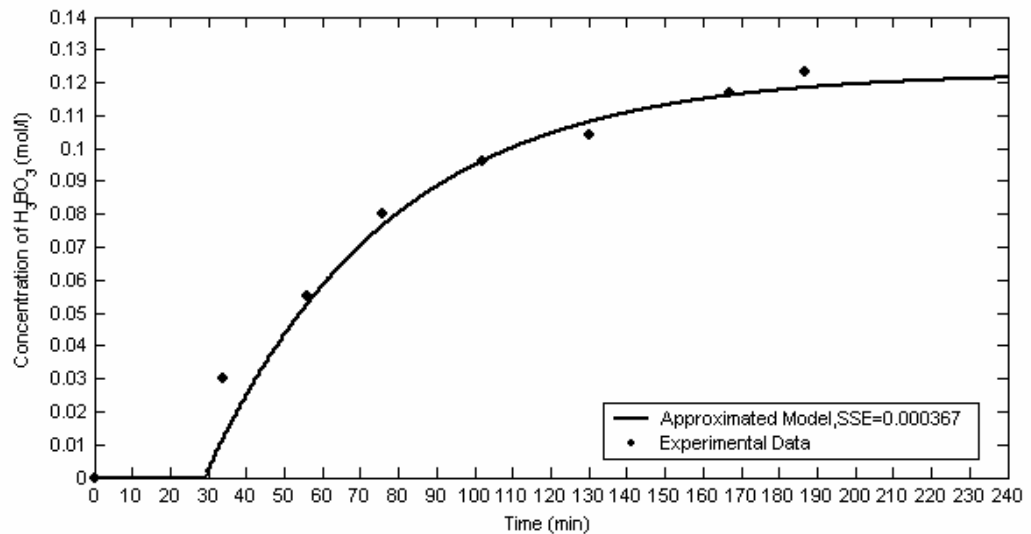


Figure 7.29: Response of boric acid concentration in Reactor IV to 1 g/min step change in colemanite flow rate obtained from approximated transfer function model for the whole system.

The comparison of Figures 7.28 and 7.29 and SSE scores reveals that the approximated transfer function for the overall system can be used satisfactorily.

7.2.2 Design of SISO-MPC

After obtaining the overall transfer functions of the process and disturbance, SISO-MPC is designed for this system by using MPC toolbox in MATLAB.

The model horizon N is found as 110 with the controller sampling time of 2 min. The control horizon M is selected as 66 to reach 60 % of the steady state. Prediction horizon P is taken as 85% of model horizon, 94. The output weight (λ_1) is taken as 1, in which the input weight (λ_2) is taken as variable, and f (λ_2/λ_1) is chosen as the tuning parameter.

7.2.2.1 Unconstrained SISO-MPC Performance in Set-Point Tracking

The performance of SISO-MPC for set point tracking is tested for a step change of 0.3 mol/l for the boric acid concentration of the fourth reactor for different f values; 1, 0.5, 0.1, 0.05, 0.02 with constant control horizon and prediction horizon. The Integral Absolute Error (IAE) score is calculated for different f values. The response of boric acid concentration and the manipulated input is presented in Figure 7.30. It is found that, the least IAE score and settling time is obtained for $f=0.02$. However, the overshoot is observed for both the controlled variable and manipulated variable. Although there is no oscillation and overshoot for $f=1.00$, the response of controlled output is slow and the IAE score is high. Therefore, the best f value is selected as 0.02. If the training parameters f is further reduced, the acid flow rate shows very high oscillations which are not preferred due to an approach which resembles on-off control.

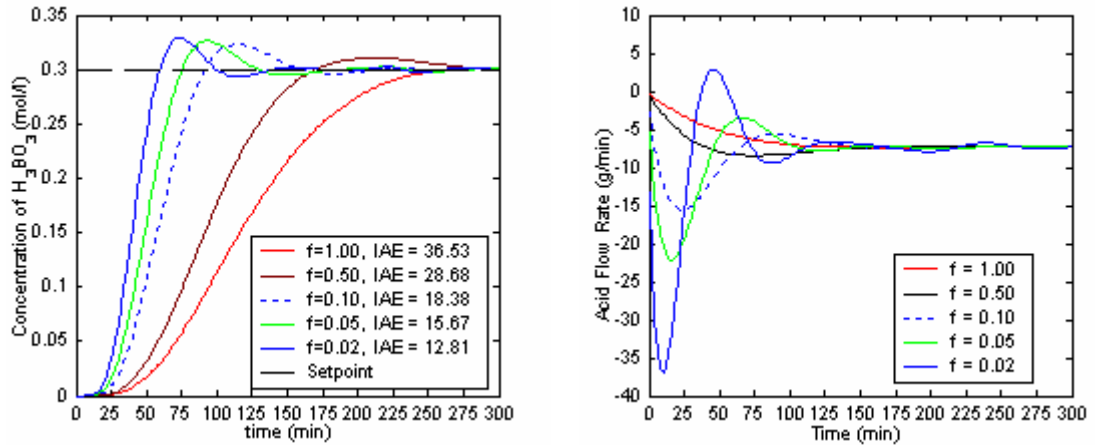


Figure 7.30: Change of controlled and manipulated variables wrt time for a 0.3 mol/l step change in the set point of boric acid concentration for $f = 1.00, 0.50, 0.10, 0.05$ and 0.02 .

7.2.2.2 Unconstrained SISO-MPC Performance in Disturbance Rejection

The disturbance rejection performance of the designed SISO-MPC is analyzed by decreasing 10 % the colemanite flow rate by 1 g/min. The responses of the controlled and manipulated variables for different f values are given in Figure 7.31. It can be seen from the figure that, the designed controller is capable of returning boric acid concentration to its initial value for all f values. The best f value is again found to be 0.02 due to small response time and least IAE score.

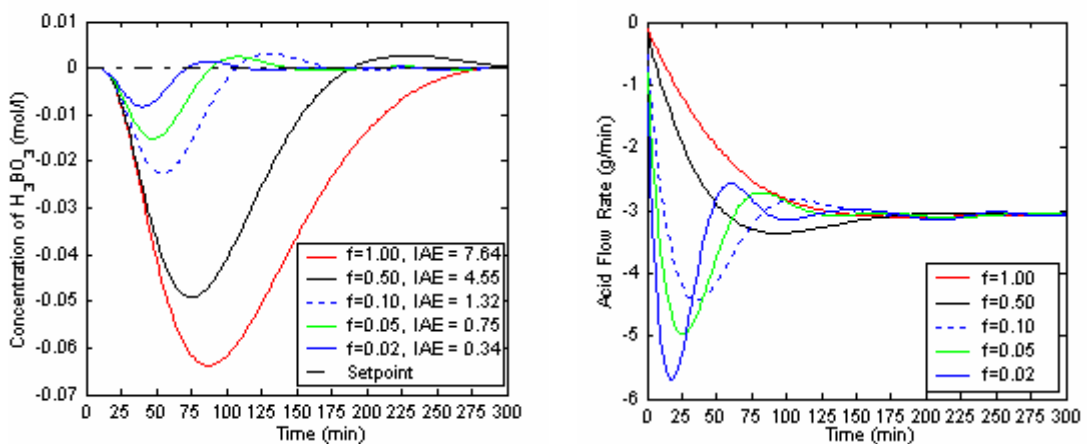


Figure 7.31: Change of controlled and manipulated variables wrt time for a 10% decrease in the colemanite flow rate for $f = 1.00, 0.50, 0.10, 0.05$ and 0.02 .

7.2.2.3 Constrained SISO-MPC Performance in Set-Point Tracking

The most important advantage of MPC is to handle input/output constraints. In the presence of unexpected conditions for the unconstrained MPC controller, input constraints can be present due to the valve saturations, and output constraints are used to avoid overshoots in the controlled variables. Thus, the designed controllers are considered to handle the constraints both in input and output to end up with appropriate control actions.

In order to eliminate overshoot in the response of boric acid concentration for $f=0.02$, the controlled variable (boric acid concentration) upper constraint is used and the performance of SISO-MPC is shown in Figure 7.32.

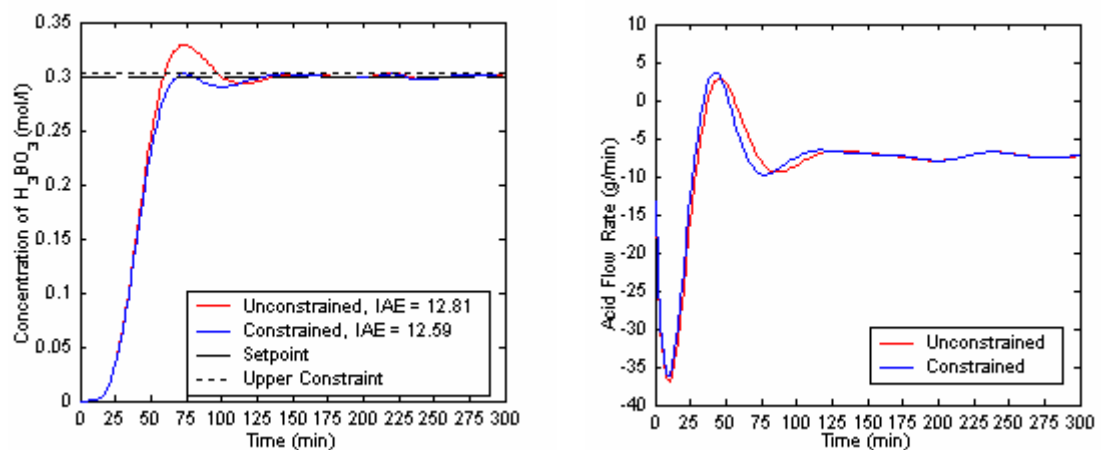


Figure 7.32: Change of controlled and manipulated variables in the presence of upper controlled variable constraint wrt time for a 0.3 mol/l step change in the set point of boric acid concentration for $f=0.02$.

It can be seen that, the overshoot of boric acid concentration is reduced significantly by giving the upper constraint to the boric acid concentration and that the IAE score for the constrained MPC is less than that of unconstrained MPC. Therefore, it is found that the constrained SISO-MPC give better performance.

In addition, the performance of SISO-MPC is investigated for manipulated variable constraints. A lower manipulated constraint is used. The performance of SISO-MPC in the presence of lower manipulated variable constraint is shown in Figure 7.33. Although the overshoot of boric acid concentration decreased in constrained case, the response time increased and therefore, the IAE score for this constrained case is higher than unconstrained case.

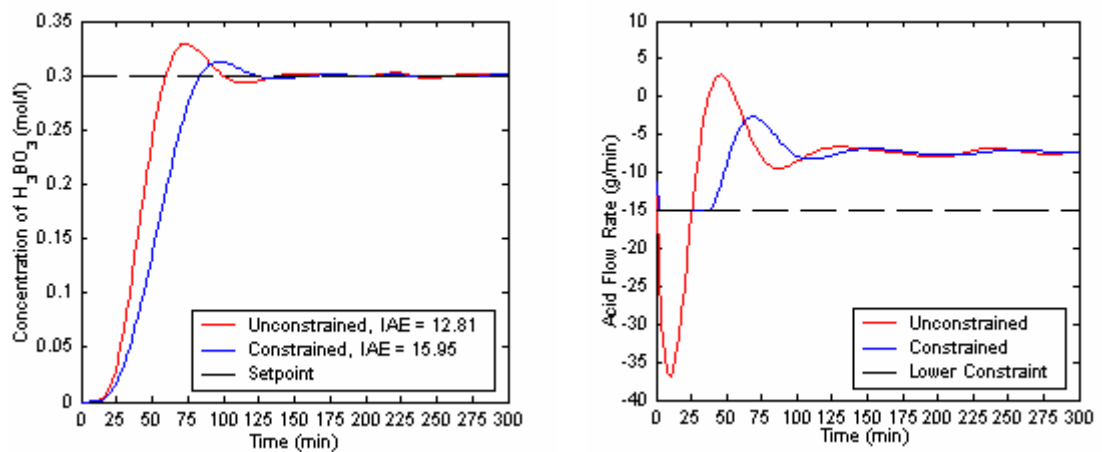


Figure 7.33: Change of controlled and manipulated variables in the presence of lower manipulated variable constraint wrt time for a 0.3 mol/l step change in the set point of boric acid concentration for $f=0.02$.

The upper manipulated variable constraint is also considered to reduce the overshoot seen in Figure 7.34. The responses of controlled and manipulated variables for a 0.3 mol/l setpoint change in boric acid concentration in the presence of upper manipulated variable constraint are shown in Figure 7.34. The overshoot in the manipulated variable is eliminated; however, in the controlled variable, overshoot is increased with an increase in IAE score.

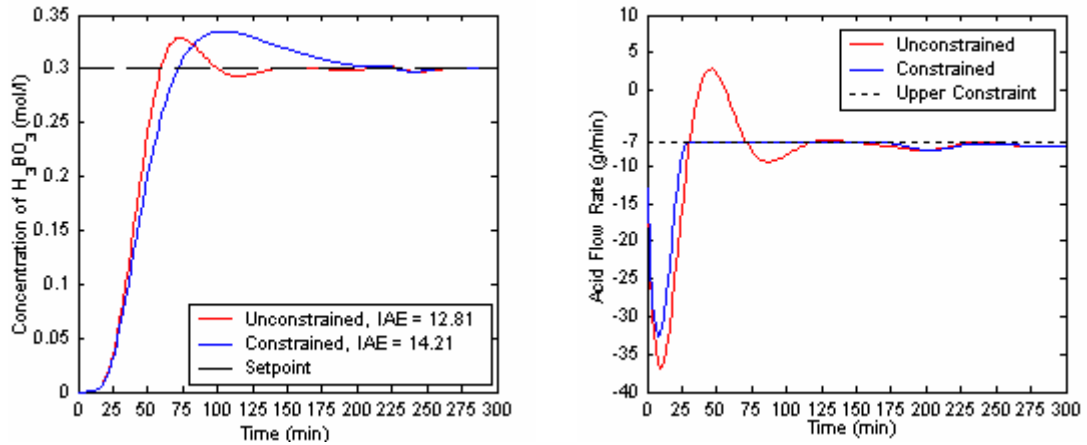


Figure 7.34: Change of controlled and manipulated variables in the presence of upper manipulated variable constraint wrt time for a 0.3 mol/l set point change in boric acid concentration for $f=0.02$.

The performance of MPC in the presence of both upper controlled and upper and lower manipulated variable constraints for a set point change of 0.3 mol/l is presented in Figure 7.35. In this case, upper manipulated variable constraint is taken as -3 since optimization program cannot solve the problem for a higher constraint. Although, an overshoot is not observed for the controlled variable in constraint case, the response time and IAE score increases due to a slower response in the controlled variable. Thus, it can be concluded that variation in the manipulated variable is reduced within the constraints. This resulted in a slower response in the controlled variable with a higher IAE score. Therefore, if these upper and lower constraints in the manipulated variable are derived, the slow response must be accepted.

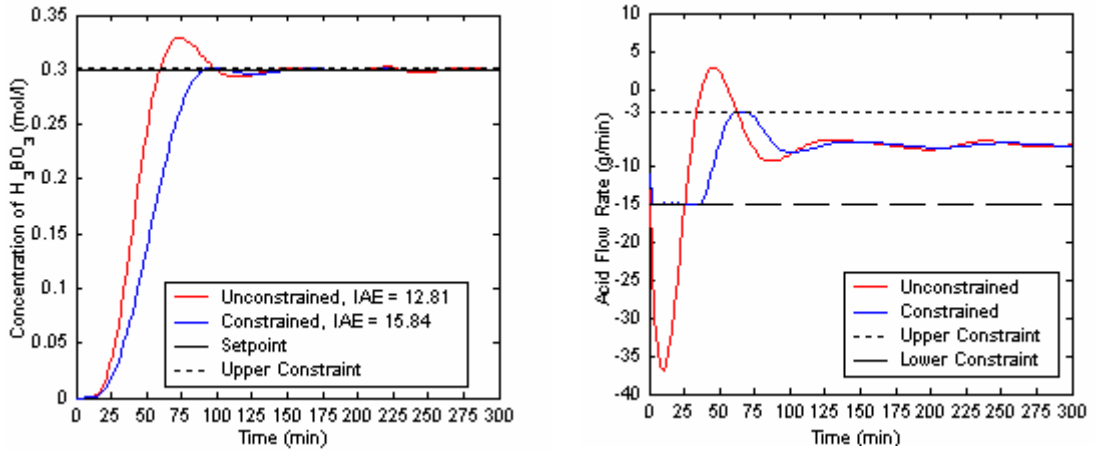


Figure 7.35: Change of controlled and manipulated variables in the presence of controlled, upper and lower manipulated variable constraint wrt time for a 0.3 mol/l set point change in boric acid concentration for $f=0.02$.

7.2.2.4 Constrained SISO-MPC Performance in Disturbance Rejection

The performance of SISO-MPC in the presence of lower controlled variable constraint for 10 % decrease in colemanite flow rate is shown in Figure 7.36. As can be seen from the figure, the IAE score of the constrained response is smaller than the unconstrained due to smaller overshoot of boric acid concentration and the faster response. Constrained controller gives better result than the unconstrained one.

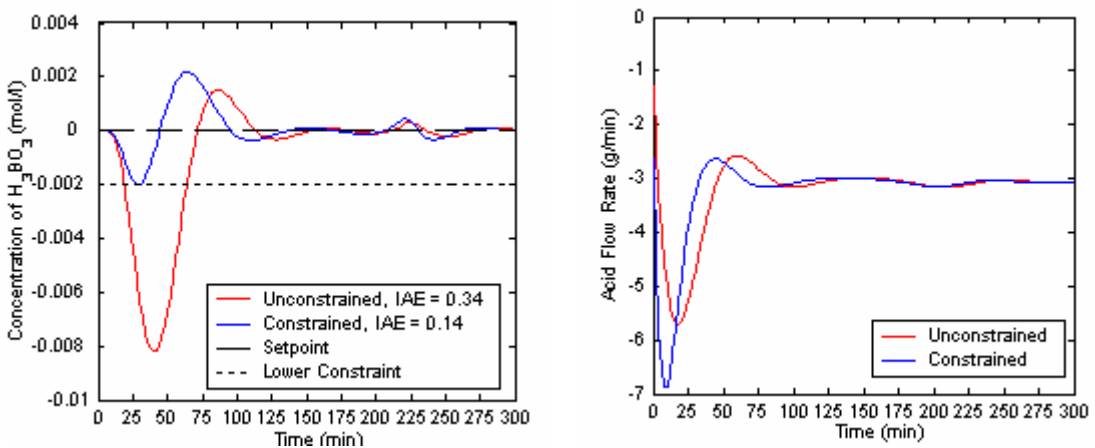


Figure 7.36: Change of controlled and manipulated variables in the presence of lower controlled variable constraint wrt time for a 10% decrease in colemanite flow rate for $f=0.02$.

The performance of designed controller is also tested in the presence of manipulated variable constraints. In Figure 7.37, the responses of the controlled and manipulated variables are given for 10 % decrease in colemanite flow rate when lower manipulated variable constraint is imposed on the controller. In constrained case, the overshoot in the boric acid concentration response is increased with a slower response resulting with a higher response time and higher IAE score. Thus, in disturbance rejection, it is not recommended to use constraint on manipulated variable which is not oscillating with high overshoot as in the case of set point tracking.

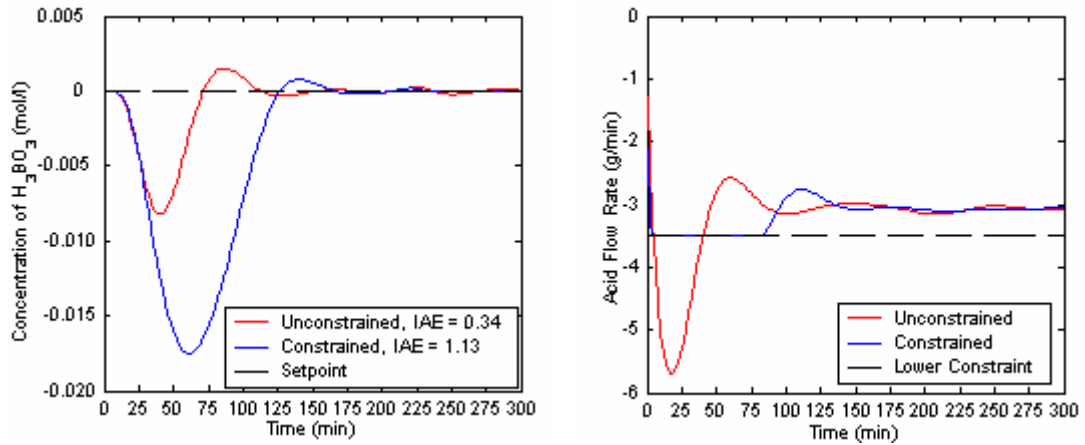


Figure 7.37: Change of controlled and manipulated variables in the presence of lower manipulated variable constraint wrt time for a 10% decrease in colemanite flow rate for $f=0.02$.

7.2.2.5 SISO-MPC Performance for Robustness

In order to analyze the robustness of SISO-MPC, the plant/model mismatch is considered as -10 % changes in time constants, time delay and gains for each reactor. Then, the overall plant transfer function is written as in Equation (7.12).

$$\begin{bmatrix} y_4' \end{bmatrix} = \begin{bmatrix} \frac{-0.0378 e^{-3.6s}}{(36s + 1)(22.5s + 1)(13.5s + 1)(4.5s + 1)} \end{bmatrix} \begin{bmatrix} u_1' \end{bmatrix} \quad (7.12)$$

The plant in Equation (7.12) is controlled by the MPC designed for the model in Equation (7.4).

The set point tracking and disturbance rejection performances of SISO-MPC are presented in Figures 7.38 and 7.39 in the presence of model/plant mismatch given above.

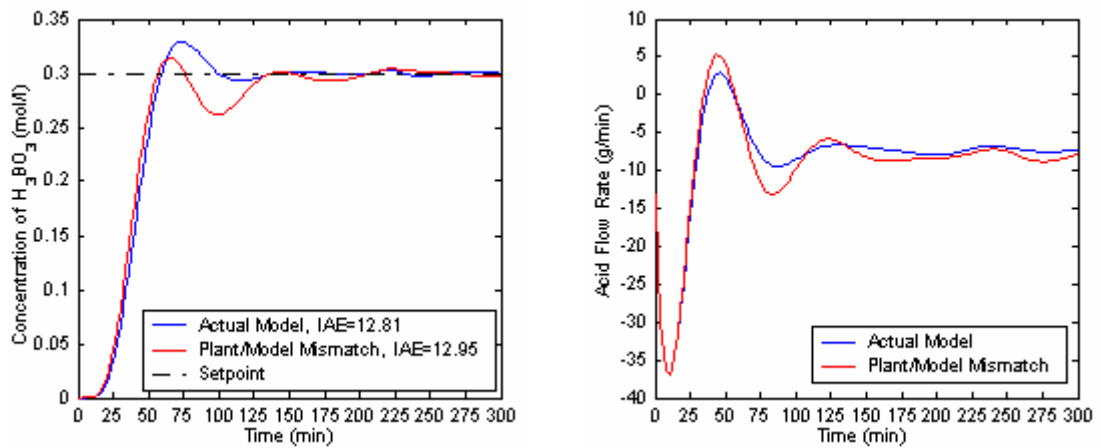


Figure 7.38: Change of controlled and manipulated variables wrt time for a 0.3 mol/l set point change in boric acid concentration when the plant is changed by -10%.

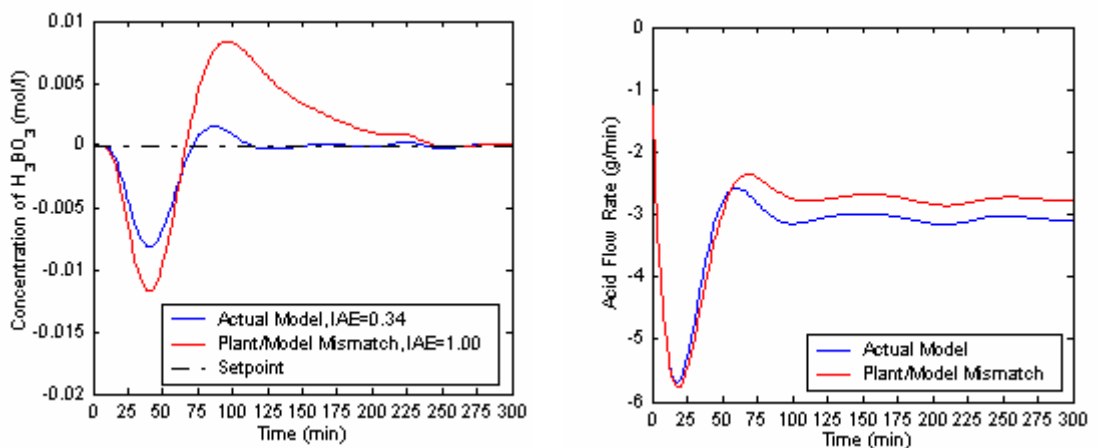


Figure 7.39: Change of controlled and manipulated variables wrt time for a 10% decrease in colemanite flow rate when the plant is changed by -10%.

It can be seen from the Figure 7.38 that the SISO-MPC performance is good in the presence of model/plant mismatch, i.e it is robust, in set point tracking. However, the performance of the same MPC in disturbance rejection is not as good as for set point tracking (Figure 7.39).

7.2.2.6 Performance of SISO-MPC by Using Approximated Transfer Function Model in Setpoint Tracking

SISO-MPC is designed by using approximated transfer function of process given in Equation (7.5). The model horizon, control horizon and prediction horizon are taken as same as the fourth order process.

The responses of boric acid concentration and the manipulated input for a set point change of 0.3 mol/l in boric acid concentration are given in Figure 7.40 for different f values. The best f value is selected as 0.02 similar to actual model based MPC due to small response time and less IAE score.

The responses of controlled and manipulated variables using the actual transfer function model and the approximated transfer function for $f=0.02$ are presented in Figure 7.41. It can be seen that the response of controlled variable for approximated transfer function model give less overshoot than that of actual transfer function model, and it gives better result with small response time and less IAE score.

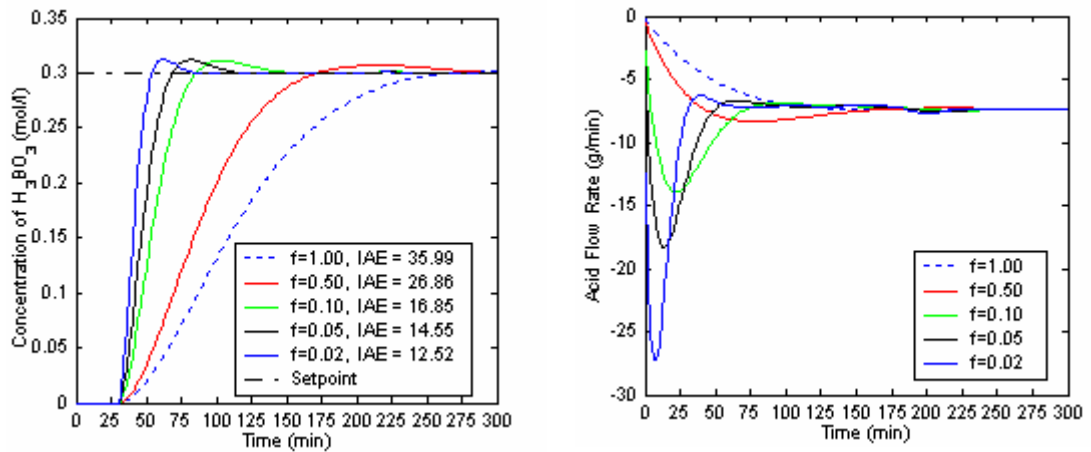


Figure 7.40: Change of controlled and manipulated variables wrt time for a 0.3 mol/l step change in the set point of boric acid concentration for $f=1.00$, 0.50, 0.10, 0.05 and 0.02.

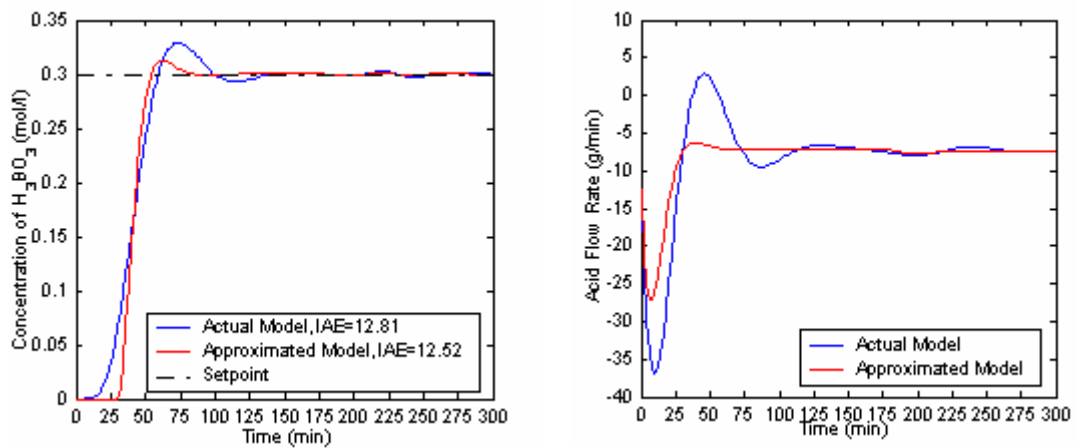


Figure 7.41: Change of controlled and manipulated variables wrt time for a 0.3 mol/l step change in the set point of boric acid concentration for actual and approximated transfer function model with $f=0.02$.

7.2.2.7 Performance of SISO-MPC by Using Approximated Transfer Function Model in Disturbance Rejection

The performance of the MPC is investigated for a 10% decrease in colemanite flow rate by using approximated transfer functions of the process and disturbance and the responses of controlled and manipulated variables are shown in Figure 7.42.

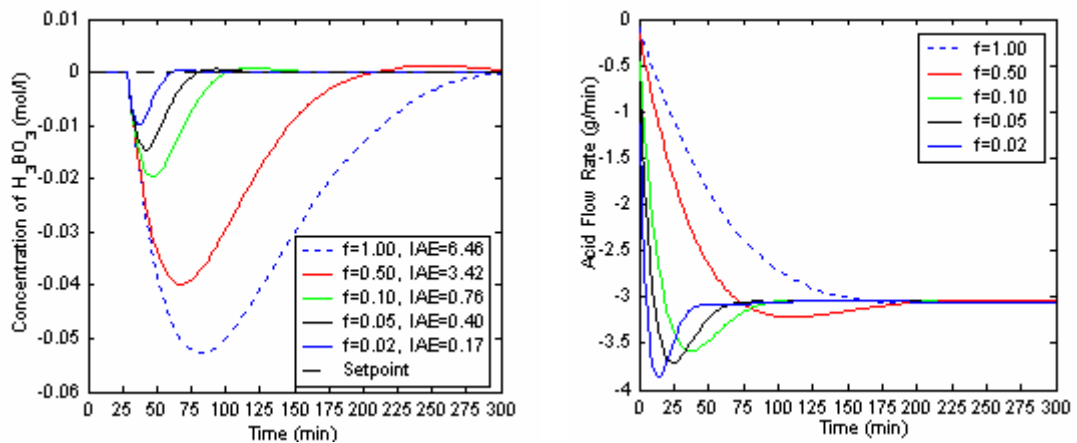


Figure 7.42: Change of controlled and manipulated variables wrt time for a 10% decrease in colemanite flow rate for $f=1.00, 0.50, 0.10, 0.05$ and 0.02 .

It can be seen from Figure 7.42 that controlled variable, boric acid concentration, returns its initial condition for all the f values when colemanite flow rate decreases by 10%. However, the best f value is chosen as 0.02 same as the actual model based MPC since the response time is fast and IAE score is low.

The changes of controlled and manipulated variables for a 10% decrease in colemanite flow rate are compared for actual and approximated transfer function model for $f=0.02$ and given in Figure 7.43. Approximated model gives better result than actual model with smaller response time and with less overshoot.

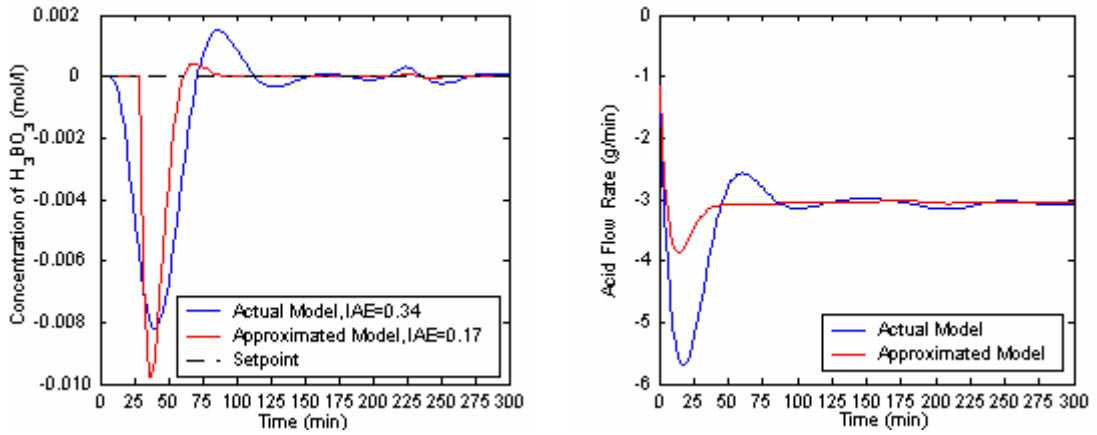


Figure 7.43: Change of controlled and manipulated variables wrt time for 10% decrease in colemanite flow rate for actual and approximated transfer function model with $f=0.02$.

7.2.2.8 Performance of SISO-MPC by Using Approximated Transfer Function Model for Robustness

In order to analyze the robustness of SISO-MPC for a proximated model, the plant/model mismatch is assumed for -10 % changes in time constants, time delay and gains for each reactor. Then, the new plant transfer function is expressed as in Equation (7.13).

$$\begin{bmatrix} y_4' \end{bmatrix} = \begin{bmatrix} \frac{-0.0378 e^{-27.9s}}{48.6s + 1} \end{bmatrix} \begin{bmatrix} u_1' \end{bmatrix} \quad (7.13)$$

The plant in Equation (7.12) is controlled by the MPC designed using the model in Equation (7.6).

The performance of designed MPC is analyzed for both setpoint tracking and disturbance rejection and robustness. The changes in the responses of controlled and manipulated variables as a function of time are presented in Figures 7.44

and 7.43. It can be said that the controller is robust in set point tracking. It is found that, similar to the actual model case in the use of the approximate model the MPC is not robust for disturbance rejection.

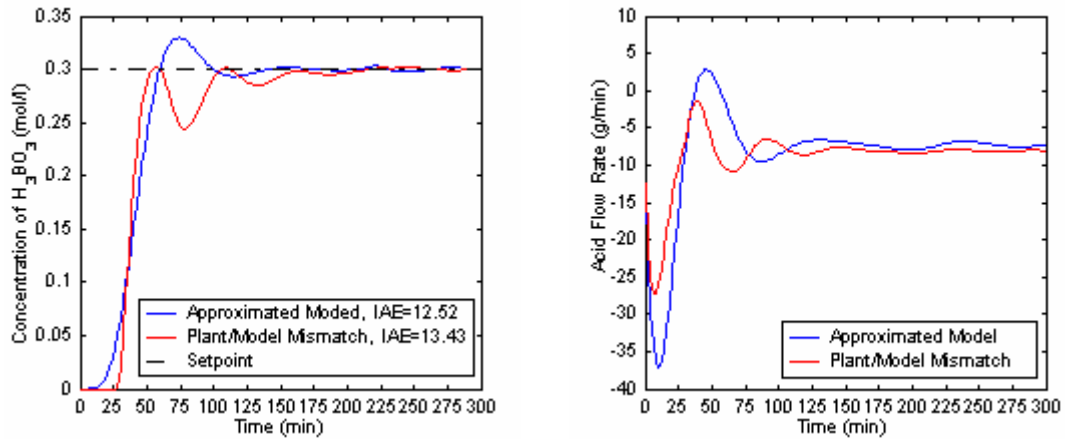


Figure 7.44: Change of controlled and manipulated variables wrt time for a 0.3 mol/l set point change in boric acid concentration when the approximated plant is changed by -10%.

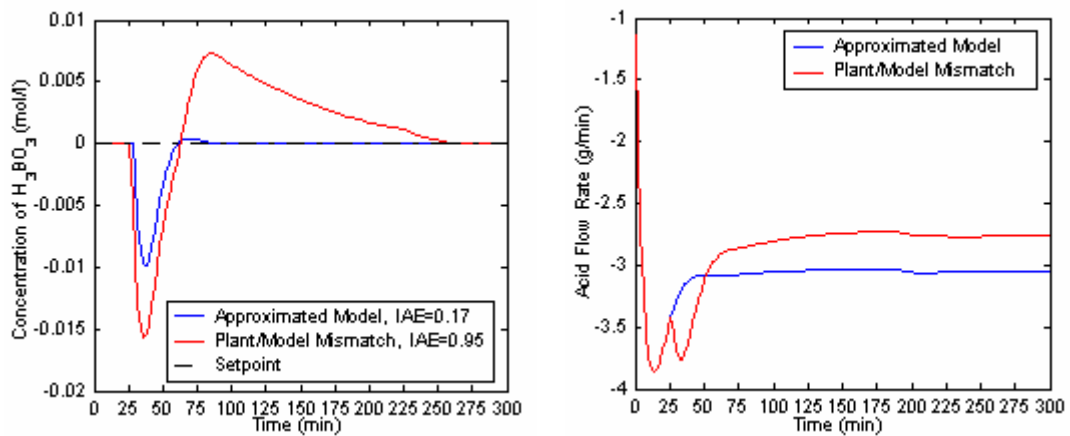


Figure 7.45: Change of controlled and manipulated variables wrt time for a 10% decrease in colemanite flow rate when the approximated plant is changed by -10%.

7.2.3 Design of Cohen-Coon (PID) and ITAE (PID) Controllers

Using the approximated transfer function of the process given in Equation (7.6), controller gain (K_C), integral time (τ_I) and derivative time (τ_D) are found as -61.3, 62.5 and 10.2 using the tuning relationship given by Cohen-Coon (PID) and -36.8, 75.9 and 9.9 for ITAE (PID)-setpoint tracking and -54.6, 42.6 and 11.8 for ITAE (PID)-load. The controller parameters calculated are given in Appendix G.2.

The performances of the controllers, namely SISO-MPC, Cohen-Coon (PID) and ITAE (PID) are compared for setpoint tracking by 0.3 mol/l changing boric acid concentration and for a disturbance rejection in a 10% decrease in colemanite flow rate as disturbance. The responses of controlled and manipulated variable are presented in Figure 7.46 and Figure 7.47.

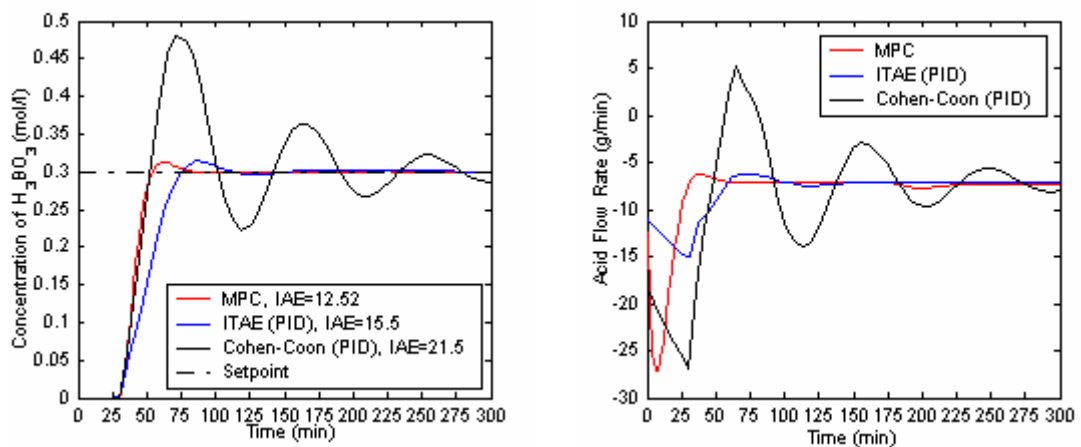


Figure 7.46: Change of controlled and manipulated variables wrt time for a 0.3 mol/l setpoint change of boric acid concentrations for different controllers.

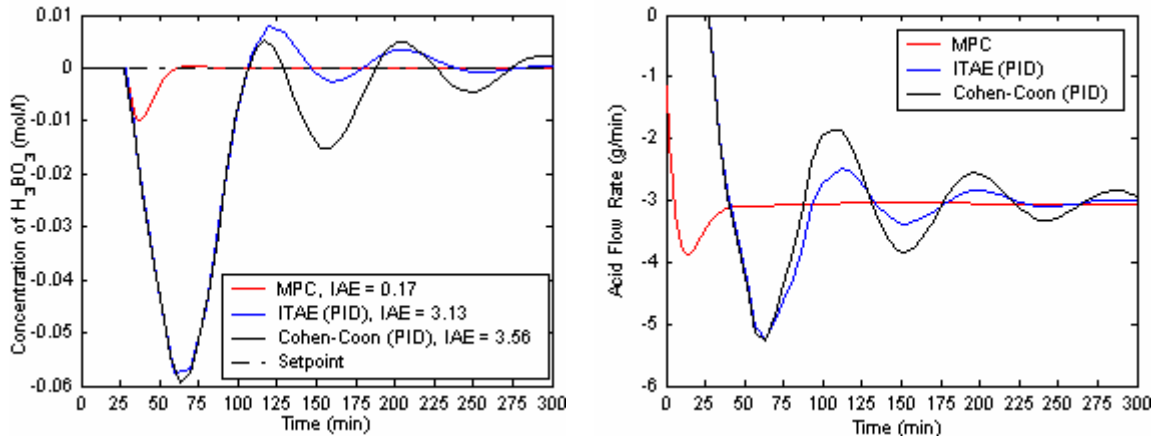


Figure 7.47: Change of controlled and manipulated variables wrt time for a 10% decrease in colemanite flow rate for different controllers.

In Figure 7.46, the best performance is obtained for SISO-MPC considering the response time and the IAE score. ITAE (PID) also gives good performance whereas oscillations are observed and setpoint is not reached for Cohen-Coon (PID) until 300 min.

It can be seen from Figure 7.47 that MPC reject the disturbance in a shorter time while Cohen-Coon (PID) and ITAE (PID) give similar performance where oscillations are observed.

CHAPTER 8

CONCLUSIONS

This study is considered to investigate the performance of the Model Predictive Controller (MPC) algorithm in CSTR's for saponification and boric acid production systems.

In saponification system;

1. The experimental and model results for a set point change in ethyl acetate, F_{ea} , are compared under unsteady-state conditions and a good match is found between them.
2. According to SVD analysis, sodium acetate concentration is coupled with ethyl acetate flow rate, and reactor temperature is coupled with cooling water flow rate for the control configuration.
3. SISO-MPC and MIMO-MPC are designed. For SISO-MPC, the tuning parameters, f and C , are found as 1×10^{-7} and 70 for controlling sodium acetate concentration, 2×10^{-3} and 14 for controlling temperature of the reactor. For

MIMO-MPC, f and C are found as 1×10^{-7} and 70 respectively for both concentration and temperature control loops.

4. It is found that, the SISO-MPC and MIMO-MPC performances are good for setpoint tracking, disturbance rejection.

5. MIMO-MPC is found to be robust.

In boric acid production system;

1. Experiments are performed in order to find the transfer functions between boric acid concentration of the fourth reactor (controlled variable) and acid flow rate (manipulated variable), and between boric acid concentration of the fourth reactor and colemanite flow rate (disturbance) as give below;

$$\text{The process transfer function, } G_p = \left[\frac{-0.042 e^{-4s}}{(40s+1)(25s+1)(15s+1)(5s+1)} \right]$$

$$\text{The disturbance transfer function, } G_d = \left[\frac{0.123 e^{-4s}}{(35s+1)(15s+1)(8s+1)(7s+1)} \right]$$

2. Approximated transfer functions of the process and the disturbance are obtained by considering first order transfer function with a time delay as;

$$G_p = \left[\frac{-0.042 e^{-31s}}{54s+1} \right]$$

$$G_d = \left[\frac{0.123 e^{-29s}}{48s+1} \right]$$

3. SISO-MPC's are designed using both actual and approximated transfer function models.
4. The tuning parameter f is found as 0.02 for both SISO-MPC and C is selected as 60% of the model horizon, $C = 66$.
5. The designed controllers give good performance for setpoint tracking and disturbance rejection. SISO-MPC's (actual and approximated) are robust for setpoint tracking whereas, for disturbance rejection they are not robust.
6. In the presence of controlled variable constraints, the designed controllers performance are good for setpoint tracking and disturbance rejection. However, the manipulated variable constraints are not recommended due to excess overshoot in the controlled variable.
7. Using approximated transfer function models, Cohen and Coon (PID) and ITAE (PID) are designed and when compared with MPC, MPC is found to be superior to others.

REFERENCES

Afonso, A.F.N.A P., Oliveira, M.C. N., A. M. Castro J.A, (1996), "Model Predictive Control of a Pilot Plant Reactor with a Simulated Exothermic Reaction", Computers and Chemical Engineering, Vol. 20, pp. S769-S774

Al-Ghazzawi, A., Ali, E., Nouh, A., Zafirou, E., (2001), "On-line Tuning Strategy for Model Predictive Controllers", Journal of Process Control, Vol. 11, pp 265-284

Bahar, A.,(2003), "An Artificial Neural Network Estimator Design for the Inferential Model Predictive Control of an Industrial Multi-Component Distillation Column", M.Sc. Thesis, Middle East Technical University, Ankara

Balland, L., Estel, L., Cosmao, J.M., Mouhab, N., (2000), "A Genetic Algorithm with Decimal Coding for the Estimation of Kinetic and Energetic Parameters", Chemometrics and Intelligent Laboratory Systems, Vol. 50, pp.121-135

Camacho, E.F., Bordons, C., (2000), "Model Predictive Control", Springer-Verlag, London

Cervantes, A.L., Agamennoni, E.A., Figueroa, J.L, (2002), "A Nonlinear Model Predictive Control System Based on a Wiener Piecewise Linear Models", Journal of Process Control, Article in Press

Clarke, D.W., Mohtadi, C., Tuffs, P.S., (1987), "Generalized Predictive Control- I. The Basic Algorithm", *Automatica*, Vol. 23, No. 2, pp. 137-148

Cutler, C.R., Ramaker, B.L., (1979), "Dynamic Matrix Control- A Computer Control Algorithm", AIChE National Meeting, Houston, Texas

Çakal, G., (2004), "Dynamic Behaviour of Continuous Flow Stirred Slurry Reactors", Ph.D. Thesis, Middle East Technical University, Ankara

Çetin, E., Eroglu, İ., Özkar, S., (2001), "Kinetics of Gypsum Formation and Growth during the Dissolution of Colemanite in Sulfuric Acid", *Journal of Crystal Growth*, Vol 231, pp. 559-567

Dokucu, M.T., (2002), "Multivariable Model Predictive Controller Design for an Industrial Distillation Column", M.Sc. Thesis, Middle East Technical University, Ankara

Fogler, S.H., (1999), "Elements of Chemical Reaction Engineering", 3rd Edition, Prentice Hall, USA

Garcia, G.E., Morhedi, A.M., (1986), "Quadratic Programming Solution of Dynamic Matrix Control (QDMC)", *Chemical Engineering Communications*, Vol. 46, pp. 73-87

Garcia, G.E., Prett, D.M., Morari, M., (1989), "Model Predictive Control: Theory and Practice-A Survey", *Automatica*, Vol. 25, pp. 335-348

Garreth, D.E., (1998), "Borates-Handbook of Deposits, Processing, Properties, and Use", Academic Press, London

Gürbüz, H., Öçgüder, S., Yavaşoğlu, N., Sayan, P., Bulutçu, A. N., (1998) "Kolemanitin Borik Asit Çözeltilerinde Çözünürlüğü", III. Ulusal Kimya Mühendisliği Kongresi, Erzurum.

Heny, C., Simanca, D., Delgado, M., (2000), "Pseudo-bond Graph Model and Simulation of a Continuous Stirred Tank Reactor", Journal of Franklin Institute, Vol. 337, pp. 21-42

Kalafatoğlu, İ. E., Özdemir, S.S., (2000), "Hisarcık Kolemanitinin Sülfürik Asitle Çözünme Davranışı", IV. Ulusal Kimya Mühendisliği Kongresi, İstanbul

Kirk-Othmer, (1992), "Encyclopedia of Chemical Technology, Vol. 4, 4th Edition, John Wiley& Sons, pp. 372-378

Lee, J., Park, S., (1994), "Adaptive Model Predictive Control for Unstable Nonlinear Processes", Journal of Chemical Engineering of Japan, Vol.27, No.6, pp.760-767

Li, S., Lim, K.Y., Fisher, D.G., (1989), "A State Space Formulation for Model Predictive Control", AIChE Journal, Vol.35, No.2, pp.241-249

Mc-Ketta, J., (1977), "Encyclopedia of Chemical Processing and Design", Vol. 5, Marcel Dektar Inc., pp. 55-65

Morari, M., Ricker, N. L., "Model Predictive Control Toolbox", The Mathworks Inc.

Nagrath, D., Prasad, V., Bequette B.W., (2002), "A Model Predictive Formulation for Control of Open-Loop Unstable Cascade Systems", Chemical Engineering Science, Vol. 57, pp. 365-378

Özbayoğlu, G., Poslu, K., (1992), "Mining and Processing of Borates in Turkey", Mineral Processing and Extractive Metallurg Review, Vol. 9, pp. 245-254

Özgülşen, F., Kendra, S.J., Çınar, A., (1993), "Nonlinear Predictive Control of Periodically Forced Chemical Reactors", AIChE Journal, Vol. 39, No. 4, pp. 589-598

Özkan, L., Kothare, M.V., Georgakis, C., (2003), "Control of a Solution Copolymerization Reactor Using Multi-Model Predictive Control", Chemical Engineering Science, Vol. 58, pp. 1207-1221

Park, M.J., Rhee, H.K., (2001), "LMI-Based Robust Model Predictive Control for a Continuous MMA Polymerization Reactor", Computers and Chemical Engineering, Vol. 25, pp. 1513-1520

Perry, R.H., Green, D., (1980), "Perry's Chemical Engineers Handbook", McGraw Hill, NewYork

Prasad, V., Schley, M., Russo, L.P., Bequette, B.W., (2002), "Product Property and Production Rate Control of Styrene Polymerization", Journal of Process Control, Vol. 12, pp. 353-372

Richalet, J., Rault, A., Testud, J.L., Papon, J., (1978), "Model Predictive Heuristic Control: Applications to Industrial Processes", *Automatica*, Vol. 14, pp. 413-428

Riggs, J.B., Rhinehart, R.R., (1990), "Comparison between two nonlinear process-model based controllers", *Computers and Chemical Engineering*, Vol. 14, No. 10, pp. 1075-1081

Rouhani, R., Mehra, R.K., (1982), "Model Algorithmic Control (MAC): Basic Theoretical Properties", *Automatica*, Vol. 18, No. 4, pp. 401-414

Santos, O. L., Afonso, A.F.N.A. P., Castro, A.A.M J., Oliveira, M.C. N., Biegler, T.L., (2001), "On-line Implementation of Nonlinear MPC: an Experimental Case Study", *Control Engineering Practice*, Vol. 9, pp. 847-857.

Seborg, D.E., Edgar, T.F., Mellichamp, D.A., (1989), "Process Dynamics and Control", John Wiley & Sons Inc., Canada

Seki, H., Ogawa, M., Ooyama, S., Akamatsu K., Ohshima, M., Yang, W., (2001), "Industrial Applications of a Nonlinear Model Predictive Control to Polymerization Reactors", *Control Engineering Practice*, Vol. 9, pp. 819-828

Sistu, P.B., Bequette, B.W., (1992), " A Comparison of Nonlinear Control Techniques for Continuos Stirred Tank Reactors", *Chemical Engineering Science*, Vol. 47, No. 9-11, pp. 2553-2558

Tunç, M., Kocakerim, M. M., (1998), "Kolemanitin H₂SO₄ Çözeltisinde Çözünme Kinetiği", III. Ulusal Kimya Mühendisliği Kongresi, Erzurum

Tübitak, (2002), "Bilim ve Teknik", pp. 38-48

Ullmann, (1985), "Encyclopedia of Industrial Chemistry", Vol. A 4, pp. 266-269

Wang, D., Romagnoli, J.A., (2003), "Robust Model Predictive Control Design Using a Generalized Objective Function", Computers and Chemical Engineering, Vol. 27, pp. 965-982

Wu, F., (2001), "LMI-Based Robust Model Predictive Control and its Application to an Industrial CSTR Problem", Journal of Process Control, Vol. 11, pp. 649-659.

APPENDIX A

FORMULATION OF CONTROLLER DESIGN

In Controller Design equation in Section 4.5:

$$P_{1,i} = \sum_{j=1}^i S_{1,j} \quad \text{for } i = 1, 2, \dots, P \quad (\text{A.1})$$

$$P_{2,i} = \sum_{j=1}^i S_{2,j} \quad \text{for } i = 1, 2, \dots, P \quad (\text{A.2})$$

$$S_{1,j} = \sum_{i=j+1}^M h_{11,i} \Delta u_{1,n+j-i} + \sum_{i=j+1}^M h_{12,i} \Delta u_{2,n+j-i} \quad \text{for } i = 1, 2, \dots, P \quad (\text{A.3})$$

$$S_{2,j} = \sum_{i=j+1}^M h_{21,i} \Delta u_{1,n+j-i} + \sum_{i=j+1}^M h_{22,i} \Delta u_{2,n+j-i} \quad \text{for } i = 1, 2, \dots, P \quad (\text{A.4})$$

The simpler form of controller design equation can be written as follows:

$$\hat{E} = -A \Delta u + \hat{E} \quad (\text{A.5})$$

If there is a perfect match between the predicted output and desired trajectory, $\hat{E} = 0$, from Equation (A.5), then:

$$0 = -A \Delta u + \hat{E} \quad (\text{A.6})$$

If control horizon and prediction horizon are equal to each other, i.e $C = P$, then

$$\Delta u = (A)^{-1} \hat{E} \quad (\text{A.7})$$

where A is of type square matrix.

In Dynamic Matrix Control (DMC), control horizon (C) is less than prediction horizon (P), so the system of equations is overdetermined. Therefore, only C control actions (Δu) are calculated. The best solution is obtained by minimizing the performance index:

$$J[\Delta u] = \hat{E}^T \hat{E} \quad (\text{A.8})$$

The optimal solution can be written as:

$$\Delta u = (A^T A)^{-1} A^T \hat{E} = K_{MPC} \hat{E} \quad (\text{A.9})$$

The benefit of this procedure is that disturbances or modeling errors are detected early and corrected by an approximate manner. However, the disadvantage of the procedure is that considerably large changes in the

manipulated variable could occur. This problem takes place if $A^T A$ matrix is ill-conditioned or singular. Therefore, another approach can be applied in order to modify the objective function by penalizing movements of the manipulated variable:

$$J[\Delta u] = \hat{E}^T W_1 \hat{E} + \Delta u^T W_2 \Delta u \quad (\text{A.10})$$

where the first term is called future errors of the systems, and the second is future control effort of the system.

Then, the resulting control law is obtained as follows:

$$\Delta u = (A^T W_1 A + W_2)^{-1} A^T W_1 \hat{E} = K_{MPC} \hat{E} \quad (\text{A.11})$$

APPENDIX B

EXPERIMENTAL DATA FOR SAPONIFICATION SYSTEM

Table B.1 Experimental Data for $F_{EA} = 40$ ml/min, $F_N = 40$ ml/min at 30°C

T (min)	V_{NaOH} (ml)	C_{NaOH} (mol/l)
15	8.0	0.020
17	8.0	0.020
19	8.1	0.019
21	8.1	0.019
23	8.2	0.018
25	8.2	0.018
27	8.2	0.018
29	8.2	0.018

Table B.2 Experimental Data after +10% step input to F_{EA} , $F_{EA} = 44$ ml/min, $F_N = 40$ ml/min at 30°C

T (min)	V_{NaOH} (ml)	C_{NaOH} (mol/l)
0	8.2	0.018
2	8.2	0.018
4	8.2	0.018
6	8.3	0.017
8	8.3	0.017
10	8.3	0.017
12	8.3	0.017
14	8.3	0.017
16	8.4	0.016
18	8.4	0.016
20	8.4	0.016
22	8.4	0.016
24	8.4	0.016
26	8.4	0.016

Table B.3: Thermodynamic and Kinetic Data

Parameters	Values
k	$1.83 \times 10^8 \times \exp(-5208/T)$ l/mol.min
C _{pN}	75.2 J/mol.K
C _{pEA}	75.2 J/mol.K
C _{pNA}	75.2 J/mol.K
C _{pE}	75.2 J/mol.K
C _{pCW}	75.2 J/mol.K
ΔH _{rxn}	-79,076J/mol

APPENDIX C

SINGULAR VALUE DECOMPOSITION (SVD) ANALYSIS

In order to determine the interactions between inputs and outputs of the system,

Singular Value Decomposition (SVD) method is used. The steady state gain matrix, G , is written as follows:

$$G = U \Sigma V^T \quad (C.1)$$

where U is left singular vector, V is right singular vector and Σ is called singular values.

Controller pairing is the most important aspect of SVD. The largest vector component of column " U_i " is paired with the largest vector component of " V_i ."

Another property of SVD analysis is focusing on condition number, CN. The condition number is defined as the ratio of the largest and smallest nonzero singular values:

$$CN = \frac{\sigma_l}{\sigma_r} \quad (\text{C.2})$$

Large condition number indicates the poor conditioning. If G is singular, then it is ill-conditioned.

APPENDIX D

SIMULATION PROGRAM FOR SAPONIFICATION SYSTEM

D.1 cstr.m

```
function cstr

% ===== Main program =====

% Clear command window
clc;
% Include all global variables
glob_decs;
% Initialize all global variables
display('Global variables are initializing ...');
glob_initial;
display('Global variables have been initialized.');
```

%----- Plant Variables

```
% NaOH Concentration (mol/l)
Cn=zeros(1);

% Ethyl acetate concentration (mol/l)
Cea=zeros(1);

% Sodium acetate concentration (mol/l)
Cna=zeros(1);

% Ethanol concentration (mol/l)
Ce=zeros(1);

% Reactor temperature (K)
T=zeros(1);

% Volume of the reactor (l)
V=zeros(1);

% Differential NaOH concentration (mol/l.min)
dCn=zeros(1);
```

```

% Differential Ethyl acetate concentration (mol/l.min)
dCea=zeros(1);

% Differential Sodium acetate concentration (mol/l.min)
dCna=zeros(1);

% Differential Ethanol concentration (mol/l.min)
dCe=zeros(1);

% Differential Reactor temperature (K/min)
dT=zeros(1);

% Differential Reactor volume (l/min)
dV=zeros(1);

% Initial concentration of NaOH (mol/lt)
Cnl=zeros(1);

% Initial concentration of Ethyl acetate(mol/lt)
Ceal=zeros(1);

% Flowrate of NaOH (lt/min)
Fn=zeros(1);

% Flowrate of Ethyl Acetate (lt/min)
Fea=zeros(1);

% Flowrate of cooling water (lt/min)
Fcw=zeros(1);

% Inlet Temperature of NaOH and Ethyl Acetate (K)
Tl=zeros(1);

% Heat of reaction at standart Temperature (J/mol)
H=zeros(1);

% Heat capacity of NaOH (J/mol.K)
cpn=zeros(1);

% Heat capacity of Sodium acetate (J/mol.K)
cpna=zeros(1);

% Heat capacity of Ethyl Acetate (J/mol.K)
cpea=zeros(1);

% Heat capacity of Ethanol (J/mol.K)
cpe=zeros(1);

% Heat capacity of water (J/mol.K)
cpw=zeros(1);

% Cooling Water Inlet temperature (K)
Twl=zeros(1);

% Overall Heat transfer coefficient times area (J/min.K)
UA=zeros(1);

% ----- Initiliaze Plant Variables

```

```

%%%%%%%%%%%%%%%%%%%%%%%%%%%%%%%%%%%%%%%%%%%%%%%%%%%%%%%%%%%%%%%%%%%%%%%%%%%%%% Initialize states

% NaOH Concentration (mol/l)
Cn=0.05;

% Ethyl acetate concentration (mol/l)
Cea=0.05;

% Sodium acetate concentration (mol/l)
Cna=0.0;

% Ethanol concentration (mol/l)
Ce=0.0;

% Initial Reactor temperature (K)
T=298.15;

% Initial Volume of the reactor (l)
V=0.04;

% Initial Error
E=zeros(1);

%%%%%%%%%%%%%%%%%%%%%%%%%%%%%%%%%%%%%%%%%%%%%%%%%%%%%%%%%%%%%%%%%%%%%%%%%%%%%% Initialize parameters

% Initial concentration of NaOH (mol/lt)
Cn1=0.1;

% Initial concentration of Ethyl acetate(mol/lt)
Ceal=0.1;

% Flowrate of NaOH (ml/min)
Fn=40;

% Flowrate of Ethyl Acetate (ml/min)
Fea=40;

% Flowrate of cooling water (ml/min)
Fcw=24;

% Inlet Temperature of NaOH and Ethyl Acetate (K)
T1=298.15;

% Heat of reaction at standart Temperature (J/mol)
H=-79076;

% Heat capacity of NaOH (J/mol.K)
cpn=75.2;

% Heat capacity of Sodium acetate (J/mol.K)
cpna=75.2;

% Heat capacity of Ethyl Acetate (J/mol.K)
cpea=75.2;

% Heat capacity of Ethanol (J/mol.K)
cpe=75.2;

```

```

% Heat capacity of water (J/mol.K)
cpw=75.2;

% Reaction rate constant  $k=1.83e8*\exp(-5208/T)$  (lt/mol.min)

% Reaction rate  $-ra=k*Cn*Cea$  (mol/lt.min)

% Cooling Water Inlet temperature (K)
Tw1=291.15;

% Cooling Water Outlet temperature (K)  $Tw2= T-(T-Tw1)*\exp(-UA/(F_{cw}*55.56*cpw))$ 

% Overall Heat transfer coefficient times area (J/min.K)
UA=18.3;

% Integral Absolute Error
E=zeros(1);

% Integral Absolute Error for Cna
E1=zeros(1);

% Integral Absolute Error for T
E2=zeros(1);

% ----- Controller Variables

% Flowrate of the Ethyl acetate (mol/min)
Fea_s = zeros(1);
% max Flowrate of the Ethyl acetate (mol/min)
Fea_s_max = zeros(1);
% min Flowrate of the Ethyl acetate (mol/min)
Fea_s_min = zeros(1);
% Cooling water flowrate (l/min)
Fcw_s = zeros (1);
% max Cooling water flowrate (l/min)
Fcw_s_max = zeros(1);
% min Cooling water flowrate (l/min)
Fcw_s_min = zeros(1);

%
Cna_max = zeros(1,n_ph);
%
Cna_min = zeros(1,n_ph);
%
T_max = zeros(1,n_ph);
%
T_min = zeros(1,n_ph);

s_Cna_Fea = zeros(1,n_mh);
s_Cna_Fcw = zeros(1,n_mh);
s_T_Fea = zeros(1,n_mh);
s_T_Fcw = zeros(1,n_mh);
h_Cna_Fea = zeros(1,n_mh);
h_Cna_Fcw = zeros(1,n_mh);
h_T_Fea = zeros(1,n_mh);

```

```

h_T_Fcw      = zeros(1,n_mh);

hessian = zeros(nu*n_ch,nu*n_ch);
eprimecoeff = zeros(nu*n_ch,ny*n_ph);
mpcgain = zeros(nu*n_ch,ny*n_ph);

gradient = zeros(1,nu*n_ch);

dyn_matrix = zeros(ny*n_ph,nu*n_ch);
dyn_matrix_Cna_Fea = zeros(n_ph,n_ch);
dyn_matrix_Cna_Fcw = zeros(n_ph,n_ch);
dyn_matrix_T_Fea = zeros(n_ph,n_ch);
dyn_matrix_T_Fcw = zeros(n_ph,n_ch);

ineq_matrix = zeros(2*nu*n_ch+2*ny*n_ph,nu*n_ch);
ineq_vector = zeros(1,2*nu*n_ch+2*ny*n_ph);

delta_u = zeros(1,nu*n_ch);
e_prime = zeros(1,ny*n_ph);
current_st = zeros(1,ny);
lambda1 = zeros(1);
lambda2 = zeros(1);
setpoint = zeros(1,ny*n_ph);

temp1 = zeros(nu*n_ch,ny*n_ph);
invhessian = zeros(nu*n_ch,nu*n_ch);

temps1 = zeros(1);
temps2 = zeros(1);
temps3 = zeros(1);
temps4 = zeros(1);

setpoint0 = zeros(1,ny);

% scalar equal to the multiple of the identity matrix added to H to
% give a positive definite matrix (output)
diag = zeros(1);
% vector of length NVAR (the number of variables) containing
% solution (output)
sol = zeros(1,nu*n_ch);
% final number of active constraints (output)
nact = zeros(1);
% vector of length NVAR containing the indices of the final active
% constraints in the first NACT positions (output)
iact = zeros(1,nu*n_ch);
% vector of length NVAR containing the Lagrange multiplier estimates
% of the final active constraints in the first NACT (output)
alamda = zeros(1,nu*n_ch);

%----- Initialization

pass          = 0;
prnt_flag    = 0;
dist_flag    = 35000;
step_flag    = 35000;
cont_flag    = 35000;

```

```

dist_int      = 100000;
step_int      = 60000;
cont_int      = 500;
prnt_int      = 500;

dist_magntd   = -1.8;
step_magntd   = -2;
time          = 0;
sim_time      = 120;
delta_t       = 0.001;
sim_time_steps = sim_time / delta_t;

uncnstrnt     = 1;
disturb       = 1;
step          = 0;

lambda1       = 1;
lambda2       = 1E-4;

% ----- Initialize Controller

controller_initialize;

for i = 1:n_ph;
    setpoint(i)      = 0.030536;
    setpoint(n_ph+i) = 302.541;
end;

setpoint0(1) = 0.030536;
setpoint0(2) = 302.541;

Fea_s = Fea;
Fcw_s = Fcw;

% % %-----

multip = 1;

for i = 1:sim_time_steps;

if (pass == prnt_flag)

    prnt_flag = prnt_flag + prnt_int;

% Write plant to screen

write_plant_to_scurr(time,delta_u(1),delta_u(n_ch+1),Cna,T,
setpoint0(2),Cn1,Fea,Fcw,E1,E2,E);

% Write plant data to file

write_plant_to_file(time, Cn, Cea, Cna, Ce, Cn1, T, V, Fea, Fcw,E);

```

```

end;
%-----Disturbances & Step Test

if ((pass == dist_flag) & (disturb == 1))
    %Fn          = Fn + dist_magntd

    Tw1          = Tw1 + dist_magntd

    %Ceal        = Ceal + dist_magntd
    dist_flag = dist_flag + dist_int;
    dist_magntd = -dist_magntd;

% if ((pass == 35000) & (disturb == 1))
%     Tw1 = Tw1 + dist_magntd
% end
%
% if ((pass==95000) & (disturb == 1))
%     Tw1 = Tw1 - dist_magntd
% end

    for i = 1:n_ph;
        setpoint(i)          = setpoint0(1);
        setpoint(n_ph+i)     = setpoint0(2);
    end;

end;

if ((pass == step_flag) & (step == 1))
    for i = 1:n_ph;
        setpoint(i)          = setpoint0(1);%*(1+step_magntd/100);
        setpoint(n_ph+i)     = setpoint0(2);%+step_magntd;

    end
    step_magntd = 0.0;
    step_flag   = step_flag   + step_int ;
end;

% if (pass>=35000)& (pass<=95000)
%     E1=E1+abs(setpoint0(1)*(1+step_magntd/100)-Cna)*delta_t;
% elseif (pass>95000)& (pass<=150000)
%     E1=E1+abs(setpoint0(1)-Cna)*delta_t;
% end

if (pass>=35000)
    E1=E1+abs(setpoint0(1)-Cna)*delta_t;
end

% if (pass>=35000)& ((pass<=95000))
%     E2=E2+abs(setpoint0(2)-2-T)*delta_t;
% elseif ((pass>95000)& ((pass<=150000)))
%     E2=E2+abs(setpoint0(2)-T)*delta_t;
%
% end
if (pass>35000)
    E2=E2+abs(setpoint0(2)-T)*delta_t;
end

```

```

    if (time==95)
        step_magntd=+2;
    end

%----- Insert Controller

if (pass == cont_flag)
    cont_flag = cont_flag + cont_int;
    current_st(1) = Cna;
    current_st(2) = T;

    eprimefinal;

    if (uncnstrnt)

        delta_u = (mpcgain*e_prime').';
    else
        eval_gradient;
        eval_ineq_vector(setpoint0, Fea, Fea_s, Fea_s_min, Fea_s_max...
                        ,Fcw, Fcw_s, Fcw_s_min, Fcw_s_max...
                        ,Cna_max,Cna_min,T_max,T_min);

        iev=ineq_vector.';

% calling qprog.dll for optimization

        delta_u = qprog(ineq_matrix,iev,gradient,hessian);

        delta_u = delta_u.';

    end;

    Fea = Fea + (Fea_s /100 * delta_u(1));
    Fcw = Fcw + (Fcw_s /100 * delta_u(n_ch+1));

    shift_control_history;
end;

%----- Calculation of derivatives

dCn=(1/V)*(1E-3*Fn*Cn1)-(1/V)*(1E-3*Fn+1E-3*Fea)*Cn-1.83e8*exp(-
5208/T)*Cn*Cea;

dCea=(1/V)*(1E-3*Fea*Cea1)-(1/V)*(1E-3*Fn+1E-3*Fea)*Cea-1.83e8*exp(-
5208/T)*Cn*Cea;

dCna=-(1/V)*(1E-3*Fn+1E-3*Fea)*Cna+1.83e8*exp(-5208/T)*Cn*Cea;

dCe=-(1/V)*(1E-3*Fn+1E-3*Fea)*Ce+1.83e8*exp(-5208/T)*Cn*Cea;

dT=(1E-3*Fn*Cn1*cpn*T1+1E-3*Fea*Cea1*cpea*T1-(1E-3*Fn+1E-
3*Fea)*(Cn*cpn+Cea*cpea+Cna*cpna+Ce*cpe)*T...

```

```

        -H*1.83e8*exp(-5208/T)*Cn*Cea*V+1E-3*Fcw*55.56*cpw*(Tw1-T)*(1-
exp(-UA/(1E-3*Fcw*55.56*cpw))))...
        /(V*(Cn*cpn+Cea*cpea+Cna*cpna+Ce*cpe));

if (time < 15)
    dV=1E-3*Fn+1E-3*Fea;
else
    dV=0;
end;

%----- Update states

Cn=Cn+dCn*delta_t;

Cea=Cea+dCea*delta_t;

Cna=Cna+dCna*delta_t;

Ce=Ce+dCe*delta_t;

T=T+dT*delta_t;

V=V+dV*delta_t;

% if (pass>=35000)
%     E=E1+E2;
% end
time = time + delta_t;
pass = pass + 1;

end;

% =====
% Close Output Files
% =====

% NaOH concentration output file
fclose(FID_NaOH_concentration);

% Ethyl Acetate concentration output file
fclose(FID_Ethylacetate_concentration);

% Sodium Acetate concentration output file
fclose(FID_Sodiumacetate_concentration);

% Initial Sodium Acetate concentration output file
fclose(FID_Initial_Sodiumacetate_concentration);

% Ethanol concentration output file
fclose(FID_Ethanol_concentration);

% Temperature output file
fclose(FID_Reactor_temperature);

% Reactor volume output file
fclose(FID_Reactor_volume);

```

```

% Main output file
fclose(FID_main);

% Integral Absolute Error file
fclose(FID_IAE);

%----- Output functions

%=====
% write_plant_to_scurr
%=====

function write_plant_to_scurr(t,u1,u2,Cnacon,Tmp,sp,Cnlcon,flowea,
flowcw,Err1,Err2,Err)

glob_decs;

fprintf('%9.4f %9.4f %9.4f %9.6f %9.4f %9.6f %9.6f %9.6f %9.6f
%9.6f%9.6f%9.6f\n',t,u1,u2,Cnacon,Tmp,sp,Cnlcon,flowea,flowcw,Err1,
Err2,Err);

%end write_plant_to_scurr

%=====
% write_plant_to_file
%=====

function write_plant_to_file(t, Cnconc, Ceaconc, Cnaconc, Ceconc,
Cnlconc, temp, vol, flowea, flowcw,Err)
glob_decs;

% NaOH concentration output file
l = prod(size(Cnconc));
formats = ''; for i=1:l; formats = [formats ' %9.6f']; end;
fprintf(FID_NaOH_concentration,['%9.4f'formats'\n'],t,reshape(Cnconc
,1,1));

% Ethyl Acetate concentration output file
l = prod(size(Ceaconc));
formats = ''; for i=1:l; formats = [formats ' %9.6f']; end;
fprintf(FID_Ethylacetate_concentration,['%9.4f'formats'\n'],t,
reshape(Ceaconc, 1, 1));

% Sodium Acetate concentration output file
l = prod(size(Cnaconc));
formats = ''; for i=1:l; formats = [formats ' %9.6f']; end;
fprintf(FID_Sodiumacetate_concentration, ['%9.4f' formats '\n'], t,
reshape(Cnaconc, 1, 1));

% Ethanol concentration output file
l = prod(size(Ceconc));
formats = ''; for i=1:l; formats = [formats ' %9.6f']; end;
fprintf(FID_Ethanol_concentration,['%9.4f'formats'\n'],t,reshape
(Ceconc, 1, 1));

```

```

% Initial Sodium Acetate concentration output file
l = prod(size(Cnlconc));
formats = ''; for i=1:l; formats = [formats ' ; %9.6f']; end;
fprintf(FID_Initial_Sodiumacetate_concentration,['%9.4f'formats'\n']
, t, reshape(Cnlconc, 1, l));
% Reactor temperature output file
l = prod(size(temp));
formats = ''; for i=1:l; formats = [formats ' ; %9.4f']; end;
fprintf(FID_Reactor_temperature,['%9.4f'formats'\n'],t,reshape
(temp, 1, l));

% Reactor volume output file
l = prod(size(vol));
formats = ''; for i=1:l; formats = [formats ' ; %9.4f']; end;
fprintf(FID_Reactor_volume, ['%9.4f' formats '\n'], t, reshape(vol,
1, l));

% Main output file
l = prod(size(flowea)) + prod(size(flowcw));
formats = ''; for i=1:l; formats = [formats ' ; %9.6f']; end;
fprintf(FID_main,['%9.4f'formats'\n'],t,reshape([flowea;flowcw],l,
l));

% Integral Absolute Error output file
l = prod(size(Err));
formats = ''; for i=1:l; formats = [formats ' ; %9.6f']; end;
fprintf(FID_IAE, ['%9.4f' formats '\n'], t, reshape([Err],l, l));

%end write_plant_to_file

% -----End Simulation loop control user interface functions----- %

```

D.2 Controller.m

```

=====Controller.m=====

```

```

function controller_initialize
glob_decs;

cntrl_hist = zeros(n_mh,nu);
w1         = zeros(ny*n_ph,ny*n_ph);
w2         = zeros(nu*n_ch,nu*n_ch);

for i = 1:n_ph;
    w1(i,i) = lambda1*1.0;
end;

for i = n_ph+1:ny*n_ph;
    w1(i,i)= lambda1*1.0;
end;

for i = 1:nu*n_ch;
    w2(i,i)= lambda2*1.0;

```

```

end;

read_step_response_coeff;
eval_imp_resp_coeff;
construct_dyn_matrix;
eval_hessian;
eval_mpcgain;

% end controller_initialize

%-----

function read_step_response_coeff
glob_decs;

for i = 1:n_mh;
    s_Cna_Fea((i))= dlmread('stepcoefficients.dat','',[i-1 0 i-1 0]);
    s_Cna_Fcw((i))= dlmread('stepcoefficients.dat','',[i-1 1 i-1 1]);
    s_T_Fea((i))= dlmread('stepcoefficients.dat','',[i-1 2 i-1 2]);
    s_T_Fcw((i))= dlmread('stepcoefficients.dat','',[i-1 3 i-1 3]);
end;

% end read_step_response_coeff

%-----

function eval_imp_resp_coeff
glob_decs;

h_Cna_Fea(1) = s_Cna_Fea(1);
h_Cna_Fcw(1) = s_Cna_Fcw(1);
h_T_Fea(1)   = s_T_Fea(1);
h_T_Fcw(1)   = s_T_Fcw(1);

for i=2:n_mh;
    h_Cna_Fea(i) = s_Cna_Fea(i) - s_Cna_Fea(i-1);
    h_Cna_Fcw(i) = s_Cna_Fcw(i) - s_Cna_Fcw(i-1);
    h_T_Fea(i)   = s_T_Fea(i)   - s_T_Fea(i-1);
    h_T_Fcw(i)   = s_T_Fcw(i)   - s_T_Fcw(i-1);
end;

% end eval_imp_resp_coeff

%-----

function construct_dyn_matrix
glob_decs;

for j=1:n_ch;
    for i=1:j-1;
        dyn_matrix_Cna_Fea(i,j) = 0.0;
        dyn_matrix_Cna_Fcw(i,j) = 0.0;
        dyn_matrix_T_Fn(i,j)    = 0.0;
        dyn_matrix_T_Fcw(i,j)   = 0.0;
    end;
end;
end;

```

```

for j=1:n_ch;
    for i=j:n_ph;
        dyn_matrix_Cna_Fea(i,j) = s_Cna_Fea(i-j+1);
        dyn_matrix_Cna_Fcw(i,j) = s_Cna_Fcw(i-j+1);
        dyn_matrix_T_Fea(i,j)   = s_T_Fea(i-j+1);
        dyn_matrix_T_Fcw(i,j)   = s_T_Fcw(i-j+1);
    end;
end;

for j=1:n_ch;
    for i=1:n_ph;
        dyn_matrix(i      ,      j) = dyn_matrix_Cna_Fea(i,j);
        dyn_matrix(i      , n_ch+j) = dyn_matrix_Cna_Fcw(i,j);
        dyn_matrix(i+n_ph ,      j) = dyn_matrix_T_Fea(i,j);
        dyn_matrix(i+n_ph , n_ch+j) = dyn_matrix_T_Fcw(i,j);
    end;
end;
% end construct_dyn_matrix

%-----

function eval_hessian
glob_decs;

templ = ((dyn_matrix)')*w1;
hessian = (templ*dyn_matrix) + w2;

% end eval_hessian

%-----

function eval_mpcgain
glob_decs;

invhessian = inv(hessian);
eprimecoeff = ((dyn_matrix)')*w1;
mpcgain      = invhessian*eprimecoeff;

%end eval_mpcgain

%-----

function shift_control_history
glob_decs;

% store the first element of the control vector on temporary space
#1
temps1 = delta_u(1);

for i = 1:n_mh;
    % store the i-th element of the control history on temporary
space #2
    temps2=cntrl_hist(i,1);
    % the new i-th element of the control history is temporary space
#1
    cntrl_hist(i,1)=temps1;
end;

```

```

% make the temporary space #1 equal to temporary space #2 which will
% make the next element of the control history equal to the the
previous one
    temps1=temps2;
end;

temps3=delta_u(n_ch+1);

for i=1:n_mh;
    temps4=cntrl_hist(i,2);
    cntrl_hist(i,2)=temps3;
    temps3=temps4;
end;

% end shift_control_history

% -----

function eprimefinal
glob_decs;

l = zeros(n_ph,ny);
s = zeros(n_ph,ny);

for j = 1:n_ph;
    for i = j+1:n_mh;
        s(j,1) = s(j,1) + h_Cna_Fea(i)*cntrl_hist(i-j,1) +
h_Cna_Fcw(i)*cntrl_hist(i-j,2);
        s(j,2) = s(j,1) + h_T_Fea(i)*cntrl_hist(i-j,1) +
h_T_Fcw(i)*cntrl_hist(i-j,2);
    end;
end;

l(1,1) = s(1,1);
l(1,2) = s(1,2);

for i=2:n_ph;
    l(i,1)=l(i-1,1) + s(i,1);
    l(i,2)=l(i-1,2) + s(i,2);
end;

for i = 1:n_ph;
    e_prime(i) = setpoint(i) - current_st(1) - l(i,1);
end;

for i = n_ph+1:ny*n_ph;
    e_prime(i) = setpoint(i) - current_st(2) - l(i-n_ph,2);
end;
% -----

function eval_gradient
glob_decs;

temp1 = (dyn_matrix) '*w1;
gradient = temp1*e_prime';

%end eval_gradient

```

```

% -----

function construct_ineq_matrix
glob_decs;

ineq_matrix = 0

% construct input constraints part of inequality matrix
for i = 1:n_ch;
    for j = 1:i;
        ineq_matrix (i+0*n_ch,    j) = -1.0;
        ineq_matrix (i+1*n_ch,n_ch+j) = -1.0;
        ineq_matrix (i+2*n_ch,    j) =  1.0;
        ineq_matrix (i+3*n_ch,n_ch+j) =  1.0;
    end;
end;

% construct output constraints part of inequality matrix
for i = 1:ny*n_ph;
    for j = 1:nu*n_ch;
        ineq_matrix (i+4*n_ch+0*n_ph,j) = -1.d0*dyn_matrix(i,j);
        ineq_matrix (i+4*n_ch+2*n_ph,j) =  1.d0*dyn_matrix(i,j);
    end;
end;

% end construct_ineq_matrix

% -----

function eval_ineq_vector(setpoint0, Fea, Fea_s, Fea_s_min,
Fea_s_max, Fcw, Fcw_s, Fcw_s_min,...
Fcw_s_max,Cna_max,Cna_min,T_max,T_min)

glob_decs;

ineq_vector = zeros(1,2*nu*n_ch+2*ny*n_ph);

Fea_scaled = (Fea-Fea_s)/Fea_s*100;
Fcw_scaled = (Fcw-Fcw_s)/Fcw_s*100;

for i = 1:n_ch;
    ineq_vector(i+0*n_ch) = Fea_scaled - Fea_s_max;
    ineq_vector(i+1*n_ch) = Fcw_scaled - Fcw_s_max;
    ineq_vector(i+2*n_ch) = Fea_s_min - Fea_scaled;
    ineq_vector(i+3*n_ch) = Fcw_s_min - Fcw_scaled;
end;

for i = 1:n_ph;
    ineq_vector(i+4*n_ch+0*n_ph) = setpoint0(1) - Cna_max -
e_prime(i);
    ineq_vector(i+4*n_ch+1*n_ph) = setpoint0(2) - T_max -
e_prime(i+n_ph);
    ineq_vector(i+4*n_ch+2*n_ph) = Cna_min - setpoint0(1) +
e_prime(i);
end;

```

```

    ineq_vector(i+4*n_ch+3*n_ph) = T_min - setpoint0(2) +
e_prime(i+n_ph);
end;

```

```

% end eval_ineq_vector

```

```

%-----

```

D.3 Global_decs.m

```

% ----- Programming Definitions ----- %

```

```

% =====

```

```

% Simulation Parameters

```

```

% =====

```

```

% -----Output File ID

```

```

%% NaOH concentration output file

```

```

global FID_NaOH_concentration;

```

```

% Ethyl acetate concentration output file

```

```

global FID_Ethylacetate_concentration;

```

```

% Sodiumacetate concentration output file

```

```

global FID_Sodiumacetate_concentration;

```

```

% Initial Sodiumacetate concentration output file

```

```

global FID_Initial_Sodiumacetate_concentration;

```

```

% Ethanol concentration output file

```

```

global FID_Ethanol_concentration;

```

```

% Reactor temperature output file

```

```

global FID_Reactor_temperature;

```

```

% Reactor volume output file

```

```

global FID_Reactor_volume;

```

```

% Main output file

```

```

global FID_main;

```

```

% Integral Absolute Error file

```

```

global FID_IAE;

```

```

global time;

```

```

% -----

```

```

% -----End Programming Definitions----- %

```

```

% -----Simulation Parameters----- %

```

```

% =====
% Physical System Definitions
% =====

% Number of outputs
global ny;
% Number of inputs
global nu;
% Model horizon
global n_mh;
% Prediction horizon
global n_ph;
% Control horizon
global n_ch;

global lambda1;
global lambda2;
% measured value at present sampling time
global current_st;
% Optimal input vector
global delta_u;
%
global e_prime;
% vector containing the values of reference setpoint
global setpoint;
% step resp coeff for sodium acetate concentration-ethyl acetate
flowrate
global s_Cna_Fea;
%global s_Cna_Fn;
% step resp coeff for sodium acetate concentration-cooling water
flowrate
global s_Cna_Fcw;
% step resp coeff for reactor temperature-ethyl acetate flowrate
global s_T_Fea;
%global s_T_Fn;
% step resp coeff for reactor temperature-cooling water flowrate
global s_T_Fcw;
% imp resp coeff for sodium acetate concentration-ethyl acetate
flowrate
global h_Cna_Fea;
%global h_Cna_Fn;
% imp resp coeff for sodium acetate concentration-cooling water
flowrate
global h_Cna_Fcw;
% imp resp coeff for reactor temperature-ethyl acetate flowrate
global h_T_Fea;
%global h_T_Fn;
% imp resp coeff for reactor temperature-cooling water flowrate
global h_T_Fcw;
%
global cntrl_hist;
%
global hessian;
%
global eprimecoeff;
%
global mpcgain;

```

```

%
global w1;
%
global w2;
%
global gradient;
%
global dyn_matrix;
%
global dyn_matrix_Cna_Fea;
%global dyn_matrix_Cna_Fn;
%
global dyn_matrix_Cna_Fcw;
%
global dyn_matrix_T_Fea;
%global dyn_matrix_T_Fn;
%
global dyn_matrix_T_Fcw;
%
global ineq_matrix;
%
global ineq_vector;

global time;

% -----

```

D.4 Glob_initial.m

```

% -----      Programming Initialization      ----- %
% =====
%                               % Simulation Parameters Settings
% =====

% -----      Output File ID Creation
fclose all; Current_Directory = cd;
% NaOH concentration output file
delete([Current_Directory '\ ' 'Cn.txt']);
FID_NaOH_concentration = fopen('Cn.txt','at');

% Ethyl acetate concentration output file
delete([Current_Directory '\ ' 'Cea.txt']);
FID_Ethylacetate_concentration = fopen('Cea.txt','at');

% Sodiumacetate concentration output file delete([Current_Directory
 '\ ' 'Cna.txt']);                               FID_Sodiumacetate_concentration =
fopen('Cna.txt','at');

% Initial Sodiumacetate concentration output file
delete([Current_Directory '\ ' 'Cn1.txt']);
FID_Initial_Sodiumacetate_concentration = fopen('Cn1.txt','at');

% Ethanol concentration output file

```

```

delete([Current_Directory '\' 'Ce.txt']);
FID_Ethanol_concentration = fopen('Ce.txt','at');

% Reactor temperature output file
delete([Current_Directory '\' 'T.txt']);
FID_Reactor_temperature = fopen('T.txt','at');

% Reactor volume output file
delete([Current_Directory '\' 'V.txt']);
FID_Reactor_volume = fopen('V.txt','at');

% Main output file
delete([Current_Directory '\' 'main.txt']);
FID_main = fopen('main.txt','at');

% Integral Absolute Error output file
delete([Current_Directory '\' 'E.txt']);
FID_IAE = fopen('E.txt','at');

% -----

% -----End Programming Initialization ----- %

% -----Simulation Initialization----- %

%Number of outputs
ny = 2;
%Number of inputs
nu = 2;
%Model horizon
n_mh = 116;
%Prediction horizon
n_ph = 99;
%Control horizon
n_ch =70;
% -----

```

D.5 stepcoefficients.dat

S_Cna_Fea	s_Cna_Fcw	s_T_Fea	s_T_Fcw
0.0000000;	0.0000000;	0.00000000;	0.00000000;
-0.0000119;	-0.0000010;	0.00500254;	-0.03193835;
-0.0000217;	-0.0000032;	0.01971825;	-0.05339092;
-0.0000291;	-0.0000061;	0.03920786;	-0.06627828;
-0.0000344;	-0.0000091;	0.05991901;	-0.07260313;
-0.0000379;	-0.0000119;	0.07949145;	-0.07422785;
-0.0000399;	-0.0000143;	0.09653106;	-0.07275286;
-0.0000408;	-0.0000163;	0.11038298;	-0.06946675;
-0.0000410;	-0.0000177;	0.12092255;	-0.06534452;
-0.0000406;	-0.0000188;	0.12837480;	-0.06107524;
-0.0000400;	-0.0000195;	0.13316741;	-0.05710551;
-0.0000392;	-0.0000198;	0.13581818;	-0.05368870;
-0.0000385;	-0.0000200;	0.13685465;	-0.05093347;
-0.0000379;	-0.0000200;	0.13676188;	-0.04884744;

-0.0000374;	-0.0000199;	0.13595289;	-0.04737398;
-0.0000371;	-0.0000198;	0.13475663;	-0.04642117;
-0.0000368;	-0.0000196;	0.13341807;	-0.04588334;
-0.0000368;	-0.0000195;	0.13210615;	-0.04565584;
-0.0000368;	-0.0000193;	0.13092583;	-0.04564436;
-0.0000368;	-0.0000192;	0.12993180;	-0.04576969;
-0.0000370;	-0.0000191;	0.12914177;	-0.04596945;
-0.0000371;	-0.0000191;	0.12854836;	-0.04619759;
-0.0000373;	-0.0000190;	0.12812902;	-0.04642255;
-0.0000376;	-0.0000190;	0.12785360;	-0.04662478;
-0.0000378;	-0.0000190;	0.12768999;	-0.04679410;
-0.0000380;	-0.0000190;	0.12760776;	-0.04692714;
-0.0000382;	-0.0000190;	0.12758036;	-0.04702513;
-0.0000384;	-0.0000190;	0.12758617;	-0.04709207;
-0.0000385;	-0.0000190;	0.12760867;	-0.04713332;
-0.0000387;	-0.0000190;	0.12763607;	-0.04715463;
-0.0000389;	-0.0000190;	0.12766070;	-0.04716145;
-0.0000390;	-0.0000190;	0.12767814;	-0.04715853;
-0.0000392;	-0.0000190;	0.12768649;	-0.04714977;
-0.0000393;	-0.0000190;	0.12768555;	-0.04713813;
-0.0000395;	-0.0000190;	0.12767625;	-0.04712576;
-0.0000396;	-0.0000190;	0.12766011;	-0.04711408;
-0.0000397;	-0.0000190;	0.12763888;	-0.04710389;
-0.0000399;	-0.0000190;	0.12761429;	-0.04709559;
-0.0000400;	-0.0000190;	0.12758787;	-0.04708924;
-0.0000402;	-0.0000190;	0.12756090;	-0.04708469;
-0.0000403;	-0.0000190;	0.12753435;	-0.04708171;
-0.0000404;	-0.0000190;	0.12750890;	-0.04707997;
-0.0000405;	-0.0000190;	0.12748500;	-0.04707918;
-0.0000407;	-0.0000190;	0.12746286;	-0.04707906;
-0.0000408;	-0.0000190;	0.12744257;	-0.04707937;
-0.0000409;	-0.0000190;	0.12742407;	-0.04707992;
-0.0000410;	-0.0000190;	0.12740726;	-0.04708058;
-0.0000411;	-0.0000190;	0.12739197;	-0.04708123;
-0.0000412;	-0.0000190;	0.12737805;	-0.04708183;
-0.0000414;	-0.0000190;	0.12736532;	-0.04708234;
-0.0000415;	-0.0000190;	0.12735361;	-0.04708274;
-0.0000416;	-0.0000190;	0.12734281;	-0.04708304;
-0.0000417;	-0.0000190;	0.12733278;	-0.04708325;
-0.0000418;	-0.0000190;	0.12732343;	-0.04708338;
-0.0000419;	-0.0000190;	0.12731469;	-0.04708345;
-0.0000420;	-0.0000190;	0.12730649;	-0.04708348;
-0.0000421;	-0.0000190;	0.12729879;	-0.04708347;
-0.0000421;	-0.0000190;	0.12729155;	-0.04708345;
-0.0000422;	-0.0000190;	0.12728473;	-0.04708342;
-0.0000423;	-0.0000190;	0.12727831;	-0.04708338;
-0.0000424;	-0.0000190;	0.12727227;	-0.04708335;
-0.0000425;	-0.0000190;	0.12726660;	-0.04708332;
-0.0000426;	-0.0000190;	0.12726127;	-0.04708329;
-0.0000426;	-0.0000190;	0.12725627;	-0.04708327;
-0.0000427;	-0.0000190;	0.12725157;	-0.04708326;
-0.0000428;	-0.0000190;	0.12724717;	-0.04708325;
-0.0000429;	-0.0000190;	0.12724305;	-0.04708324;
-0.0000429;	-0.0000190;	0.12723918;	-0.04708324;
-0.0000430;	-0.0000190;	0.12723557;	-0.04708324;
-0.0000431;	-0.0000190;	0.12723218;	-0.04708324;
-0.0000431;	-0.0000190;	0.12722901;	-0.04708324;
-0.0000432;	-0.0000190;	0.12722604;	-0.04708324;

-0.0000432;	-0.0000190;	0.12722326;	-0.04708325;
-0.0000433;	-0.0000190;	0.12722066;	-0.04708325;
-0.0000434;	-0.0000190;	0.12721822;	-0.04708325;
-0.0000434;	-0.0000190;	0.12721594;	-0.04708325;
-0.0000435;	-0.0000190;	0.12721380;	-0.04708325;
-0.0000435;	-0.0000190;	0.12721180;	-0.04708325;
-0.0000436;	-0.0000190;	0.12720993;	-0.04708325;
-0.0000436;	-0.0000190;	0.12720817;	-0.04708325;
-0.0000437;	-0.0000190;	0.12720652;	-0.04708325;
-0.0000437;	-0.0000190;	0.12720498;	-0.04708325;
-0.0000437;	-0.0000190;	0.12720354;	-0.04708325;
-0.0000438;	-0.0000190;	0.12720219;	-0.04708325;
-0.0000438;	-0.0000190;	0.12720092;	-0.04708325;
-0.0000439;	-0.0000190;	0.12719973;	-0.04708325;
-0.0000439;	-0.0000190;	0.12719862;	-0.04708325;
-0.0000441;	-0.0000190;	0.12719483;	-0.04708325;
-0.0000441;	-0.0000190;	0.12719403;	-0.04708325;
-0.0000441;	-0.0000190;	0.12719328;	-0.04708325;
-0.0000442;	-0.0000190;	0.12719257;	-0.04708325;
-0.0000442;	-0.0000190;	0.12719191;	-0.04708325;
-0.0000442;	-0.0000190;	0.12719129;	-0.04708325;
-0.0000442;	-0.0000190;	0.12719072;	-0.04708325;
-0.0000443;	-0.0000190;	0.12719017;	-0.04708325;
-0.0000443;	-0.0000190;	0.12718967;	-0.04708325;
-0.0000443;	-0.0000190;	0.12718919;	-0.04708325;
-0.0000444;	-0.0000190;	0.12718874;	-0.04708325;
-0.0000444;	-0.0000190;	0.12718833;	-0.04708325;
-0.0000444;	-0.0000190;	0.12718794;	-0.04708325;
-0.0000444;	-0.0000190;	0.12718757;	-0.04708325;
-0.0000444;	-0.0000190;	0.12718723;	-0.04708325;
-0.0000445;	-0.0000190;	0.12718690;	-0.04708325;
-0.0000445;	-0.0000190;	0.12718660;	-0.04708325;
-0.0000445;	-0.0000190;	0.12718632;	-0.04708325;
-0.0000445;	-0.0000190;	0.12718606;	-0.04708325;
-0.0000445;	-0.0000190;	0.12718581;	-0.04708325;
-0.0000446;	-0.0000190;	0.12718558;	-0.04708325;
-0.0000446;	-0.0000190;	0.12718536;	-0.04708325;
-0.0000446;	-0.0000190;	0.12718516;	-0.04708325;
-0.0000446;	-0.0000190;	0.12718497;	-0.04708325;
-0.0000446;	-0.0000190;	0.12718479;	-0.04708325;
-0.0000447;	-0.0000190;	0.12718462;	-0.04708325;

APPENDIX E

EXPERIMENTAL DATA FOR BORIC ACID PRODUCTION SYSTEM

Table E.1 Experimental Data in Reactor I for Run I

Time (min)	V_{NaOH} (ml)	C_{H3BO3} (mol/l)
0	26.80	2.680
25	26.44	2.644
60	26.25	2.625
95	26.01	2.601
128	25.88	2.588
156	25.79	2.579
176	25.83	2.583

Table E.2 Experimental Data in Reactor II for Run I

Time (min)	V_{NaOH} (ml)	C_{H3BO3} (mol/l)
0	26.23	2.623
26	25.96	2.596
53	25.76	2.576
92	25.59	2.559
125	25.39	2.539
149	25.33	2.533
181	25.27	2.527

Table E.3 Experimental Data in Reactor III for Run I

Time (min)	V_{NaOH} (ml)	C_{H3BO3} (mol/l)
0	26.41	2.641
28	26.22	2.622
51	26.01	2.601
89	25.88	2.588
123	25.67	2.567
148	25.60	2.560
183	25.54	2.554

Table E.4 Experimental Data in Reactor IV for Run I

Time (min)	V_{NaOH} (ml)	C_{H3BO3} (mol/l)
0	26.84	2.684
19	26.70	2.670
40	26.58	2.658
63	26.47	2.647
98	26.31	2.631
120	26.16	2.616
145	26.08	2.608
187	25.99	2.599

Table E.5 Experimental Data in Reactor I for Run II

Time (min)	V_{NaOH} (ml)	C_{H3BO3} (mol/l)
0	32.11	3.211
30	31.60	3.160
50	31.34	3.134
80	31.27	3.127
105	31.15	3.115
128	31.09	3.109
156	31.00	3.100
180	31.06	3.106

Table E.6 Experimental Data in Reactor II for Run II

Time (min)	V_{NaOH} (ml)	C_{H₃BO₃} (mol/l)
0	32.14	3.214
32	31.83	3.183
64	31.56	3.156
83	31.42	3.142
106	31.33	3.133
130	31.21	3.121
158	31.08	3.108
175	31.13	3.113

Table E.7 Experimental Data in Reactor III for Run II

Time (min)	V_{NaOH} (ml)	C_{H₃BO₃} (mol/l)
0	31.80	3.180
34	31.56	3.156
65	31.33	3.133
85	31.17	3.117
108	31.05	3.105
133	30.94	3.094
154	30.82	3.082
181	30.77	3.077

Table E.8 Experimental Data in Reactor IV for Run II

Time (min)	V_{NaOH} (ml)	C_{H₃BO₃} (mol/l)
0	32.30	3.230
20	32.15	3.215
50	31.99	3.199
73	31.79	3.179
94	31.66	3.166
119	31.54	3.154
145	31.37	3.137
189	31.23	3.123

Table E.9 Experimental Data in Reactor I for Run III

Time (min)	V_{NaOH} (ml)	C_{H3BO3} (mol/l)
0	27.15	2.715
30	27.96	2.796
57	28.14	2.814
83	28.35	2.835
107	28.29	2.829
136	28.41	2.841
155	28.48	2.848
175	28.45	2.845

Table E.10 Experimental Data in Reactor II for Run III

Time (min)	V_{NaOH} (ml)	C_{H3BO3} (mol/l)
0	27.26	2.726
28	27.89	2.789
59	28.14	2.814
81	28.29	2.829
111	28.33	2.833
138	28.42	2.842
157	28.49	2.849
178	28.54	2.854

Table E.11 Experimental Data in Reactor III for Run III

Time (min)	V_{NaOH} (ml)	C_{H3BO3} (mol/l)
0	27.40	2.740
33	27.84	2.784
61	28.12	2.812
78	28.33	2.833
109	28.42	2.842
134	28.50	2.850
161	28.59	2.859
184	28.66	2.866

Table E.12 Experimental Data in Reactor IV for Run III

Time (min)	V_{NaOH} (ml)	C_{H3BO3} (mol/l)
0	27.53	2.753
34	27.83	2.783
56	28.08	2.808
76	28.33	2.833
102	28.49	2.849
130	28.57	2.857
167	28.70	2.870
186	28.76	2.876

Table E.13 Experimental Data in Reactor I for Run IV

Time (min)	V_{NaOH} (ml)	C_{H3BO3} (mol/l)
0	24.70	2.470
25	25.37	2.537
55	25.54	2.554
80	25.68	2.568
110	25.90	2.590
132	25.77	2.577
160	25.84	2.584
175	25.87	2.587

Table E.14 Experimental Data in Reactor II for Run IV

Time (min)	V_{NaOH} (ml)	C_{H3BO3} (mol/l)
0	24.84	2.484
27	25.37	2.537
58	25.56	2.556
84	25.72	2.572
113	25.88	2.588
135	25.82	2.582
155	25.91	2.591
180	25.97	2.597

Table E.15 Experimental Data in Reactor III for Run IV

Time (min)	V_{NaOH} (ml)	C_{H3BO3} (mol/l)
0	24.90	2.490
30	25.33	2.533
60	25.54	2.554
86	25.70	2.570
115	25.85	2.585
135	25.79	2.579
158	25.91	2.591
184	26.01	2.601

Table E.16 Experimental Data in Reactor IV for Run IV

Time (min)	V_{NaOH} (ml)	C_{H3BO3} (mol/l)
0	25.12	2.512
20	25.29	2.529
50	25.64	2.564
80	25.81	2.581
105	25.93	2.593
130	25.97	2.597
163	26.11	2.611
188	26.19	2.619

APPENDIX F

MPC TOOLBOX IN MATLAB AND SIMULATION PROGRAMS FOR BORIC ACID PRODUCTION SYSTEM

F.1 MPC Toolbox in MATLAB

The MPC toolbox is composed of functions (commands) that are made use of for the analysis and design of model predictive control systems. The routines involved in the MPC toolbox were divided into two basic categories; routines using a step response model and routines using a state-space model.

MIMO step response coefficient matrix is written as in Equation (F.1) for n_m inputs and n_y outputs.

$$A_i = \begin{bmatrix} a_{1,1,i} & a_{1,2,i} & \cdots & a_{1,n_m,i} \\ a_{2,1,i} & & & \vdots \\ \vdots & & & \vdots \\ a_{n_y,1,i} & a_{n_y,2,i} & \cdots & a_{n_y,n_m,i} \end{bmatrix} \quad (\text{F.1})$$

where $a_{l,m,i}$ is the i^{th} step response coefficient relating the m^{th} input to the l^{th} output and A_i is the step response coefficient matrix at the i^{th} step.

The step response model can be achieved from identification experiments, or generated from a continuous or discrete transfer function or state-space model. In this study, step-response models are created from continuous transfer functions obtained in the identification experiments.

The step response model is kept in MPC Toolbox as in Equation (F.2).

$$\text{model} = \begin{bmatrix} & A_1 & & & \\ & A_2 & & & \\ & \vdots & & & \\ & A_n & & & \\ \text{nout}(1) & 0 & \dots & 0 & \\ \text{nout}(2) & 0 & \dots & 0 & \\ \vdots & \vdots & & \vdots & \\ \text{nout}(n_y) & 0 & \dots & 0 & \\ n_y & 0 & \dots & 0 & \\ \text{deltt} & 0 & \dots & 0 & \end{bmatrix}_{(n.n_y+n_y+2) \times n_m} \quad (\text{F.2})$$

The elements of the transfer function matrix are transferred to the MPC toolbox in Equation (F.3).

$$g_{ij} = \text{poly2tfd}[\text{num}, \text{den}, \text{delt}, \text{delay}] \quad (\text{F.3})$$

The function *poly2tfd* converts a transfer function (continuous or discrete) from the standard MATLAB poly format into the MPC *tf* format. In Equation (F.3), *num* consists of the coefficients of the transfer function numerator, and *den* includes the coefficients of the transfer function denominator, *delt* is sampling time, if a discrete time transfer function is used, *delt* must be specified, and for continuous time system, *delt* is zero. The *delay* is the time delay in the transfer function.

The function *tfd2step* calculates the MIMO step response of a model in the MPC tf format and converts a model MPC *tf* format to MPC step format as in Equation (F.4).

$$\text{model} = \text{tfd2step} \left[\text{tfinal}, \text{deltt}, n_y, g_j \right] \quad (\text{F.4})$$

After the model is stored in MATLAB, the function *mpccon* calculates MPC controller gain, K_{MPC} , using a model in MPC step format as in Equation (F.5).

$$K_{mpc} = \text{mpccon}(\text{model}, ywt, uwt, M, P) \quad (\text{F.5})$$

where *model* is the model of the process to be used in the controller design in the stepformat, *ywt* is the output weight and *uwt* is input weight, *M* is the control horizon and *P* is the prediction horizon.

The MPC is simulated by using *mpcsim* as expressed by Equation (F.6).

$$[y, u] = \text{mpcsim}(\text{plant}, \text{model}, K_{MPC}, \text{tend}, r) \quad (\text{F.6})$$

In Equation (F.6), *plant* is a model in the MPC step format that is to represent the plant, *model* is a model in the MPC step format that is to be used for state estimation in the controller, K_{MPC} is the MPC controller gain matrix, *tend* is the simulation time and *r* is the set-point changes.

In order to simulate MPC for disturbance, Equation (F.7) is used.

$$[y, u] = \text{mpcsim}(\text{plant}, \text{model}, K_{\text{MPC}}, \text{tend}, r, \text{usat}, \text{tfilter}, \text{dplant}, \text{dmodel}, \text{dstep}) \quad (\text{F.7})$$

where *usat* is a matrix giving the limits on the manipulated variables, *tfilter* is a matrix of time constants for the noise filter and the unmeasured disturbances entering at the plant output, *dplant* is a model in MPC step format representing all the disturbances (measured and unmeasured) that affect plant, *dmodel* is a model in MPC step format representing the measured disturbances. If *dmodel* is provided, then input *dstep* is also required. If there are no measured disturbances, set *dmodel*= [].

In case of constraints on manipulated variables or controlled variables, the model predictive controller is simulated by using *cmpc* function expressed in Equation (F.8), for disturbance rejection Equation (F.9) is used.

$$[y, u] = \text{mpcsim}(\text{plant}, \text{model}, \text{ywt}, \text{uwt}, M, P, \text{tend}, r, \text{ulim}, \text{ylim}) \quad (\text{F.8})$$

where *ulim* is a matrix giving the limits on the manipulated variables, *ylim* is same as *ulim*, but for the lower and upper bounds of the outputs.

$$[y, u] = \text{mpcsim} \left(\begin{array}{l} \text{plant}, \text{model}, K_{\text{MPC}}, \text{tend}, r, \text{ulim}, \text{ylim}, \text{usat}, \text{tfilter}, \\ \text{dplant}, \text{dmodel}, \text{dstep} \end{array} \right) \quad (\text{F.9})$$

F.2 MPC Simulation Program for Boric Acid Production System

```
% SISO-MPC Design

% Sampling time

deltt=2;

% Truncation time

tfinal=220;

% Model Horizon, N=tfinal/deltt

N=110;

% Process model

g11=poly2tfd(-0.042,[75000 24875 2375 85 1],0,4);
% Number of Outputs

ny=1;

% Model of transfer function

model=tfd2step(tfinal,deltt,ny,g11);

% Plant/Model Mismatch

plant=model;

% Weights on Outputs

ywt=[1];

% Weights on Inputs

uwt=[0.02];

% Control Horizon

M=66;

% Prediction Horizon

P=94;

% MPC Gain

Kmpc=mpccon(model,ywt,uwt,M,P);
```

```

%-----Set-Point Tracking-----

%Simulation time
tend=300;

%Set Point Change
r=[0.300];

% For unconstrained Case

% MPC Simulation

[y,u]=mpcsim(plant,model,Kmpc,tend,r);
% IAE Calculation

e=abs(r*ones(size(y))-y);

t=0:deltt:tend;

trapz(t,e);

ploteach(y,u,deltt);

%For Constrained MPC

ulim=[];
ylim=[-inf 0.302];

[y,u]=cmprc(plant,model,ywt,uwt,M,P,tend,r,ulim,ylim);

% IAE Calculation

e=abs(r*ones(size(y))-y);

t=0:deltt:tend;

trapz(t,e)

ploteach(y,u,deltt);

%-----Disturbance Rejection-----

%Simulation time
tend=300;

% Disturbance model
gd=poly2tf(0.123,[29400 10675 1331 65 1],0,4);

```

```

% Disturbance plant
dplant=tf2step(tfinal,deltt,ny,gd);

% Disturbance Model
dmodel=dplant;

%Set Point Change
r=[0];

usat=[];

tfilter=[];

% Step Change in Input
dstep=[-1];

%MPC Simulation
[y,u]=mpcsim(plant,model,Kmpc,tend,r,usat,tfilter,dplant,dmodel,dstep);
% IAE Calculation
e=abs(r*ones(size(y))-y);

t=0:deltt:tend;

trapz(t,e)

ploteach(y,u,deltt);

%-----Robustness-----

% A plant/model mismatch was assumed for -10 % changes in time
constants,
%time delay and gains for each reactor

% Plant model
p11=poly2tfd(-0.0378,[49207.5 18133.9 1923.8 76.5 1],0,3.6);

% Plant
plant=tf2step(tfinal,deltt,ny,p11);

%Simulation time
tend=300;

%Set Point Change
r=[0.3];

```

```
%MPC Simulation
[y,u]=mpcsim(plant,model,Kmpc,tend,r);
% IAE Calculation
e=abs(r*ones(size(y))-y);
t=0:deltt:tend;
trapz(t,e)
ploteach(y,u,deltt);
```

F.3 Cohen and Coon (PID) Model by Simulink

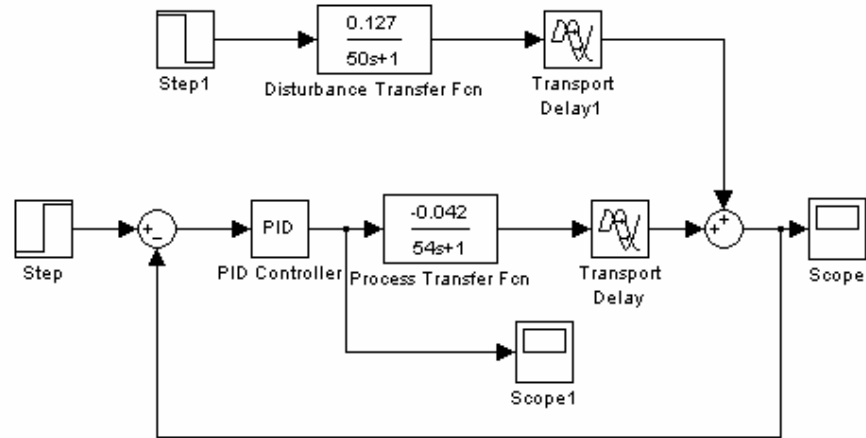


Figure F.1: Cohen and Coon Model by Simulink

F.4 ITAE (PID) Model by Simulink

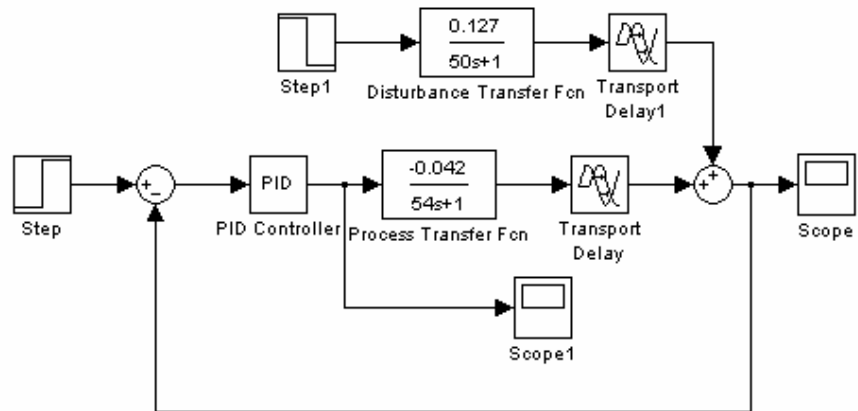


Figure F.2: ITAE (PID) Model by Simulink

APPENDIX G

SAMPLE CALCULATIONS

G.1 Calculation of Sodium Hydroxide Concentration for Saponification

System

$$T=30^{\circ}\text{C}$$

$$F_{\text{NaOH}} = 40 \text{ ml/min}$$

$$F_{\text{EtOAc}} = 40 \text{ ml/min}$$

$$M_{\text{HCl}} = 0.1 \text{ M}$$

$$V_{\text{HCl}} = 10 \text{ ml}$$

$$V_{\text{NaOH}} = 8.2 \text{ ml (from titration)}$$

$$M_{\text{NaOH}} = 0.1 \text{ M}$$

$$V_{\text{sample}} = 10 \text{ ml}$$

Unreacted amount of NaOH is found from back-titration;

$$V_{\text{HCl}} * M_{\text{HCl}} - V_{\text{NaOH}} * M_{\text{NaOH}} = C_{\text{NaOH-unreacted}} * V_{\text{sample}} \quad (\text{G.1})$$

$$10 \text{ ml} * 0.1 \text{ M} - 8.2 \text{ ml} * 0.1 \text{ M} = C_{\text{NaOH-unreacted}} * 10 \text{ ml}$$

$$C_{\text{NaOH-unreacted}} = 0.018 \text{ mol/l}$$

G.2 Calculations of Cohen-Coon (PID) and ITAE (PID) Design Parameters

From Approximated Transfer Function of Process in Equation (7.5):

$$K = -0.042, \tau = 54, \theta = 31$$

For Cohen and Coon (PID): (Seborg, 1989)

$$K_c = \frac{1}{K} \frac{\tau}{\theta} \left[\frac{16\tau + 3\theta}{12\tau} \right] \quad (\text{G.2})$$

$$\tau_I = \frac{\theta [32 + 6(\theta/\tau)]}{13 + 8(\theta/\tau)} \quad (\text{G.3})$$

$$\tau_D = \frac{4\theta}{11 + 2(\theta/\tau)} \quad (\text{G.4})$$

By using Equations (G.2), (G.3) and (G.4), K_c , τ_I and τ_D are calculated as -61.3, 62.5 and 10.2 respectively.

For ITAE (PID)- Setpoint:

$$KK_c = 0.965(\theta/\tau)^{-0.85} \quad (\text{G.5})$$

$$\tau/\tau_I = 0.796 - 0.1465(\theta/\tau) \quad (\text{G.6})$$

$$\tau_D/\tau = 0.308(\theta/\tau)^{0.929} \quad (\text{G.7})$$

By using Equations (G.5), (G.6) and (G.7), K_C , τ_I and τ_D are calculated as -36.8, 75.9 and 9.9 respectively.

For ITAE (PID)- Load:

$$KK_C = 1.357(\theta/\tau)^{-0.947} \quad (G.8)$$

$$\tau/\tau_I = 0.842(\theta/\tau)^{-0.738} \quad (G.9)$$

$$\tau_D/\tau = 0.381(\theta/\tau)^{0.995} \quad (G.10)$$

Using Equations (G.8), (G.9) and (G.10), K_C , τ_I and τ_D are calculated as -54.6, 42.6 and 11.8 respectively.

G.3 Determination of Boric Acid Concentration

The substances used to determine boric acid concentration were H_2SO_4 (1/3 by volume), 6N NaOH, 0.5 N NaOH, mannitol, methyl red indicator, phenolphthalein indicator.

In the experimental studies, 2-3 drops methyl red indicator was added to 5 ml sample of solution. Then, H_2SO_4 (1/3 by volume) was added to the solution up to color change was occurred from yellow to pink. The mixture was titrated with 6 N NaOH until it became yellow. H_2SO_4 was then mixed with the solution until the color of solution was changed from yellow to pink. The solution was titrated with 0.5 N NaOH solution until the pH of solution became 4.5. After that, 2-3 g mannitol was added to the solution. The solution was then titrated with 0.5 N

NaOH until the pH of the solution was equal to 8.5. This volume was used to find boric acid concentration.

Boric acid concentration was calculated by using Equation (G.11).

$$[\text{H}_3\text{BO}_3] = (V_{\text{NaOH}} \times F_{\text{NaOH}} \times N_{\text{NaOH}}) / V_{\text{sample}} \quad (\text{G.11})$$

where

V_{N} : Volume of NaOH for titration after adding mannitol to the solution (ml)

F_{N} : Factor of 0.5 N NaOH solution, (1)

N_{N} : Normalite of NaOH, (0.5 N)

V_{sample} : Volume of sample taken from filtering, (5 ml)